DEVELOPMENT OF NEW ANALYTICAL METHODS TO CHARACTERIZE THE HETEROGENEITY OF CELLULOSE ACETATES

Vom Fachbereich Chemie

der Technischen Universität Darmstadt

zur Erlangung des akademischen Grades eines

Doktor rerum naturalium (Dr. rer. nat.)

genehmigte

Dissertation

vorgelegt von

Hewa Othman Ghareeb, M.Sc.

aus Al-Sulaimaniyah, Irak

Referent:	**Prof. Dr. Matthias Rehahn**
Korreferent:	**Prof. Dr. Markus Busch**
Tag der Einreichung:	**21. Dezember 2012**
Tag der mündlichen Prüfung:	**11. Februar 2013**

Darmstadt 2013

D17

To my Parents, brothers and sisters
For all the support and encouragement

It is a pleasure to thank many people who have accompanied and supported me throughout this scientific work. I am honoured to pay my sincere thank to my research supervisor Prof. Dr. Matthias Rehahn for giving me the opportunity to work in his fascinating research group.

I wish to extend my deepest appreciation to Dr. Wolfgang Radke for providing this very interesting and challenging topic. His constant willingness to discuss and numerous suggestions have contributed to the success of the work. I am also thankful in particular for the necessary freedom that I had in dealing with the present research work.

My further heartfelt thanks go to Dr. Frank Malz for the NMR measurements and sharing his areas of expertise with me.

I am deeply indebted to Dr. Tibor Macko for his many helpful ideas and valuable advices and also to group mates Karsten Rode and Christoph Brinkmann for their contributions in technical assistance and equipment needs.

I would also like to express my gratitude for the rest of my colleagues from DKI for the pleasant working atmosphere and the cooperativeness in everyday matters. It was nice to meet you all and thank you very much for the beautiful moments that we spent together.

I gratefully acknowledge the German Academic Exchange Service (DAAD) for granting me a PhD scholarship, as well as for several enjoyable tour invitations and excellent care.

Last but not least, I am ever so grateful to my dearest Mom, Dad, brothers, sisters, and my relatives for their moral support, endless love, trust, and understanding during my study. Their motivational nature and enthusiasm in both good and difficult times will remain in my memory.

Diese Arbeit wurde am Deutschen Kunststoff-Institut (DKI) unter Leitung von Prof. Dr. M. Rehahn in der Zeit von November 2008 bis Mai 2012 durchgeführt. Am 1. Juli 2012 wurde das DKI als Bereich “Kunststoffe” in das Fraunhofer-Institut für Betriebsfestigkeit und Systemzuverlässigkeit LBF integriert.

Publication:

1. Hewa Othman Ghareeb, Wolfgang Radke, Peter Kilz
   "SEC method for cellulose acetates of wide DS-range"
   LC-GC Europe, 2011, 24 (12), S22

2. Hewa Othman Ghareeb, Frank Malz, Peter Kilz, Wolfgang Radke
   "Molar mass characterization of cellulose acetates over a wide range of high DS by size exclusion chromatography with multi-angle laser light scattering detection"
   Carbohydrate Polymers, 2012, 88 (1), 96-102

3. Hewa Othman Ghareeb, Wolfgang Radke
   "Separation of cellulose acetates by degree of substitution"
   Submitted to Polymer, 2012

4. Hewa Othman Ghareeb, Frank Malz, Wolfgang Radke
   "Characterization of cellulose acetates by two-dimensional liquid chromatography"
   In preparation, 2012

Oral Presentation:

1. "Liquid chromatography for the separation of cellulose derivatives by DS"
   Summer School (Cellulose: Combining Contradictions: Recognize, Understand, Surmount, Change and Use Structural Properties)
   August 30th – September 1st 2010, Bomlitz, Germany

2. "Chromatographic separation of polysaccharides by degree of substitution"
   SCM-5 (Fifth International Symposium on the Separation and Characterization of Natural and Synthetic Macromolecules)
   January 26th – 28th 2011, Amsterdam, The Netherlands

3. "Chromatographic separation of cellulose acetates by degree of substitution"
   Doctoral workshop
   December 14th 2011, Darmstadt, Germany

4. "New developments in the characterization of cellulose derivatives:
   Chromatographic separations by degree of substitution"
   HPLC 2012 (38th International Symposium on High Performance Liquid Phase Separations and Related Techniques)
   June 16th – 21st 2012, Anaheim, California, USA

Poster:

1. "Development of a chromatographic method to separate cellulose acetates by degree of substitution"

   a) SCM-5 (Fifth International Symposium on the Separation and Characterization of Natural and Synthetic Macromolecules)
      January 26th – 28th 2011, Amsterdam, The Netherlands

   b) Doctoral workshop
      July 13th 2011, Darmstadt, Germany

   c) NoSSS-6 (The Nordic Separation Science Society, Sixth International Conference on Separations and Related Techniques)
      August 24th – 27th 2011, Riga, Latvia

2. "Molar mass characterization of cellulose acetates over a wide range of high DS by size exclusion chromatography with multi-angle laser light scattering detection"
   NoSSS-6 (The Nordic Separation Science Society, Sixth International Conference on Separations and Related Techniques)
   August 24th – 27th 2011, Riga, Latvia

3. “Separation of cellulose acetate (CA) and sodium carboxymethyl cellulose (CMC) according to DS by gradient chromatography and its correlation with molar mass by 2D chromatography”

   Rolduc Polymer Meetings (Sustainability in Polymer Materials)

   May 20th – 23th 2012, Kerkrade, The Netherlands

Content

1. German Summary

Cellulose ist das häufigste natürliche Polymer. Die Bedeutung von Cellulose resultiert nicht nur aus den hervorragenden physikalischen Eigenschaften der Cellulose selbst, sondern auch aus der Tatsache, dass Cellulose zu Cellulosederivaten mit interessanten Eigenschaften umgewandelt werden kann. Cellulosederivate sind komplexe Copolymere, die zumindest in bezüglich der Molmasse und der chemischer Zusammensetzung heterogen sind. Diese Heterogenität wirkt sich kritisch auf viele der Eigenschaften aus, wie beispielweise die Haftfestigkeit, Löslichkeit, Viskoelastizität, Transparenz und die Fähigkeit der kontrollierten Wirkstofffreisetzung aus hydrophilen Tabletten. Deshalb ist die Untersuchung der Heterogenität von Cellulosederivaten von großer Bedeutung.

Trotz der großen Anzahl von Anwendungen umfassen die heutige Charakterisierungsstrategien für Cellulosederivate hauptsächlich die Charakterisierung der mittleren Molmassen und Molmassenverteilungen, des mittleren Substitutionsgrades (DS) und die Verteilung der Substituenten in den einzelnen Anhydroglucoseeinheiten (AGU), d.h. die partiell Substitutionsgrade in den Positionen O-2, O-3 und O-6.

Die Größenausschlusschromatographie (SEC) wird dabei zur Charakterisierung von Molmassen und deren Verteilung eingesetzt. NMR-Techniken werden verwendet, um die mittlere Substitutionsgrade und die Verteilung der Substituenten in den AGUs zu ermitteln.

Jedoch ist die Eignung von Cellulosederivaten für eine bestimmte Anwendung stark abhängig von der Verteilung der Substituenten zwischen den Polymerketten (Heterogenität der ersten Ordnung) und entlang der Polymerketten (Heterogenität der zweiten Ordnung). Um Informationen zur Verteilung der Monomerbausteine zu erlangen werden Cellulodederivate oftmals (partiell) durch Verwendung von Säuren oder Enzymen abgebaut. Hieraus resultieren Mischungen von Monomeren und/oder Oligomeren in unterschiedlichen Zusammensetzungen. Die resultierenden Produkte werden getrennt und anschließend detailliert bezüglich der Zusammensetzung und der Substituentenverteilung auf die Oligomere charakterisiert, wobei verschiedene analytische Techniken, wie SEC, Anionenaustauscherchromatographie (AEC), Gas-Flüssigkeitschromatographie (GLC) und Massenspektrometrie (MS) allein oder in Kombination, eingesetzt werden. Hierdurch erhält man Informationen zur Verteilung der verschieden substituierten AGUs entlang der Polymerkette (Heterogenität der zweiten Ordnung).

Durch den vollständigen oder partiellen Abbau gehen jedoch die Information darüber verloren, ob die unterschiedlichen monomeren oder oligomeren Einheiten aus der gleichen oder aus unterschiedlichen Ketten stammen. Die Charakterisierung der chemischen Heterogenität von Cellulosederivaten auf der Ebene intakter Polymerketten ist auch heute noch immer eine hochgradig herausfordernde Aufgabe.

Die Gradienten-HPLC stellt ein leistungsfähiges Verfahren Tool zur Trennung von (Co)Polymeren nach der chemischen Zusammensetzung dar. Derartige Trennungen erlauben die Berechnung der chemischen Zusammensetzung Verteilung (CCD) der Copolymeren. Jedoch sind bislang Informationen zur Trennung von Cellulosederivaten, besonderes von Celluloseacetat (CA), nach dem Substitutionsgrad in der Literatur nur sehr begrenzt verfügbar.

Die vorliegende Arbeit befasste sich daher hauptsächlich mit der Anwendbarkeit der Flüssigchromatographie zur Charakterisierung der molekularen Heterogenität von CAs.

Hierbei konnten die folgenden wesentlichen Ergebnisse erhalten werden:

1. Bei der Synthese der CA Proben, wurde gezeigt, dass die alkalische partielle Verseifung einer CA mit hohem Substitutionsgrad ein geeignetes Verfahren zur Herstellung von CAs mit unterschiedlicher mittlerer Substitutionsgraden ohne Veränderung der Polymerisationsgrad darstellt. Der Vergleich der berechneten theoretischen Substitutionsgrade mit den durch ^{1}H-NMR bestimmten zeigte, dass die Deacetylierungsreaktion kann durch die Menge an Natriumhydroxid (NaOH) kontrolliert werden.

2. Die FTIR/ATR konnte verwendet werden, um auch mit sehr geringen Probenmengen die Substitutionsgrade zu bestimmen. Hierdurch war es möglich, auch chromatographische Fraktionen bezüglich ihrer Substitutionsgarde zu charakterisieren.

3. Durch Löslichkeitstests wurden Dimethylsulfoxid (DMSO) und Dimethylacetamid (DMAc)/Lithiumchlorid (LiCl) als geeignete Lösungsmittel identifiziert um CA Proben im Bereich DS = 1,5 – 2,9 unabhängig von ihrem Substitutionsgrad zu lösen. Daher wurden diese beiden Lösungsmittel für chromatographische Experimente verwertet.

4. Es wurde eine SEC-Methode zur Charakterisierung der Molmassen und Molmassenverteilungen von CAs im Bereich DS = 1,5 – 2,9 entwickelt. Durch SEC mit Vielwinkel-Lichtstreudetektion (MALLS) konnte gezeigt werden, dass in reinem DMSO

und reinem DMAc Aggregate vorliegen, die durch den Zusatz von LiCl komplett unterdrückt werden können. Für die SEC-Untersuchungen wurde DMAc gegenüber DMSO bevorzugt, weil das spezifischen Brechungsindexinkrement (dn/dc) für CA in DMAc signifikant höher war als in DMSO. Proben unterschiedlicher Substitutionsgrade, die jedoch auf dem gleichen Ausgangsmaterial basierten zeigten nahezu identische Elutionsprofile und Kalibrierkurven. Dies deutet darauf hin, dass Variationen des Substitutionsgrades in den Bereich von 1,5 bis 2,9 nicht merklich das hydrodynamische Volumen verändern. Demzufolge können in diesem DS-Bereich alle Proben unabhängig vom Substitutionsgrad mittels der gleichen Kalibrierkurve ausgewertet werden. Die Vergleichbarkeit der durch Lichtstreuung erhaltenen mit den PMMA-äquivalenten Molmassen zeigte, dass letztere die wahren Werten deutlich überschätzen. Deshalb wurden Korrekturfaktoren ermittelt, die innerhalb des DS-Bereiches DS = 1,5 – 2,9 und unabhängig vom vorliegenden DS die Bestimmung der korrekten Molmassen basierend auf einer PMMA Kalibrierkurve ermöglichen.

5. Es konnte weiterhin eine Gradienten HPLC Methode erarbeitet werden, die es erlaubt CAs im Bereich DS = 1,5 – 2,9 nach dem Substitutionsgrad zu trennen. Durch Kopplung der Flüssigkeitschromatographie mit der Infrarotspektroskopie konnte gezeigt werden, dass mit der Gradientenmethode nicht nur Proben, die sich in ihrer mittleren DS-Werten deutlich unterscheiden, getrennt werden können, sondern dass auch innerhalb einer einzigen Probe eine Trennung nach Substitutionsgrad erfolgt. Die erarbeitete Gradientenmethode ermöglicht somit zum ersten Mal, um die experimentelle Bestimmung der Heterogenität der ersten Ordnung von intakten CAs, unabhängig von Substitutionsgrad.

6. Nachdem Trennmethoden nach Substitutionsgrad und Molmasse erarbeitet waren, konnten die Korrelationen zwischen Substitutionsgrad und Molmasse untersucht werden. Um dies zu tun, werden zweidimensionale Trennungen durchgeführt. Zuerst wurde eine chromatographische Trennung nach Substitutionsgrad unter Verwendung der neu entwickelten Gradienetenmethode durchgeführt. Die so erhaltenen Fraktionen, von denen angenommen wurde, dass sie bezüglich der Zusammensetzung homogen sind, wurden anschließend durch SEC getrennt. Diese neu entwickelte 2D-LC-Methode erlaubte neue Einblicke in die Heterogenität von CAs.

2. Introduction

2.1. Cellulose and cellulose derivatives

The increasing price and rapid depletion of crude oil as source for synthetic and petrochemical-based polymers, as well as the environmental conservation issues are the main driving forces towards "green" polymers based on sustainable natural resources. Cellulose, one of the world's most abundant natural biopolymers, is renewable and biodegradable and thus it has shown its great economically and environmentally significances in this direction. The annual natural production of cellulose amounts to $10^{11} – 10^{12}$ tons [1].

Cellulose is a polydisperse homopolymer consisting of D-anhydroglucose units (AGU) linked successively through β-1,4-glycosidic bonds. As seen in figure 1 every second AGU ring is rotated by 180° resulting in a linear arrangement and the AGUs at both ends of the formed chain possess one reducing and one non-reducing hydroxyl function at C_1 and C_4, respectively.

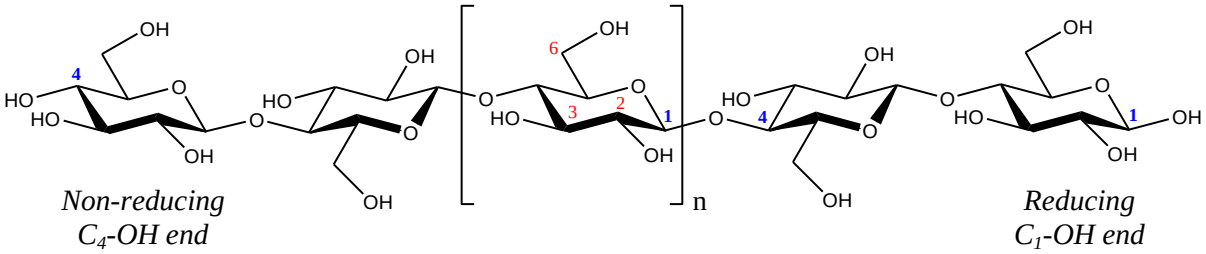

Figure 1: Molecular structure of cellulose with assignments of reaction sites in the AGU monomer: O-2, O-3 and O-6.

The degree of polymerization (DP, defined as the average number of AGUs per chain) of a cellulose sample varies between 100 and 15000 [2] and depends on the cellulose source as well as the method used for isolation. The commercial sources of cellulose include cotton linters and wood pulp. Cellulose is also produced by some microbes and animals. Pure cellulose is mainly used for paper production and, to a minor extent, in textile production. However, the two fundamental challenges in working with cellulose are its poor solubility in common solvents and non-thermoplastic behaviour (not melt-processable). These properties are attributed to the extensive intramolecular hydrogen bonding between two neighbouring AGUs

(i.e. C_2-OH with C_6-OH and C_3-OH with endocyclic oxygen) and the intermolecular hydrogen bonding between C_3-OH and C_6-OH which result in highly crystalline regions within the cellulose. These difficulties can be overcome through cellulose derivatization. The derivatization of cellulose yields products with new useful properties, thereby extending the application range of cellulose. Due to the high DP, the OH end groups of the cellulose chains are usually neglected and only the three free OH groups located in positions O-2, O-3, and O-6 of the AGUs are considered as the main reaction sites (see figure 1). The extent of the chemical modification can be described by the degree of substitution (DS), which refers to the average number of substituted OH groups per monomer unit:

$$DS = \frac{Number\ of\ substituted\ OH\ groups}{Number\ of\ AGUs} \qquad \textbf{Equation 1}$$

Therefore, DS can take values between 0 and 3 for unbranched cellulose derivatives. For example, in a cellulose acetate with a DS of 1.5, half of the OH groups are acetylated while the other half remains unsubstituted, resulting in an average of 1.5 acetyl moieties per AGU. The substituents in cellulose derivatives can be of one single type such as in cellulose acetate (CA) or a combination of different types such as in cellulose acetopropionate (CAP), which contains acetate and propionate substituents. Sometimes there is the possibility of side chain propagations by substituents having free OH groups of their own, like in hydroxypropyl cellulose (HPC). In these cases, the extent of the derivatization is characterized in addition to DS by the molar substitution (MS) which can be defined as the average number of moles of substituents per monomer unit:

$$MS = \frac{Number\ of\ moles\ of\ substituent}{Number\ of\ AGUs} \qquad \textbf{Equation 2}$$

Therefore, the MS value can exceed 3. Due to the statistics inherent in any polymer analogous reaction DS and MS values given usually represent average values.

Among the most important cellulose derivatives commercially produced today are organic and inorganic cellulose esters. The principle routes of their syntheses comprise carboxylation, nitration, sulfation or phosphorylation of cellulose. Furthermore, mixed cellulose esters containing acetate and any of propionate, butyrate or phthalate are also commercially produced by carboxylation reaction [3]. The unique chemical and physical properties of these cellulose esters such as solubility, adhesion strength, non-toxicity, viscoelasticity,

transparency, ability to control drug release from hydrophilic tablets etc. play vital roles in a large number of applications including coatings, cosmetics, films, fibres, membranes, flame retardancies, packagings and pharmaceuticals just to name a few [3-11]. The suitability for a given application is primary determined by the type of the substituents and the average DS and/or average MS. Cellulose derivatives as synthetic polymers consist of a mixture of molecules differing in chain lengths. Thus, the molar mass and molar mass distribution have to be considered. Many studies have related the physical properties of cellulose derivatives to the molar mass and molar mass distribution [12]. However, often cellulose derivatives obtained from the same source having the same chemical composition and molar mass vary significantly in performance if applied in a particular application. Thus, the influence of the chemical heterogeneity (substituent distribution) and its correlation with molar mass on the properties have to be taken into account additionally. For instance, Fischer et al. investigated the influence of the substituent distribution along the chains of CA on particle size and shape of cellulose microsphere beads. For this purpose they applied size exclusion chromatography with multi-angle laser light scattering, refractive index and ultraviolet (SEC/MALLS/RI/UV) detection [13]. They concluded that CAs similar in average DS and molar mass distribution but with non-uniform distribution of the substituents can form larger and hollow-shaped particles which subsequently influence their applications as drug delivery systems and in extracorporeal blood purification systems.

Thus, a fundamental understanding of the influence of the structure of cellulose derivatives on application properties, and hence performances requires a comprehensive characterization of the samples in terms of molar mass, DS and chemical heterogeneity. The latter has to be considered on various structural levels. The chemical heterogeneity results from the distribution of substituents within the individual AGUs, i.e. the substitution of the three chemically different hydroxyl functions of the AGUs, as well as the polymer chains.

Depending on the number of different substituents (A) introduced, the number of differently substituted AGU structures increases as A^3 (where A = number of different substituents including unsubstituted H). For instance, for one substituent such as in CA eight different substitution monomers (unsubstituted, 2-acetyl, 3-acetyl, 6-acetyl, 2,3-diacetyl, 2,6-diacetyl, 3,6-diacetyl and 2,3,6-triacetyl AGU monomers) exist as illustrated in figure 2a. The distribution of substituents within the AGUs is caused by the different reactivities of OH groups of the AGU.

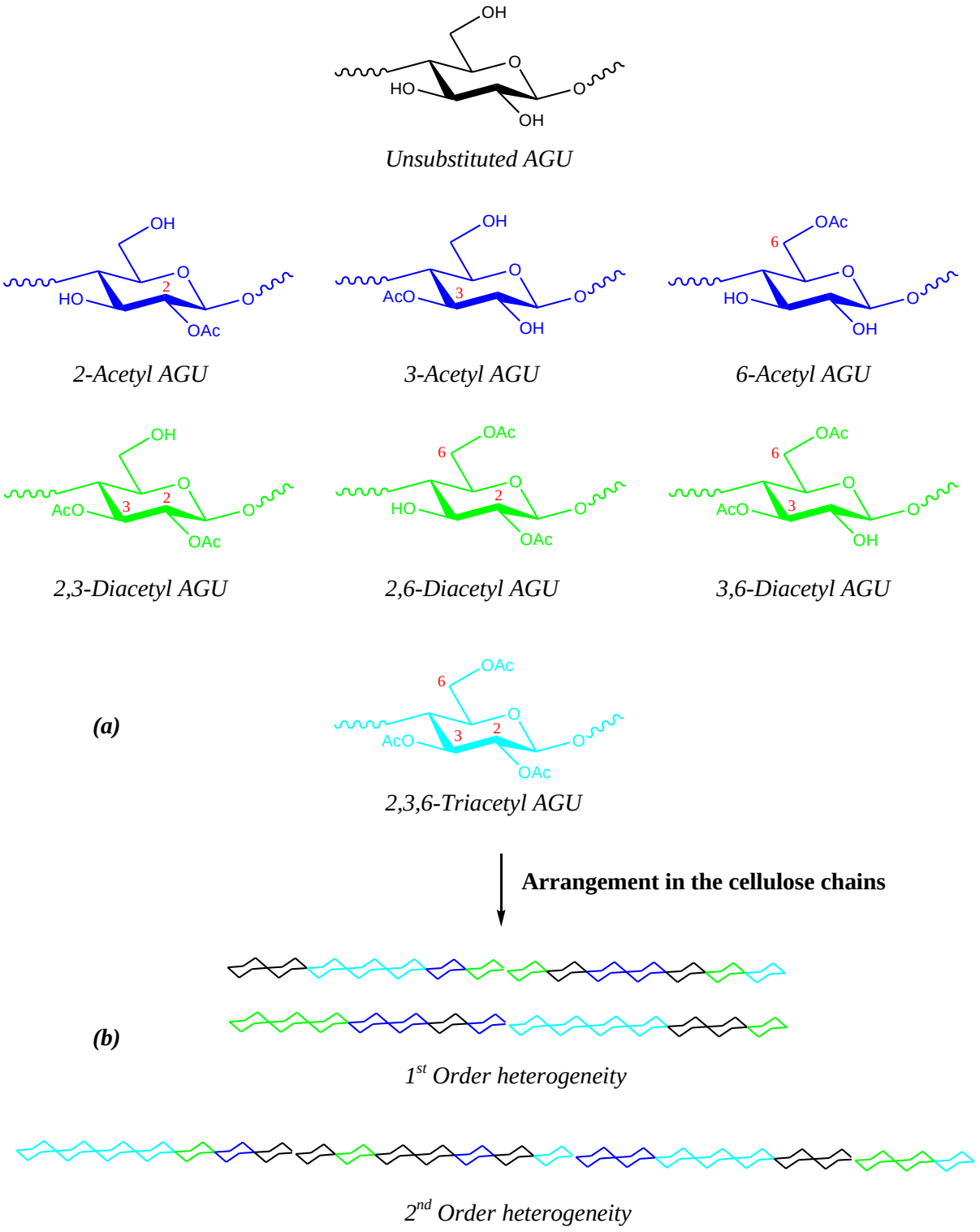

Figure 2: The eight possible substitution patterns of the acetylated cellulose (**a**) and their distributions among (heterogeneity of 1st order) and along (heterogeneity of 2nd order) the cellulose chains (**b**).

The relation between water solubility and the substituent distribution on the monomer units has been investigated for CAs of low DSs prepared under different homogeneous conditions.

Soluble products could be obtained only when there were little differences in the partial DS among O-2, O-3, and O-6 positions. Contrary to that, higher acetylated O-6 position relative to O-2 and O-3 resulted in insoluble products [14].

If cellulose chains are equally accessible to the reagent attack during the substitution reaction, i.e. under homogeneous conditions, the resulting un-, mono-, di-, and trisubstituted monomer residues are expected to be arranged in a more or less statistical manner among the chains. In contrast, derivatizations under heterogeneous conditions lead to deviations from the statistical distribution of the corresponding monomers. However, to date, cellulose derivatization on the industrial scale is carried out as heterogeneous process. This means that the pretreatments and solvent systems used for the activation of cellulose prior to functionalization are not sufficient to completely dissolve the cellulose molecules. The OH groups in the solubilized amorphous areas are more readily available for the reaction than those in the highly ordered and less reactive crystalline areas. As a consequence, the substituents introduced will be distributed in an irregular pattern.

For instance, two CA samples with average DSs around 2.5 and 2.6 were synthesized by Heinrich et al. under different conditions [15]. Cellulose triacetate (CTA) was heterogeneously synthesized by direct acetylation of cellulose with acetic anhydride/H_2SO_4 followed by subsequent hydrolysis to DS 2.5, while CA DS 2.6 was homogeneously prepared by direct acetylation of cellulose under alkaline conditions. The heterogeneous distribution of the acetyl groups in the first case is due to the incomplete activation of cellulose under acidic conditions. The activation of cellulose in alkaline medium results in a better accessibility of OH groups to the reagent and therefore a more regular substituent distribution.

Due to the different accessibility of the reagents to the amorphous and crystalline regions, the ratio of both parts, i.e. the so-called degree of crystallinity, has a major impact on the chemical functionalization of cellulose. The different accessibility gives rise to differences in substituent distribution on the polymer level. The chemical heterogeneity can be classified as the distribution of the substituents among the polymer chains (heterogeneity of 1^{st} order) and along the polymer chains (heterogeneity of 2^{nd} order). Figure 2b shows the 1^{st} order and the 2^{nd} order chemical heterogeneity of CA.

From the above it is obvious that the characterization of chemical heterogeneities on both the monomer and the polymer levels as well as the characterization of the molar mass and molar mass distributions are crucial steps for a thorough understanding of the structure-property relationship of cellulose derivatives with regard to their application performances. Therefore, to provide information on all aspects of molecular heterogeneities of cellulose derivatives, a

combination of different analytical techniques has to be used. Each technique has its own advantage and disadvantage. Preferably the technique employed should be sensitive, quantitative and fast. Therefore, recent research in cellulose chemistry is particularly directed to the improvement of existing and the development of new analytical methods to characterize the different distributions.

2.2. Current state of cellulose derivative characterization

Cellulose acetate (CA) is a general term that refers to celluloses being substituted by acetyl groups. Cellulose diacetate (CDA) refers to cellulose acetates having an average DS in the range DS = 1.8 – 2.5, whereas cellulose triacetate (CTA) is used for cellulose acetates of DS higher than 2.7 [3]. CA, as one of the most intensively studied cellulose derivative, was first synthesized by Schützenberger in 1865 by reacting cellulose with acetic anhydride at 180 °C in a sealed glass tube [16]. Addition of a catalyst to the system allowed lowering the temperature, thus avoiding excessive degradation. A number of acetylation catalysts have been identified; however, the most predominant catalyst used up to now is sulfuric acid.

Presently, the majority of CA produced commercially - either continuously or batch-wise - is synthesized by the acetic acid process [6, 17, 18]. In this process, cellulose is mixed with a solution of acetic acid and the sulfuric acid as catalyst. An excess of acetic anhydride (or rarely, acetyl chloride) is then added to form CTA followed by subsequent hydrolysis where several acetyl groups are cleaved to achieve acetone-soluble CDA. The reaction scheme is illustrated in figure 3.

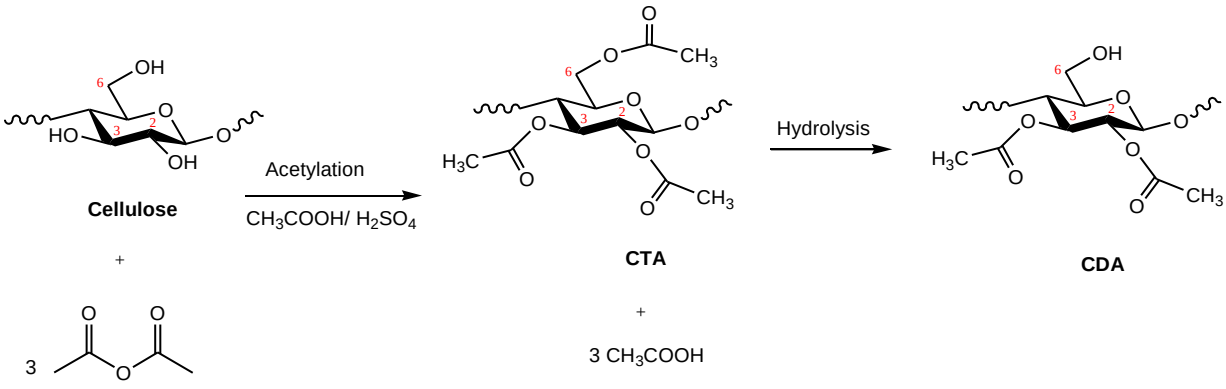

Figure 3: Scheme of the acetic acid process.

To ensure a fast and more uniform acetylation reaction with a high degree of conversion, several pretreatment procedures for the cellulose have been elaborated. The pretreatment should interrupt the hydrogen bonds and thus provide a uniform accessibility of the OH groups to the acetylating reagents. The most convenient procedure used for the activation of cellulose is the swelling of the sample in water, aqueous alkalines or other solvents. In addition, the cellulose raw material must be pure to obtain high quality products and the catalyst concentration and reaction temperature have to be controlled to minimize degradation, especially when a high molar mass product is desired [17, 19, 20]. Even if these requirements are met, a complete acetylated product cannot be obtained because the sulfuric acid itself can react to some extent with the hydroxyl groups of the cellulose [21-23].

Similar kinds of reaction processes are carried out when preparing mixed cellulose esters by esterification with acetic acid and butyric acid or propionic acid [6].

Another industrial process employed in the past was the methylene chloride (or dichloromethane, DCM) process. In this process, perchloric acid was used as catalyst for the esterification reaction. Contrary to sulfuric acid, the perchloric acid did not yield perchloric acid esters with cellulose allowing to reach virtually completely acetylated cellulose (i.e. CTA) [6, 24]. In the methylene chloride process the fibrous structure of cellulose could be maintained throughout the reaction and methylene chloride was a better solvent than acetic acid for CTA. However, this process was closed down because of the high costs. Additionally, perchloric acid is corrosive and its salts are explosive.

A number of solvents and solvent systems have been established to effectively dissolve the supramolecular structure of cellulose and thus allow performing the derivatization reaction under homogeneous conditions [25, 26]. Examples for such solvents are N,N-dimethyl acetamide/

lithium chloride (DMAc/LiCl) [27, 28], dimethyl sulfoxide/tetrabutylammonium fluoride (DMSO/TBAF) [29, 30] or ionic liquids [31, 32].

The advantages of these systems are the dissolution of high DP celluloses, the direct synthesis of partially acetylated cellulose and the control of the distribution of acetyl substituents on the monomer units to design novel application materials [33, 34].

A common property of each of these homogeneous media for derivatizing cellulose is the fact that they are all hygroscopic; meaning that, they tend to absorb moisture which results in hydrolyzing part of the substituents and thus lowering the DS of the product. Moreover, the homogeneous reaction systems have yet been applied only in laboratory scale, where low concentrations of cellulose are used. None of them achieved industrial importance so far, due to economic reasons e.g. expensive solvent recovery.

Besides homogeneous partial acetylation of cellulose, it is possible to produce CAs of low DS by partial hydrolysis of a highly acetylated CA. The hydrolysis of CAs of high DS can be performed by acidic or alkaline catalysis. In industrial hydrolysis of CTA sulfuric acid is used as catalyst [17]. In fact, this acidic hydrolysis is the second step of the acetic acid process to produce CDA. After the acetylation reaction has been completed, the acidic hydrolysis is initiated by the addition of water. The concentrations of water and catalyst are usually adjusted to control the rate of hydrolysis of the ester groups. The higher water content leads to an increase in the primary OH groups, indicating that O-6 acetyl group is hydrolyzed faster than O-2 and O-3 acetyl groups (hydrolysis rate: O-6 > O-2 and O-3) [35]. When a desired DS is reached, the catalyst is neutralized by the addition of an acetate salt.

However, one of the disadvantages of acidic catalysis of CA is the susceptibility of the glycosidic bonds resulting in hydrolytic chain length degradation [36]. Alkaline hydrolysis conditions do not favour chain degradation, offer short reaction times and are simply to perform [36-39]. In alkaline hydrolysis of CAs the order of deacetylation is O-2 and O-3 > O-6 [35].

As a consequence of the polymer analogous reactions, it is not feasible to obtain chemically uniform products (i.e. control the substituent distribution on the polymer level). The chemical heterogeneity might vary among different samples having the same chemical composition. It may lead, for instance, to serious solubility problems in solvents that are used, if the substituents are not uniformly distributed among the polymer chains and/or within a chain itself. To understand the interaction between structure and resulting properties of such complex copolymers suitable characterization tools are required. Investigations of cellulose derivatives are conducted in different fields in order to determine the chemical structure

(molar mass, molar mass distribution, chemical composition, chemical composition distribution on various architectural levels…) and the properties (solubility, crystallinity, gelation, film formation…) for potential applications.

Today cellulose derivatives are mainly characterized in terms of molar mass and molar mass distribution, average DS and the distribution of the substituents on both monomer and oligomer levels. Size exclusion chromatography (SEC) provides a convenient way for the characterization of molar masses and molar mass distributions of cellulose and cellulose derivatives [40].

The average DS can be determined by elemental analysis, functional group analysis, titration, NMR or other methods [41-43] depending on the nature of the substituent. The great advantage of NMR over the other methods is the straightforward measurement of average DS without the need of depolymerization or further sample preparation steps. NMR techniques are also applied to intact cellulose derivative chains providing a first insight in the partial DS in positions of O-2, O-3, and O-6 [44-51]. However, the low solubility and high viscosity of samples like cellulose ethers are drawbacks since highly viscous solutions of low concentration samples result in a low signal-to-noise- (S/N-) ratio. To overcome the resolution and sensitivity limitations of the NMR, complete or partial degradation (methanolysis, acid hydrolysis, or mild reductive cleavage) or enzymatic cleavage of the polymer chains is often utilized. The degradation of the sample results in a mixture of monomers and/or oligomers present in different molar ratios. The resulting products are separated and characterized subsequently in detail. Besides by NMR techniques [52-57], the hydrolyzed products were further investigated by other techniques such as size exclusion chromatography with differential refractometer (SEC-RI) or with multi-angle light scattering detection (SEC-MALS) [56, 58], anion-exchange chromatography with pulsed amperometric detection (AEC-PAD) [59], gas-liquid chromatography with flame ionization detection (GLC-FID) [46, 49, 58, 60], electrospray ionization-mass spectrometry (ESI-MS) [60] and matrix-assisted laser desorption/ionization - time of flight - mass spectrometry (MALDI-TOF-MS) [61] to provide information on the monomer composition.

Concerning the distribution of substituents on the oligomer levels, the resulting hydrolyzed products were quantitatively analyzed by various analytical techniques like SEC [62, 63], AEC [59, 61-65], GLC [64, 66] and MS [60, 64-71] and compared with the product distribution expected for a random substituent distribution at a certain DP. This procedure yields the distribution of the differently substituted AGUs along the polymer chain (heterogeneity of 2nd order).

Acidic hydrolysis can attack any glycosidic linkages irrespective of whether the neighbouring AGUs are substituted or not, while enzymes have less accessibility to the glycosidic linkages adjacent to modified AGUs. Therefore, if substituents of a cellulose derivative are randomly distributed along the chains, no or very few un- and/or low substituted AGUs should result from selective enzymatic hydrolysis. Thus, a direct comparison of chemical heterogeneity between two samples of the same average DS can be made based on the amount of AGUs released from enzymatic hydrolysis. The higher the amount of AGUs liberated, the more the distribution differs from a random substituent distribution. Therefore, the selective enzymatic degradation can reveal information on the distribution of the substituents along the polymer chains (heterogeneity of 2nd order) based on the quantification of the hydrolyzed products. However, enzymatic degradation is not applicable for cellulose derivatives of high DSs. For example, regardless the enzyme family, CAs can only be degraded up to DS 2.3 [70], methyl celluloses (MC) to DS 2.1 [59, 72], carboxymethyl celluloses (CMC) to DS 1.6 [72] and cellulose sulfates to DS 1.5 [73].

In general, any or at least a large amount of information is lost on whether the different monomeric or oligomeric units result from the same or from different chains, if the sample is fully or partially degraded. Therefore, establishing methods to characterize the chemical heterogeneity of cellulose derivatives on the level of intact polymeric chains and especially for cellulose derivatives of high DSs are still a highly challenging task.

Gradient HPLC has been shown to be a powerful tool for separating (co)polymer molecules according to chemical composition [74, 75]. Such separations can be achieved under suitable chromatographic conditions. Different separation mechanisms such as adsorption-desorption which uses the differences in interaction energy between the polymer components and the stationary phase or precipitation-redissolution which uses differences in the solubilities of the different sample components are used [76-78]. These separation methods allow calculating the chemical composition distribution (CCD) of the copolymers. Nevertheless, knowledge on the separation of cellulose derivatives with respect to chemical composition (DS) is still very limited and attempts to perform separations of such polymers according to chemical heterogeneity are scarcely found in literature.

Without suitable separations, the heterogeneities of the different types cannot be differentiated. The efforts on separation and characterization of cellulose derivatives reported in literature are briefly discussed here:

SEC with MALLS/RI/UV detections has been used to gain insight on the substitution distribution along the chains of cellulose xanthate (CX), CMC and CA [13, 79]. The procedure

requires the presence of UV-active groups that can be detected by a UV-detector in relation to the molar mass distribution (MMD) determined by MALLS/RI. It was found that each fraction different in molar mass can have a different DS with the low molar mass fractions being higher substituted than the high molar mass fractions for both CX and CMC, while the opposite case was observed for CA. However, the DS gradient over the MMD curve does not represent a real separation in terms of DS, because SEC separation is based on size, not on chemical composition. Furthermore, since the derivatives like CMCs or CAs do not contain UV-active groups, they have to be modified to the respective amide derivatives. Thus, the modification procedures have to be quantitatively performed in order to achieve reliable results.

Fitzpatrick et al. investigated the dependence of DS on molecular size for fractions of intact and enzymatically hydrolyzed MC by SEC-MALLS/RI/NMR. The data were correlated with cloud-point measurements. The results revealed no significant dependence of the DS on the molecular size for the fractions of the intact sample and nearly the same clouding curves for the fractions of different size were obtained. However, significant differences in the clouding behaviour of the fractions from the enzymatic degradation, the DS of which decreased with decreasing the size, were observed. Thus, the changes in clouding behaviour was explained by differences in the DS and DS-distribution [80].

Another technique applied in the characterization of cellulose derivatives is capillary electrophoresis (CE) connected with fluorescence, UV or MS as detection and identification methods [81, 82]. Oudhoff et al. reported on the separation of CMC according to DS by CE-UV, allowing determination of the DS-distribution. They found that the electrophoretic mobility as a function of DS was linear till DS = 1 and became non-linear at high DS. This small linear range is not sufficient to provide reliable calculation of the DS-distribution. The separation is also not purely DS dependent as an effect of size was observed additionally. Furthermore, it is very difficult by CE to collect fractions large enough for subsequent (spectroscopic) characterization [82].

Other techniques used in the separation and analysis of cellulose derivatives are solvent fractionation, precipitation fractionation and thin layer chromatography (TLC). Stepwise solvent fractionation involves extracting a solid polymer with successively stronger solvents or solvent mixtures. The solvents or solvent mixtures are chosen such that they dissolve a fraction of the polymer within a selective DS-range. Increasing the polarity of the solvent mixture allows extracting fractions of decreasing DS. Therefore, this technique can provide information on heterogeneity of 1st order [83, 84]. Application of this method to CA is however

very limited. Fractionated precipitation involves dissolving a solid polymer in a good solvent and then precipitating the desired fractions stepwise by decreasing the solubility as a result of adding controlled volumes of a poor solvent [85]. This method was extensively used to fractionate CA using acetone or chloroform as the solvent and water, ethanol or n-hexane as the non-solvent. In most cases, the isolated fractions varied in DP but were of the same DS [86-90]. Despite the intensive studies on solvent and precipitation fractionations, these methods are laborious, require large amounts of solvents and samples, are not very selective and difficult to automate.

Kamide et al. evaluated the use of TLC for the separation of CAs and cellulose nitrates according to DS and molar mass [91-93]. By changing stepwise the eluent composition, they were able to identify experimental conditions where clear dependences of retardation factor (R_f) on either DS or molar mass were observed. R_f is defined as the ratio of the distance travelled by a substance to the distance travelled by the solvent front. The resulting separations according to DS and molar mass were found to be independent of molar mass and DS, respectively. The methods allowed calculating both DS-distributions and MMDs. However, TLC is difficult to quantify and has a poor reproducibility.

Very recently Greiderer et al. reported on the two-dimensional reversed-phase liquid chromatography-size exclusion chromatography (2D RPLC-SEC) separation to characterize hydroxypropyl methylcelluloses (HPMC) [94]. A reversed-phase gradient system and an aqueous SEC system were used in the first and second dimension, respectively. A large impact of column temperature on the retentions in both dimensions was observed. This was attributed to the occurrence of thermal gelation phenomena within the columns, requiring performing the experiments at a low well-controlled temperature. At this temperature, a separation according to molar hydroxylpropyl substitution was established in the first dimension, the retention time increased with increasing the molar substitution, while a separation according to molar mass in the second dimension was obtained. The separation method provided information about molar mass and chemical heterogeneities of the samples and their correlations.

2.3. Motivation

Regarding the application of adsorption liquid chromatography to CA, two chromatographic separation systems for different DS-ranges were mentioned in literature. Both systems

followed reversed-phase liquid chromatography under different conditions. The first system reported by Floyd et al. allowed for the separation of cellulose diacetate (CDA) in the range of DS = 2.3 – 2.7 [95]. The reversed-phase separation was carried out on Hamilton PRP-1 (polystyrene-divinyl benzene based column) in a linear gradient from acetone/water/MeOH (4:3:1) to acetone in 15 min at a flow rate of 0.8 mL/min. The samples eluted in the order of increasing average DS. The second system reported by Asai et al. was applied for the separation of cellulose triacetate (CTA) in the range of DS = 2.7 – 2.9 [96]. The separation was performed on a Waters Novapak-phenyl column in a gradient from chloroform-MeOH (9/1) : MeOH-water (8/1) [2:8] to 100% in 28 min at a flow rate of 0.7 mL/min.

Both systems allowed calculating DS-distributions from a linear correlation between DS and retention volume. However, the applicability of both methods is confined to the DS-ranges investigated.

Therefore, it was the task of the present work to develop a single phase system capable of running all CAs irrespective of DS or applicable over a wide DS-range. Such a system should allow calculating the 1st order degree of heterogeneity of intact CAs irrespective of DS.

The second experimental task of the present work was the development of an SEC method for characterization of molar mass and molar mass distribution of the CAs. Since the DS alters the polarity, solubility and aggregation behaviour of CAs, the SEC methods found in literature are usually applicable only within narrow DS-ranges. However, as already stated CAs are heterogeneous in both molar mass and chemical composition. Thus, SEC methods useful for larger DS-ranges are required, in order to allow molar mass characterization of samples heterogeneous in DS. In addition, such methods should allow running samples of different DS using the same chromatographic conditions instead of adjusting the phase system to the DS of the sample under investigation.

Having established separations by DS and by molar mass, the correlations between DS and molar mass shall be investigated. In order to do so, two-dimensional separations will be performed. First, a chromatographic separation according to DS is carried out using the separation method developed before. The fractions, which are assumed to be homogeneous in composition, were subsequently separated by SEC. Therefore, this PhD thesis focused on the suitability of liquid chromatography for the comprehensive characterization of CAs.

3. Theoretical Perspectives

The analysis of molecular heterogeneity of CAs was the main focus in this research. As previously mentioned, these derivatized products of cellulose are commercially produced from a heterogeneous two-step process of acetylation and deacetylation, where the reaction conditions cannot be easily controlled. This results in inhomogeneous products and their characterizations are a very challenging work. It should be mentioned that the inhomogeneities are inherent in any polymer analogous reaction due to statistical nature of the substitution reaction. CAs are heterogeneous with respect to several features i.e. molar mass as well as DS on both AGUs and cellulose chains. Therefore, it is foreseeable that a combination of several methods will be required to comprehensively describe the products. In general, the chemical structures present in a polymer sample can be characterized through two primary steps:

1. Application of chromatographic separation techniques to fractionate the polymer samples into more homogeneous fractions,
2. Characterization of each fraction by spectroscopic or spectrometric techniques in order to get precise chemical information on the fraction. As a result, a distribution profile of the characterized feature can be obtained.

Frequently, it is desirable to hyphenate different techniques by coupling a chromatographic separation technique either with a spectroscopic method or another chromatographic separation technique. In the latter case, the correlation between two molecular features of the polymer sample (for example: chemical composition and molar mass distributions) may be analyzed [97]. When a chromatographic separation is coupled with a spectroscopic or spectrometric method, both qualitative and quantitative information on the chemical composition of the polymer fractions can be obtained [98, 99]. Thus, hyphenation of a separation step with a spectroscopic or spectrometric method provides information on the chemical composition distribution of the polymer sample in comparison to the average chemical composition which is obtained by using the spectroscopic technique alone. Since this PhD thesis focussed on the development of methods to characterize the molecular heterogeneity of CAs, the following section is divided into two chapters. The first chapter gives an overview on the modes and principles of liquid chromatographic techniques available particularly for the analysis of natural and synthetic polymers. In the second chapter, a description of the hyphenation of a liquid chromatographic technique online and/or off-line either with another

chromatographic technique or a chemical selective or molar mass sensitive method, their principles and the provision of the potential information, will be addressed.

We assume that cellulose derivatives behave identical to other types of copolymers, despite the higher number of monomers (differently substituted AGUs) present.

3.1. High performance liquid chromatography (HPLC) of polymers

High performance liquid chromatography (HPLC) is an effective separation method for characterizing distributions in polymer systems. The separation can be achieved when the polymer components spend different times on their way through a chromatographic column. The different retention times of the components are caused by differences in the adsorption or partition equilibrium between the stationary phase and the mobile phase. This distribution is described by the distribution (or partition) coefficient, K_d [100]:

$$K_d = \frac{c_{SP}}{c_{MP}} \qquad \textbf{Equation 3}$$

where c_{SP} and c_{MS} are the concentrations of the analyte in the stationary phase and mobile phase, respectively. The distribution coefficient is related, thermodynamically, to the Gibbs free energy difference, ΔG, of the analytes in both the stationary and the mobile phases [74, 75]. This difference in free energy comprises enthalpic and entropic contributions. The dependence of K_d on these contributions can be written as follows:

$$\Delta G = \Delta H - T\Delta S = -RT \ln K_d \qquad \textbf{Equation 4}$$

After rearrangement:

$$\ln K_d = \frac{-\Delta G}{RT} = \frac{-\Delta H + T\Delta S}{RT} \qquad \textbf{Equation 5}$$

where R is the universal gas constant, T the absolute temperature, ΔH and ΔS are the changes in interaction enthalpy and conformational entropy, respectively. ΔH is caused by attractive or repulsive interactions of the polymer molecules with both the stationary and the mobile

phases while the ΔS arises from the fact that these macromolecules have different sizes which can present different accessibility to the pore volume of the stationary phase.

The relation between K_d and retention volume of sample molecules in a defined chromatographic system can be given in the following equation:

$$V_R = V_I + K_d V_P \qquad \textbf{Equation 6}$$

where V_R is the retention volume (or elution volume, V_e) of the analyte, V_I the interstitial volume of the stationary phase and V_P the entire pore volume of the stationary phase. The sum of V_P and V_I is defined by the void (hold-up) volume of the chromatographic system, V_0, ($V_0 = V_P + V_I$) [101]. V_0, corresponding to the volume occupied by the mobile phase between the injector and the detector and can be estimated by injecting a low molar mass sample. It is possible to determine K_d experimentally from the equation 6.

The retention volume can also be expressed in time scale instead of volume, since retention time (t_R) and the retention volume (V_R) are related by the flow rate of the mobile phase (F) as follows:

$$t_R = \frac{V_R}{F} \qquad \textbf{Equation 7}$$

The retention volume is however more practical to be used instead of retention time because it allows direct comparing the chromatographic results for the same system at different flow rates.

Depending on the choice of the stationary and mobile phases as well as the column temperature, three modes of liquid chromatography for polymer separations i.e. size exclusion chromatography (SEC), liquid adsorption chromatography (LAC) and liquid chromatography at critical conditions (LC-CC) can be distinguished. These modes differ in their dependences of elution volume on molar mass.

In the following parts, the principles of the chromatographic modes with their potential for polymer analysis will be discussed.

3.1.1. Size exclusion chromatography (SEC)

In size exclusion chromatography (SEC), the macromolecules are not enthalpically interacting with the stationary phase and thus are separated according to their size in solution (hydrodynamic volume, V_h). The stationary phase is packed with a porous material, mostly silica or semirigid (highly crosslinked) organic gels, with a certain pore size distribution. The mobile phase should be a good eluent for the polymer in order to avoid non-exclusion effects e.g. interactions between the stationary phase and the macromolecules [102].

SEC is a ΔS-controlled separation mode of liquid chromatography. When a macromolecule enters a pore from the free mobile phase, this causes a loss of conformational entropy due to its steric hindrance. The bigger the macromolecule, the larger is the loss in the entropy. In addition, certain conformations of the macromolecules simply do not fit into the pore [103]. Thus, macromolecules with the largest volume in solution are eluted first followed by the smaller ones.

In ideal case of SEC, where no enthalpic interaction (i.e. $\Delta H = 0$) exists between the stationary phase and the macromolecules, separation takes place exclusively due to the hydrodynamic size of the macromolecules. Therefore, the rewritten K_d from equation 5 is given by:

$$K_d = K_{SEC} = e^{\frac{\Delta S}{R}} \qquad \textbf{Equation 8}$$

Since $\Delta S < 0$, K_{SEC} ranges from 0 to 1, with $K_{SEC} = 0$ for macromolecules larger than the largest pore (exclusion limit) and $K_{SEC} = 1$ for small macromolecules, which have access to the entire pore volume (separation limit). Those macromolecules with sizes between both limits will be separated according to decreasing size. Thus, according to equation 6 the retention volume will be smaller than the dead volume of the system ($V_R < V_0$ or $V_P + V_I$). In other words, the macromolecules will be eluted before the solvent peak. The size of a linear macromolecule increases with its molar mass. Thus, larger macromolecules will be stronger excluded from the pores of the column than smaller ones, resulting in an increase of the K_d and therefore in an increase of retention volume with decreasing molar mass (see figure 4 for SEC).

After a suitable calibration, the molar mass distribution, the molar mass averages and the dispersity with respect to molar mass of a polymer sample can be determined. However, if the calibrants are not chemically identical to the sample, the obtained molar mass distribution, the

molar mass averages and the dispersity of the sample will only be relative with respect to the calibrant used. If a molar mass sensitive detector e.g. multi-angle laser light scattering (MALLS) is added, absolute molar masses and molar mass distribution of the sample can be obtained. The principle of MALLS will be given in 3.2.2.2.

Two molar mass averages which are usually determined from the molar mass distribution of a polymer are the number average molar mass (M_n) and the weight average molar mass (M_w). The definitions of both M_n and M_w are given bellow:

$$M_n = \frac{\sum_{i=1}^{\infty} N_i M_i}{\sum_{i=1}^{\infty} N_i}$$ **Equation 9**

$$M_w = \frac{\sum_{i=1}^{\infty} N_i M_i^2}{\sum_{i=1}^{\infty} N_i M_i}$$ **Equation 10**

where N_i is the number of chains with molar mass M_i of a polymer sample. The width of the distribution curve is expressed by the molar mass dispersity ($Đ_M$) which is defined as the ratio of M_w to M_n. Since M_w is always equal or larger than M_n, $Đ_M$ has a value ≥ 1. If a sample contains chains of nearly the same molar mass then its $Đ_M$ value is expected to be close to 1. The higher the $Đ_M$ the broader is the molar mass distribution.

3.1.2. Liquid adsorption chromatography (LAC)

In liquid adsorption chromatography (LAC), separation is usually achieved by differences in interaction strengths between the polymer molecules and the stationary phase. These interactions determine the elution volume of the analyte and can be controlled by the experimental conditions (i.e. mobile phase composition and/or temperature) [104]. In fact, LAC is classically employed in the separations of small molecules where ΔS does not play a significant role.

In ideal case of LAC, $\Delta S = 0$ because of the absence of exclusion effects due to the small molecular size. Thus, the separation mechanism is driven only by the enthalpic contribution

(ΔH) which describes the adsorptive interactions of the molecules with the functional groups of the stationary phase. K_d in ideal adsorption mode taken from equation 5 after rewriting is given by:

$$K_d = K_{LAC} = e^{\frac{-\Delta H}{RT}}$$ **Equation 11**

Since ΔH is negative for adsorptive interactions, the K_d values exceed unity. The higher the K_d of a molecule the stronger are the interactions. If this interaction is sufficiently strong, the molecule will be retained by the stationary phase and hence will be eluted later than the solvent peak. This means that according to equation 6 the retention volume will be larger than the dead volume of the system ($V_R > V_0$ or $V_P + V_I$).

LAC is also progressively used in the separation of polymers. In this situation, the retention behaviour of macromolecules is different from that of small molecules (low molar mass). Since macromolecules are able to present large conformation variation, the entropic contributions, ΔS, can also exist. However, the effective enthalpic contributions, ΔH, remain the most predominant factor in the separation mechanism ($\Delta H >> T\Delta S$). Therefore, the overall K_d is larger than 1 [75].

For chemically homogeneous polymers, the number of repeating units increases with the molar mass. If one unit has the ability to adsorb on the stationary phase, theoretically all similar units of the chain show the same susceptibility for interaction. As a result, the K_d value increases dramatically, resulting in large retention volumes even if the adsorptive interaction of a single repeating unit with the stationary phase is very weak. This behaviour can be explained by a multiple attachment mechanism [105]. A macromolecule of a high number of adsorbing monomer units (i.e. high molar mass polymer) elutes later than a macromolecule containing less of these monomers (i.e. lower molar mass polymer). Hence, the opposite molar mass dependence of retention volume in LAC is observed as compared to SEC (see figure 4 for LAC). Even at conditions of very weak interaction, high molar mass polymer molecules may be irreversibly retained in the column. Consequently, in isocratic LAC, where the mobile phase composition remains the same throughout the experiment, the elution of a high molar mass disperse polymer sample in reasonable experimental time scales is only possible in a very small range of interaction strength.

Since already a very weak interaction of a repeating unit causes extremely high retention volumes for high molar mass polymers even a small change in the mobile phase composition

often results in a sudden transition from infinite retention to complete desorption (i.e. LAC to SEC). Therefore, the elution behaviour of polymers in LAC seems to occur by an on-off mechanism, unlike the elution of low molar mass substances. That is why LAC is mostly applied for the analysis and efficient separation of oligomers according to chemical composition [106, 107].

For high molar mass polymers, gradient LAC is a preferable alternative to isocratic LAC for separations by chemical composition. In gradient mode, the interaction strength can be systematically varied by changing the mobile phase composition during the chromatographic experiments. In this way, a complete elution within a reasonable time can be achieved [108]. It is also possible to apply a temperature gradient as has been shown by Chang et al. which results in high resolution separations [109, 110]. The principles of gradient chromatography will be given in 3.1.4.

3.1.3. Liquid chromatography at critical condition (LC-CC)

Liquid chromatography at critical conditions (LC-CC) (also called LC at critical point of adsorption) is a unique method for polymeric solutes at which the entropic size exclusion effect on elution volume is exactly compensated by the enthalpic interaction [75]. Therefore according to equation 5, K_d at LC-CC is given by:

$K_d = 1$ at LC-CC **Equation 12**

Under critical conditions, it is possible to elute homopolymers of a given chemical structure independent of molar mass at the same retention volume (see figure 4 for LC-CC). Therefore, homopolymers at critical condition are often referred to as being chromatographically "invisible" since the polymer molecules elute at the void volume of the chromatographic system being neither adsorbed on the stationary phase nor excluded from it ($V_R \approx V_0$ or $V_P + V_I$). Given a stationary phase with a defined pore size and configuration, the critical conditions for polymers can be obtained by choosing an appropriate composition of the mobile phase, usually a mixture of solvents [111, 112].

If a certain type of polymer has an additional part other than the chromatographically invisible repeating units, separations according to the other active parts of the polymer such as

functional end groups (also known as functionality type distribution (FTD)) in telechelic oligomers and polymers [113, 114], tacticity differences [115, 116] or separation of blends [117, 118] can be realized at critical condition. LC-CC is also useful for characterization of the block length distribution within a block copolymer. For example taking a block copolymer -A-B- the separation is completely controlled by the interactions of polymer -A- with the stationary phase at the critical condition for polymer -B- and vice versa [119-122].

Critical conditions have been established for a variety of polymers [123]. In spite of that, the application of the LC-CC is limited because the determination of the critical conditions of elution for a polymer is frequently a long and difficult experimental process. In addition, it is not easy to reproduce the critical condition since only a slight variation of the eluent composition can change the retention mode to either SEC or LAC. If this is the case, then flushing and re-equilibration of the column are highly necessary. Therefore, a simple, fast and effective approach to determine critical conditions for a given polymer will be a substantial advantage to improve the use of LC-CC.

3.1.4. Gradient LAC

Since a small decrease in eluent strength in isocratic LAC may cause irreversible adsorption of high molar mass polymer molecules even at conditions of very weak interactions, gradient chromatography is preferably used for separating polymers of very different adsorption strengths. In gradient liquid chromatography the eluent strength is systematically increased during the chromatographic run, such that the adsorptive interaction decreases and the polymer molecules elute within a reasonable time as a function of their affinity to the stationary phase. Furthermore, the chromatographic peaks become narrower and more symmetrical in comparison with isocratic elution [75].

The gradient elution mechanism can be clarified as follows: similar to isocratic LAC both enthalpic and entropic effects are operative in polymer gradient elution again with the more predominant contributions being the enthalpic ones (i.e. $\Delta H >> T\Delta S$). In the beginning of the gradient, the polymer molecules are strongly adsorbed in the weak initial eluent on the stationary phase (i.e. $K_d > 1$). Polymer molecules of high molar mass are more strongly adsorbed than those of lower molar mass since the number of interaction units is proportional to the molar mass. By increasing the eluent strength desorption occurs (i.e. the value of K_d decreases). The weakly adsorbed molecules (i.e. low molar mass molecules) are desorbing

first at eluent compositions well lower than the critical one. When these molecules become desorbed, they will start moving with a velocity lower than that of the eluent. The following stronger adsorbed molecules (i.e. higher molar mass molecules) require stronger eluents to desorb from the column. Since the eluent moves faster than the polymer, compositions of increasing eluent strength will overtake the polymer molecules, resulting in an acceleration of them. In this case, the eluent compositions required for elution of the molecules are approaching the critical eluent composition with increasing molar masses. The condition of the polymer velocity being equal to the eluent velocity corresponds to the critical conditions ($K_d = 1$). Under this condition especially at sufficiently high molar masses, a nearly molar mass independent retention volume is observed (see figure 4 for gradient LAC).

Apart from adsorption/desorption, another type of the gradient elution mechanism involved in chromatographic separation of polymers is the precipitation-redissolution mechanism. It is related to the solubility properties of the polymers in the solvent gradient. In this case, the polymer solution is injected into an initial eluent of low solvent strength. If this is a non-solvent for the polymer, precipitation may occur at the time of injection. By increasing the solvent strength during the chromatographic run the precipitated polymer molecules will redissolve at a certain solvent composition. The solvent composition at redissolution depends on the molar mass and the chemical composition of the polymer molecules. Thus, a gradient of varying solvent strength can result in a separation of the polymer molecules.

In general, the separation achieved by gradient elution chromatography depends on a number of factors, namely the applied eluent system (weak solvent or non-solvent), the column temperature, the type of column (polar or non-polar), the gradient profiles (shape and slope), and injection conditions (concentration, volume, and sample solvent) [74].

The role of the weak solvent/non-solvent systems is abovementioned. Both the adsorption-desorption and the precipitation-redissolution mechanisms are highly affected by the column temperature; therefore temperature control is one of the major requirements for reproducible and reliable polymer separations.

The choice of the column, whether polar or non-polar, is as important as that of the solvent systems. Thereby, there are two different modes of gradient liquid chromatography: normal-phase liquid chromatography (NPLC) and reversed-phase liquid chromatography (RPLC).

NPLC is carried out using a polar stationary phase and a combination of eluents increasing in polarity. The most common polar stationary phases used in NPLC are made of silica, either as packed spherical particles or monolithic column [124, 125]. The surface of these stationary phases

is covered with silanol groups, SiOH, which enhance polar interactions with analyte molecules resulting in a separation according to increasing polarity. Other kinds of polar stationary phases contain support-bonded amino (NH_2), cyano (CN), nitro (NO_2), or diol phases. Hydrophobic and/or non-polar molecules cannot adsorb on the surface of the stationary phase and remain mainly in the mobile phase. Therefore, they elute before more polar ones which adsorb on the column. Desorption can be achieved by changing the composition of the mobile phase using a more polar eluent in a gradient profile. The more polar eluent reduces the interaction strength between the macromolecules and the stationary phase, resulting in an elution order from lowest to higher polar macromolecules.

Aluminium, titanium, and zirconium oxides have been extensively studied as alternatives for silica substrates due to their much higher pH stability of approximately 0-13 [126, 127]. However, the high activity of the surfaces of these inorganic oxides has diminished the widespread use of these substrates.

In contrast to NPLC, the RPLC is applied using a non-polar stationary phase in combination with an eluent of decreasing polarity. The great majority of the stationary phases used in RPLC are silica substrates grafted with large non-polar aliphatic ligands such as octadecyl (C18). The polarity of the stationary phase can be tuned by carefully choosing the grafted ligand. Stationary phases with different grafted ligands are commercialized such as chemically bonding octyl (C8), butyl (C4), or phenylhexyl [128, 129]. Another group of RPLC stationary phases is based on synthetic polymers such as styrene-divinylbenzene, crosslinked polymethacrylates or polyvinylalcohol [130]. Despite their high pH stability, some drawbacks including limited pressure resistance, hindered mass transfer in pore structure and swelling/shrinking processes have prevented their widespread applications. In case of RPLC, the mobile phase gradient runs from a polar to a less polar solvent which leads to a separation according to decreasing polarity of the molecules. Therefore, the elution order is reversed as compared to NPLC. A typical example for both kinds of separations is the separation of styrene/ethylmethacrylate copolymer mixtures. It was demonstrated that these copolymers can be separated either by NPLC on a silica column, in which the sample of the lowest ethylmethacrylate content eluted first, while the RPLC separation on a C18 column resulted in early elution of the sample of the highest content of ethylmethacrylate [131].

Another factor influencing the separation in gradient liquid chromatography is gradient slope. A very steep gradient may compress the eluting peaks because of the fast increase in mobile phase elution strength and thus reduce resolution while a very shallow gradient may cause detection problems since the concentration of the analyte decreases.

In addition, the initial eluent strength or solubility needs to be low enough to retain the polymer molecules on the column. Therefore, optimization of several parameters is a prerequisite to yield a reliable gradient based separation method.

In gradient LAC, the mobile phase composition at the time of elution (Φ_e) can be determined by the following equation:

$$\Phi_e = \Phi_0 + G\,(V_R - V_0) \qquad \textbf{Equation 13}$$

where Φ_0 is the initial mobile phase composition, V_R the retention volume of the analyte and V_0 the void (hold-up) volume of the chromatographic system. G, the gradient slope, can be defined as the total change in the mobile phase composition ($\Delta\Phi$) divided by the product of flow rate (F) and gradient time (t_G): $G = \frac{\Delta\Phi}{F \times t_G}$. It should be noticed that the equation 13 assumes that there is no dwell volume (V_d, i.e. volume between mixing chamber and injector) in the chromatographic system. However, the gradient is started at the pump and not at the injector. Therefore, a more accurate value for the Φ_e is obtained when the gradient delay caused by the mixing chamber volume is taken into account. In this case, V_0 in the equation 13 has to be replaced by the total volume of solvent in the system (i.e. $V_T = V_0 + V_d$). Considering the above definitions, equation 13 can be rewritten as follows [132]:

$$\Phi_e = \Phi_0 + \frac{\Delta\Phi}{F \times t_G}(V_R - V_0 - V_d) \qquad \textbf{Equation 14}$$

Sometimes in gradient chromatography an optimum separation of a polymer sample with different chemical composition can only be achieved by multi-step or multi-linear gradients, which can be described by a series of isocratic and linear gradient steps.

All the isocratic modes of liquid chromatography (i.e. SEC, LAC, LC-CC) along with gradient LAC mentioned above can usually be summarized on the same diagram showing the chromatographic retention behaviour of polymer molecules as a function of the molar mass (see figure 4).

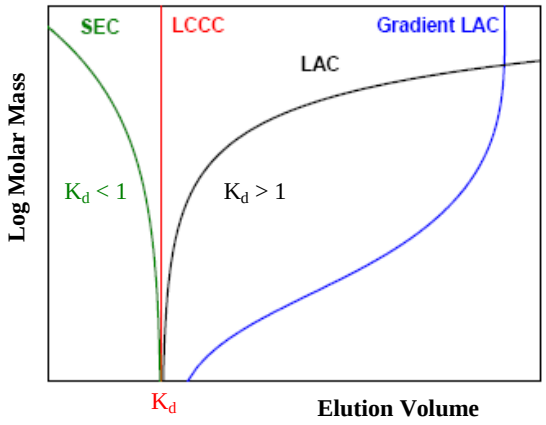

Figure 4: Schematic representation of the molar mass dependences of the elution volume in polymer liquid chromatography. SEC, LC-CC, and LAC modes operate under isocratic conditions of eluent whereas in gradient LAC, the eluent strength is changed (weak to strong) with time. (Figure taken from [133])

The polymeric components are separated in SEC mode when the changes in the conformational entropy control the distribution of the components between the stationary phase and the mobile phase ($K_d < 1$) and they elute before the solvent peak. If the enthalpic interactions of the polymeric components with the stationary phase dominate the distribution, the polymeric components are separated by the isocratic or gradient LAC ($K_d > 1$) and they elute after the solvent peak. The transition between SEC and LAC is observed under a unique critical condition at which the molar mass dependence of the polymer retention vanishes and the travelling velocity of the polymeric components is identical to the travelling solvent velocity. This is the point of enthalpy-entropy compensation ($K_d = 1$).

3.2. Hyphenated techniques in chromatography of polymers

3.2.1. Two-dimensional liquid chromatography (2D-LC)

All the chromatographic separation modes described can provide information only on one of the structural features of a complex polymer sample, either the chemical composition distribution or molar mass distribution. It is not possible to characterize several distributions simultaneously. By coupling two different liquid chromatographic separation methods, which is called two-dimensional liquid chromatography (2D-LC), it is however possible to increase

the informational content of an experiment. For example, when adsorption chromatography (LAC/LC-CC) is coupled with SEC, information on both chemical composition distribution and molar mass distribution of a polymer sample can be obtained [134]. The experimental implementation of the 2D-LC can be performed either off-line or online. A schematic illustration of the constructions of an online 2D chromatographic system (a) and an off-line one (b) are shown in figure 5.

The off-line systems require a fraction collection device to fractionate the polymer sample in the first dimension and then the collected fractions will manually be injected into the second dimension. In online 2D systems the transfer of fractions is preferentially done by an automatic eight port switching valve equipped with two storage loops. In this way, a fraction of the first dimension is collected into a first storage loop, while the contents of the second loop (i.e. a previous fraction) is injected and analyzed in the second dimension. As a result, an elugram for each fraction of the second dimension analysis can be obtained. The data of both dimensions can be combined in a contour plot wherein the first dimension is shown along the y-axis and the second dimension along the x-axis. The signal intensity is described by the z-axis and is displayed by a colour coding (see figure 5).

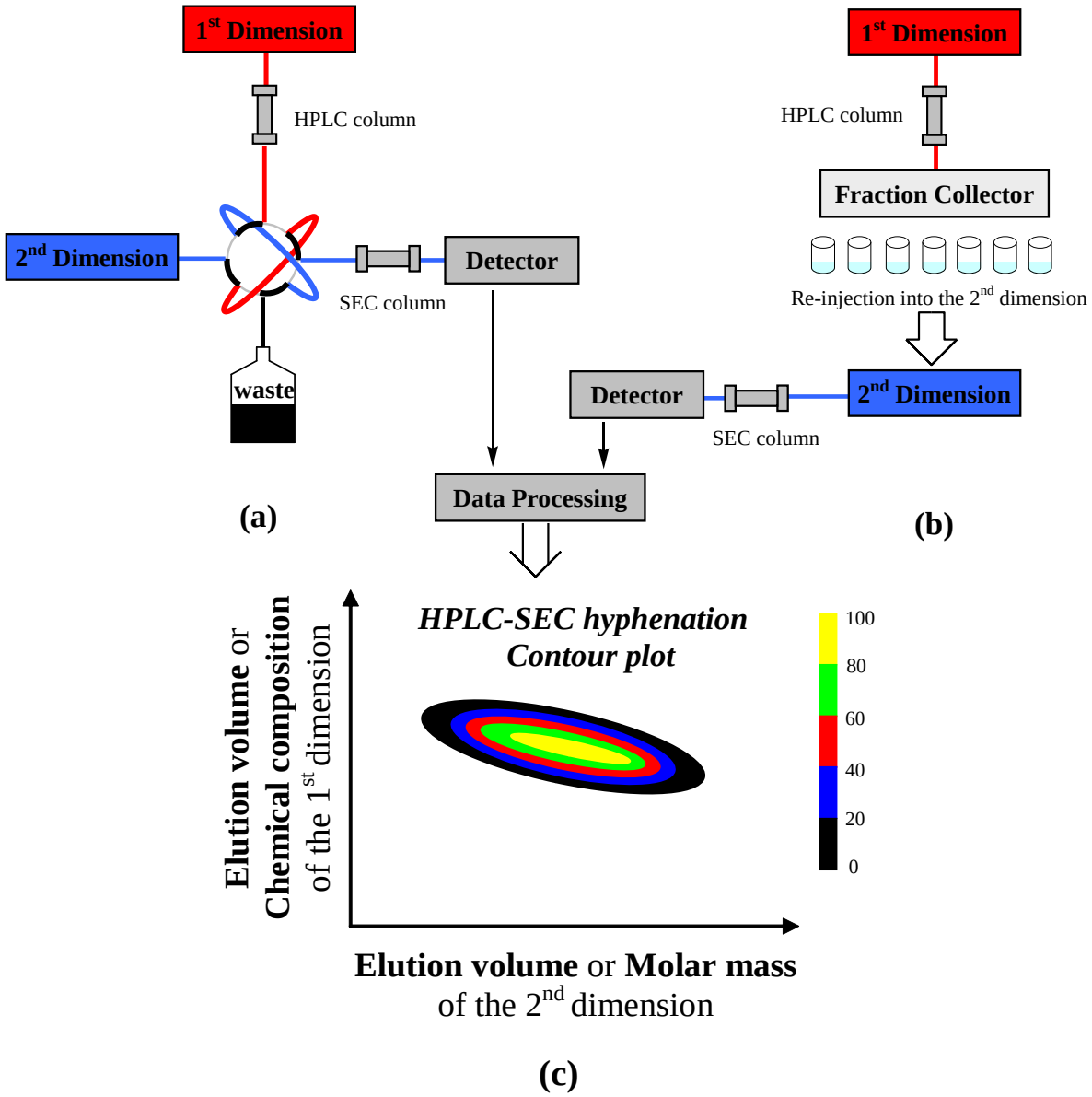

Figure 5: Schematic diagram of 2D-LC system: online (a) and off-line (b) with a 2D contour plot (c) (the colour from yellow to black corresponds to the highest to lowest analyte concentration, respectively).

There are some requirements which must be fulfilled in order to get a proper 2D-LC system. Since the second dimension is repeated multiple times on first dimension fractions, the two flow rates of the first and second dimensions must be well-matched: the flow rate of the first dimension must be low whereas the flow rate of the second dimension should be chosen as fast as possible in order to keep the run time of a 2D experiment low but maintaining its separation capacities and to avoid sample loss [135]. In principle, coupling any kinds of LC techniques is conceivable. However, several couplings are easier to set-up and others either technically not possible or worthless in terms of obtained information [97].

The most often used combination in 2D chromatography is a gradient HPLC in the first dimension coupled to SEC in the second dimension (gradient HPLC × SEC) [136-138]. The principal reasons are:

- It is not necessary to equilibrate the column in the second dimension after each experimental run since the SEC is performed isocratically. In contrast, performing the analysis by SEC × gradient HPLC is technically much more difficult as a reconditioning period is needed after each gradient run. Each second dimension run lasts very long and consequently the flow rate in the first dimension is too low to be properly controlled by the pump.
- Parameters such as temperature, mobile phase and stationary phase can be adjusted in the first dimension to improve separation efficiency.
- Better fine-tuning separation in the first dimension gives more homogeneous fractions.
- Breakthrough effects are absent upon transferring the fractions from the first dimension into the second dimension (elution of polymer within a solvent peak in gradient chromatography is called breakthrough peak [139]).
- A higher sample concentration can be loaded onto the stationary phase without loss of separation efficiency because column overloading in gradient HPLC is less pronounced compared to SEC. This is particular beneficial since the fractions in the first dimension are diluted with the eluent in the second dimension.

Another frequently used 2D combination involves LC-CC and SEC (LC-CC × SEC). Such system is utilized for analyzing functional homopolymers, block and graft copolymers [140-144].
A fully automated 2D system combining two chromatographs was first developed by Kilz et al. [97, 145]. In the first dimension, a gradient LAC separation, governed by enthalpic interactions allowed determining the chemical composition distribution of the polymer sample while in the second dimension the macromolecules were eluted as a function of their decreasing hydrodynamic volume using SEC.
A number of reviews have been published describing 2D-LC systems for investigating complex polymer samples [135, 146, 147].

3.2.2. Coupling liquid chromatography with chemical selective or molar mass sensitive detector

After the polymer molecules are separated in the column according to a structural feature, they can be analyzed by several detection methods. These methods can be used online or off-line with the chromatographic system to provide the desired information. They can be either chemical selective detection methods such as infrared (IR) to measure specific functional groups in the polymers or molar mass sensitive detection methods such as light scattering to measure molar mass distribution of the polymers.

3.2.2.1. Liquid chromatography-Infrared (LC-IR)

Infrared (IR) is a selective detection device applicable to all kinds of materials. IR spectroscopy deals with the quantitative measurement of the interaction between IR radiation and materials, revealing molecular vibrational transitions and thus provides characteristic information on molecular structure. Liquid chromatography can be combined with IR detector for specific detection and/or identification of separated sample constituents [148]. Two approaches are usually distinguished in the combination of LC and IR. The first approach (online combination) uses a flow cell through which the mobile phase from the chromatographic column is directly passed to the IR instrument where the spectra are continuously acquired in real time [149, 150].

However, the application of the online approach is very limited because the solvents used in chromatography are strong IR adsorbers, obscuring most absorbance regions of the low concentration analyte fractions. The drawback of solvent bands can be overcome by removing the solvents from the eluting fractions. Therefore, the second approach uses a solvent-elimination interface which is called LC-Transform for evaporating the solvent and depositing the polymeric fractions on a suitable substrate (e.g. an IR transparent Germanium disc) prior to recording the IR spectra [151-153]. In such a two-step process (deposition of LC fractions and IR measurement), solvent-free IR spectra of the deposited fractions can be obtained independently from the LC conditions.

A detailed description of the LC-IR experiments will be given in 4.2.2 on page 85.

3.2.2.2. Size exclusion chromatography–multi-angle laser light scattering (SEC-MALLS)

The absolute molar mass and molar mass distribution of polymer samples over a wide molar mass range ($10^3 – 10^9$ g/mol) can directly be determined by a light scattering detector (i.e. low angle laser light scattering, LALLS, right angle laser light scattering, RALLS, two/three angle laser light scattering, TALLS or multi-angle laser light scattering, MALLS). These detectors are mainly used online after SEC separation. Compared to LALLS and TALLS, the MALLS detector can also provide reliable root mean square radius or radius of gyration (R_g) and further information about branching and structure.

The principle of online light scattering detectors follows the theoretical basis of static light scattering as applied to polymer solutions [154-158]. When a MALLS is coupled to an SEC, the intensity of light scattered by each chromatographic slice or fraction eluting from the column is measured at many angles (θ) simultaneously (see figure 6). The angles are typically in the range of 30° – 150°. Since the response of such detectors is proportional to the molar mass and concentration of the fractions, a concentration detector has to be added to the system in order to measure the concentration. The molar mass of the polymer sample is obtained by performing a double extrapolation to the zero angle and the zero concentration.

One of the concentration sensitive detectors widely used is the differential refractive index (RI)-detector (differential refractometer) [159-164]. The measuring principle of the RI-detector is based on the refractive index change between the polymer analyte and the pure solvent during the experiments. A linear relationship between the refractive index and the concentration of a polymer solution (c) is indicated by refractive index increment (dn/dc). This relationship is given by:

$$\frac{dn}{dc} = \lim_{c \to 0} \left(\frac{n - n_0}{c}\right) \qquad \textbf{Equation 15}$$

where n is the refractive index of polymer solution, n_0 the refractive index of pure solvent, c the polymer concentration and dn/dc the refractive index increment of the polymer and has the units of cm^3/g. At very low concentration of the dissolved substance, the refractive index increment is independent of the concentration and it becomes also independent of molar mass above a molar mass of about 20000 g/mol.

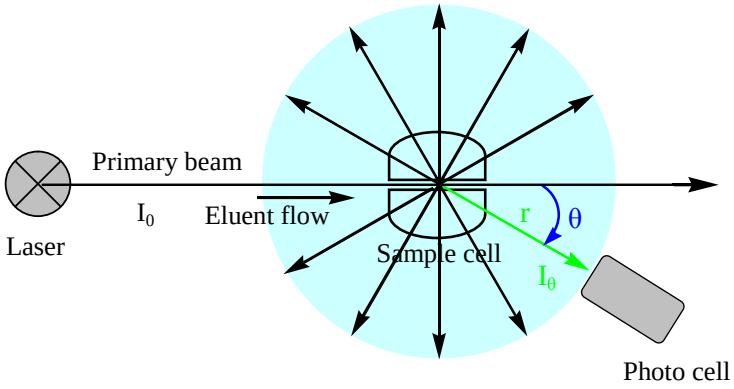

Figure 6: Schematic representation of a MALLS detector.

The relation between the intensity of scattered light and the Rayleigh ratio (R_θ), which is the ratio of the scattered to incident light per unit volume, is given by:

$$R_\theta = \frac{I_\theta \, r^2}{I_0 \, V_D} \qquad \textbf{Equation 16}$$

where I_0 is the intensity of incident light, I_θ the intensity of scattered light at a scattering angle θ, V_D recorded scattering volume, and r the distance between detector and scattering volume. R_θ at the angle θ from a dilute polymer solution is related to molar mass and concentration as described by [165, 166]:

$$\frac{R_\theta}{Kc} = MP(\theta)(1 - 2A_2 cMP(\theta) + ...) \qquad \textbf{Equation 17}$$

where M is the molar mass of the polymer (M is the weight average molar mass, M_w, if the polymer is a disperse sample), c the polymer concentration, A_2 the second virial coefficient. A_2 describes the interactions between the polymer and solvent molecules. The second term in the parentheses accounts for interactions between the polymer molecules [167, 168]. K, an optical constant, is defined by the following equation when vertically polarized incident light:

$$K = \frac{4\pi^2 n_0^2}{N_A \lambda_0^4}\left[\frac{dn}{dc}\right]^2 \qquad \textbf{Equation 18}$$

where n_0 is the refractive index of the pure solvent, N_A Avogadro's number, λ_0 the wavelength of the incident light in vacuum, and dn/dc the refractive index increment of the polymer in the given solvent and at the given temperature.

The particle scattering factor, P(θ), describes the angular dependence of the intensity of scattered light which is the excess Rayleigh ratio at the observation angle θ divided by that at zero angle ($P(\theta) = R_\theta/R_0$). For small molecules, whose molecular diameters are smaller than approx. λ/20, the intensity of the scattered light is independent of the scattering angle. Therefore, in this case, $P(\theta) = 1$ for all angles. However, for larger particle diameters (> λ/20), $P(\theta) \neq 1$ and thus its dependence of scattering angles has to be considered. P(θ) can be given at a certain angle from the following equation (the higher order is neglected) which is used to determine the radius of gyration of the scattering particle (R_g):

$$P(\theta) = 1 - \frac{16}{3}\frac{\pi^2}{\lambda^2}\left\langle R_g^2 \right\rangle_z \frac{\sin^2\theta}{2} \qquad \textbf{Equation 19}$$

where λ is the wavelength of the incident light in the solvent which is the ratio of the primary wavelength and refractive index of the solvent ($\lambda = \lambda_0/n_0$). The R_g describes the size of a particle in the solution regardless of its structure and is not identical to the geometrical radius. Since R_g is changed with conformation of flexible polymer chains in solution, only the average R_g has the practical meaning.

4. Results and Discussions

In this section, the results of this study will be discussed in detail. The first part of this section is divided in two chapters. The first chapter is dedicated to the synthesis of CA samples via alkaline partial saponification of a high DS CA and the characterization of average DS of the samples using ^{1}H-NMR and FTIR/ATR. The second chapter is about the solubility results of CAs in the DS-range investigated.

The second part of this section will discuss the chromatographic experiments on the CAs. The chromatographic results are divided in three main chapters. In the first chapter an SEC method for molar mass characterization of the CA samples will be set up. The second chapter will present the chromatographic method development for the separation of CAs according to DS. The correlation of both molecular features, i.e. DS and molar mass, will be discussed in the last chapter. The aim of these investigations is to fully resolve the complex molecular structure of cellulose derivatives which may affect their physicochemical properties such as adhesion strength, solubility, thermoreversible gelation…etc.

4.1. Synthesis and solubility of CA

4.1.1. Synthesis and characterization of CA varying in DS

As mentioned in the theoretical section CAs of high DS can be partially hydrolyzed by acidic or alkaline catalysis. Taking the benefits of alkaline over acidic hydrolysis, partial alkaline saponification of a highly substituted CA (sample 16, DS = 2.60) in 1,4-dioxane was therefore chosen in this investigation. The degree of saponification was adjusted by changing the amount of sodium hydroxide (NaOH) added.

After the synthesis, the average DS of CA samples was determined by quantitative ^{1}H-NMR spectroscopy in DMSO [43]. Figure 7 depicts the spectrum of one of the investigated samples (sample 12, DS = 2.27). As can be seen, the resonance lines of the CH_3-protons of the acetyl groups at (2.2 – 1.6 ppm) are separated from the proton signals of the cellulose unit at (5.5 – 2.8 ppm). The sharp and intense signal at 3.14 ppm is due to residual H_2O and HDO in the solvent and needs to be accounted for when determining DS. Since no traces of

1,4-dioxane can be seen at 3.57 ppm, this confirms the thorough purification of the CA precipitates in the washing step of the synthetic procedure.

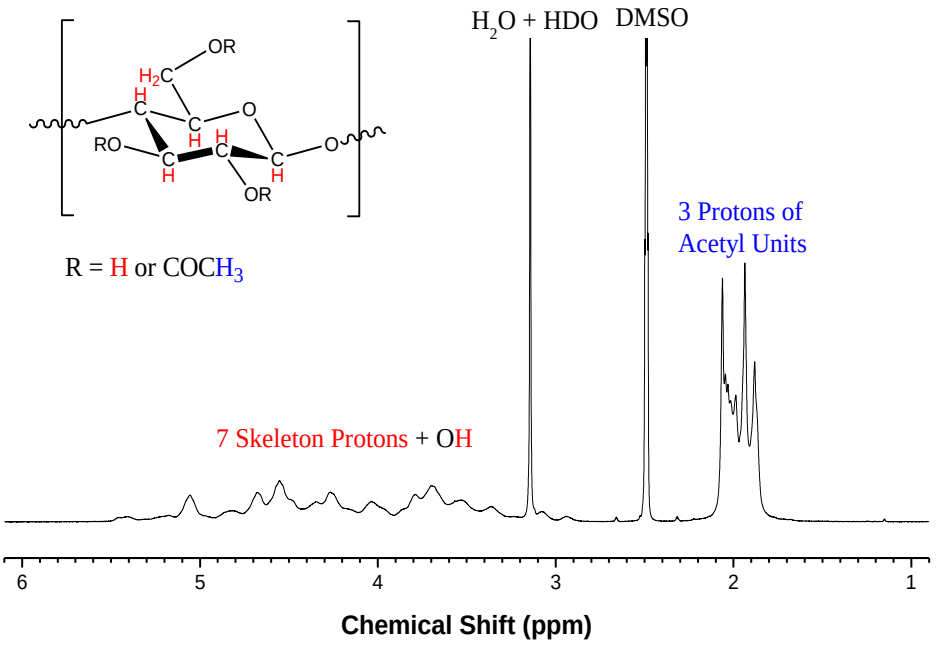

Figure 7: ^{1}H-NMR spectrum of CA (sample 12, DS = 2.27).

The quantification of average DS is based on the integral ratio between the CH_3-protons of acetyl units and the cellulosic ring protons using the following equation:

$$DS = \frac{10 \times \frac{I_{Acetyl}}{I_{AGU}}}{3 + \frac{I_{Acetyl}}{I_{AGU}}} \qquad \textbf{Equation 20}$$

where I_{Acetyl} is the integral of CH_3-protons of the acetyl units and I_{AGU} the integral of protons of anhydroglucose units. It should be mentioned that the region from 5.5 ppm to 2.8 ppm in the spectrum includes both the protons of the anhydroglucose units and the protons of the OH groups because of the use of DMSO as solvent. This fact was considered in the calculation of the average DS values.

The reliability of the deacetylation procedure for the synthesis of CA samples was checked by comparing the theoretical and calculated average DS values. In figure 8 the percentage of NaOH added relative to the acetyl groups is plotted against the DS determined by ^{1}H-NMR. In addition, the theoretical DS is added for a better comparison.

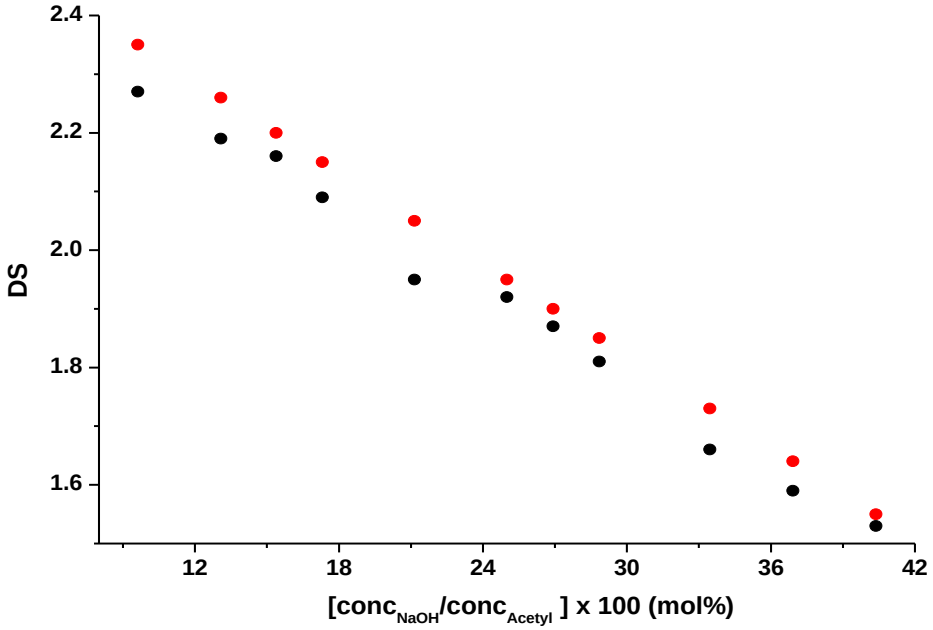

Figure 8: Dependence of DS on the amount of NaOH for partial deacetylation of CA in 1,4-dioxane. The red symbols represent the theoretical DS.

There is a good agreement between the theoretical DS values and the ones obtained from ^{1}H-NMR. The systematic deviation to slightly lower values might be the result of the additional reaction of water with acetyl groups since only the NaOH concentration was considered for the calculation of the theoretical DS. As expected, a decrease of DS with increasing amount of NaOH is observed. Nevertheless, the results show that alkaline partial saponification is a suitable method for the preparation of CA of various DS.

While ^{1}H-NMR is a direct method for the characterization of average DS of CAs, it, however, needs a large amount of sample to result in spectra of high signal-to-noise-ratio (S/N-ratio). In addition, costly instrumentations are used. Therefore, an alternative straightforward method for a fast estimation of average DS was required. For this purpose, the suitability of FTIR spectroscopy using ATR technique was investigated. Due to the high sensitivity, FTIR analysis can be adapted to much smaller sample quantities as compared to NMR. A further advantage of FTIR is that no solvents are required in preparation of the samples. In order to investigate whether DS can be derived from FTIR spectra, FTIR/ATR spectra were acquired for the samples. During these measurements we observed differences in the spectra of a single sample obtained by different experiments, which would complicate determination of DS. These spectral changes might be due to the existence of particle size differences in the sample. The reliability of the results was therefore improved by repeating the experiments several times and averaging the band ratios. The spectra of all CAs were recorded in

extinction mode. Annotation of the spectral bands of CA according to the literature [169-171] and changes of the normalized band intensities due to differences of the average DS of selected samples are shown in figure 9.

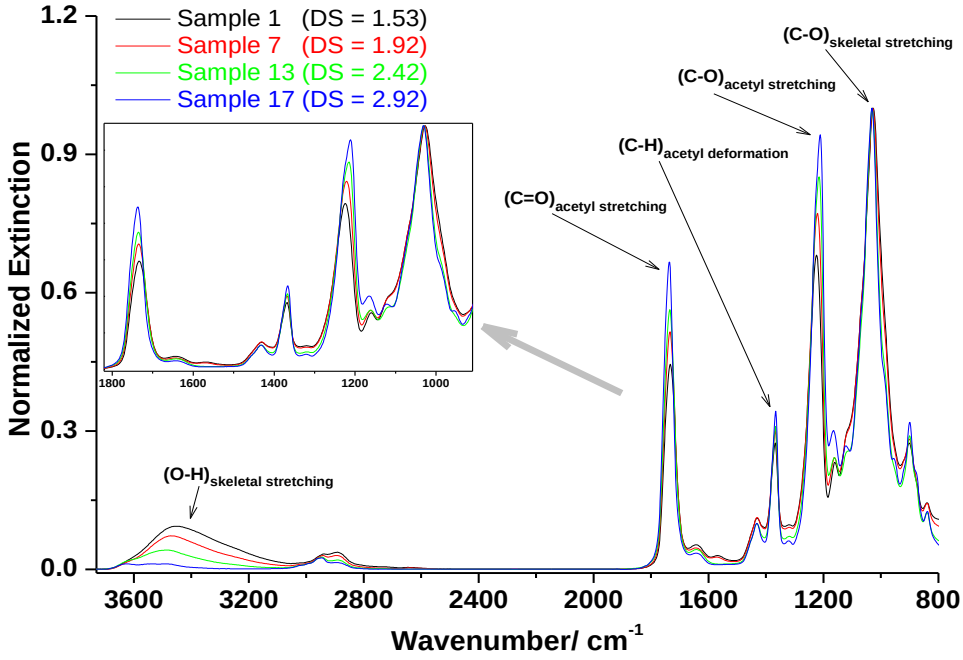

Figure 9: Assignment of the bands of superimposed FTIR/ATR spectra of CAs with different DS.

The bands at around 1030 cm^{-1} and 3450 cm^{-1} are characteristic for the C-O and O-H stretching vibrations of the skeleton, respectively, whereas the bands at around 1220 cm^{-1}, 1370 cm^{-1} and 1735 cm^{-1} are characteristic for the C-C-O stretching, CH_3 symmetric deformation and C=O stretching of the acetyl units, respectively. It can be observed that the relative intensities of the bands attributed to the acetyl groups increase from low to the high DS while the intensity of O-H skeletal stretching decreases in the same direction. These variations are due to the fact that at lower DS values more OH groups exist, causing more intensive O-H band in the spectrum. Similarly, the less acetyl groups are present (the lower DS) the bands representative for these groups show lower intensities.

Since the absolute intensities in FTIR/ATR depend on a variety of experimental parameters, e.g. sample contact with ATR-crystal and sample coverage of the crystal, the area ratios for spectral bands representative for the acetyl side groups and the anhydroglucose ring were taken as follows: The band area of each C=O stretching (1664 – 1826 cm^{-1}), C-H deformation (1336 – 1405 cm^{-1}) and C-O stretching (1182 – 1303 cm^{-1}) of the acetyl groups were divided by the band area of C-O skeletal stretching (933 – 1141 cm^{-1}). The baseline settings were set

identical to the integration limits. Some authors have chosen one specific band ratio such as C=O group for the quantitative determination of acetyl contents of CA films [172]. However, it is worthwhile to consider all the band ratios, since the environmental conditions such as temperature, humidity…etc. may cause variations in the band intensities of the functional groups in the spectrum, which will be diminished by using different band ratios. The correlations of the band ratios with the DS values determined by ^{1}H-NMR are represented in figure 10.

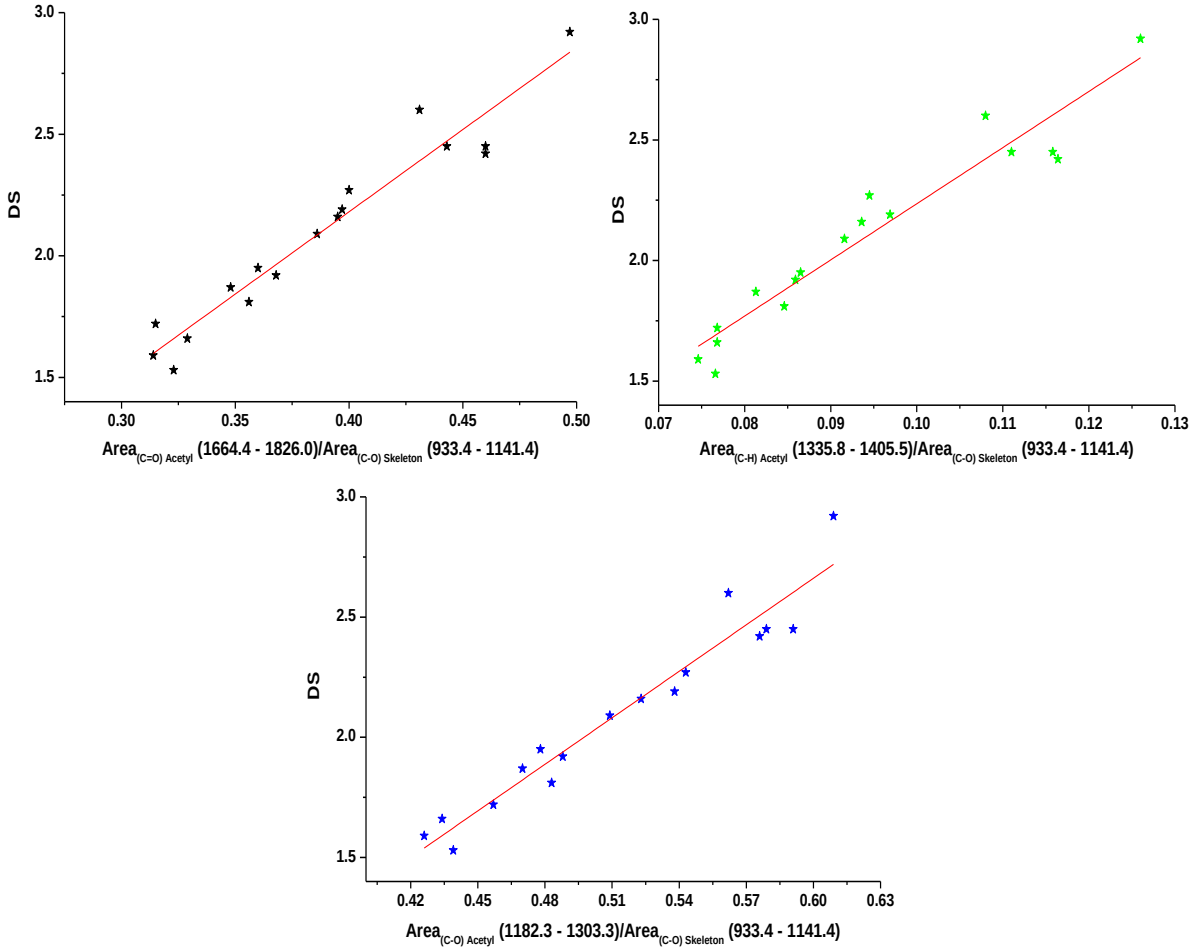

Figure 10: Correlations of the defined FTIR signal area ratios (C=O, C-H, and C-O of acetyl group and C-O skeleton) with the DS values determined by ^{1}H-NMR spectroscopy of CA samples.

Although the relations between the DSs and the corresponding band ratios of the samples show some scattering, the tendencies are apparent. The correlations were fitted by linear regression. The calibration curves could be described by the following equations:

$$DS_1 = -0.52 + 6.8 \times \frac{A_{(C=O)\,Acetyl}}{A_{(C-O)\,Skeleton}}$$ **Equation 21**

$$DS_2 = -0.09 + 23.3 \times \frac{A_{(C-H)\,Acetyl}}{A_{(C-O)\,Skeleton}}$$ **Equation 22**

$$DS_3 = -1.2 + 6.4 \times \frac{A_{(C-O)\,Acetyl}}{A_{(C-O)\,Skeleton}}$$ **Equation 23**

where A is the FTIR peak areas of respective spectral bands of acetyl and anhydroglucose units.

For the determination of DS from FTIR spectra the DS values calculated from the different band ratios were averaged:

$$DS = (DS_1 + DS_2 + DS_3)/3$$ **Equation 24**

These equations can be directly utilized for the quantification of the average DS of any unknown CA sample once the FTIR spectrum is available. Since the FTIR correlations have been proven useful to determine DS with very low amounts of sample, they might be used for characterization of chromatographic fractions (see LC-FTIR experiments in 4.2.2 on page 86).

4.1.2. Solubility of CA over a wide DS-range

The solubility of CAs in organic solvents is primarily related to their acetyl content. The large span of solubility characteristics given in literature is summarized in table 1.

Table 1: Solubility of CA at various degrees of substitution range [4, 6].

DS	Acetyl, wt%	Solubility
0.6 – 0.9	13.8 – 19.4	Water
1.2 – 1.8	24.3 – 32.6	2-Methoxy ethanol
2.2 – 2.7	37.2 – 42.2	Acetone
2.8 – 3.0	43.1 – 44.8	DCM or Chloroform

By increasing the acetyl content the polymer tends to be less polar and, thus, the solubility decreases in polar solvents while it increases in non-polar ones.

In order to perform liquid chromatography of CAs, a single solvent or a single solvent mixture is needed to dissolve all the samples, irrespective of DS. To identify suitable solvents for dissolution, five samples (samples 2, 4, 9, 16 and 17), having DS values of DS = 1.59, 1.72, 2.09, 2.60 and 2.92, respectively, were selected and their solubilities were tested in a large variety of different solvents and solvent mixtures. Therefore, 1.0 mL of the solvent or the solvent mixture was added to 1.0 mg of the polymer and the mixture was left overnight with agitation.

The solubilities evaluated by visible inspection at three different temperatures of 25 °C, 55 °C and 90 °C are collected in table 2 . Most of the solvents or the solvent mixtures are found either to be ineffective in the dissolution process or dissolve only selected samples, i.e. a particular DS-range. If we compare the results in table 2 with the literature-based data given in table 1, some inconsistencies can be seen. For example, 2-methoxy ethanol was found by us to be incapable to dissolve the sample of DS 1.59 whereas a soluble DS-range of CA (DS = 1.2 – 1.8) for this solvent is reported in literature. Since the solubility of cellulose derivatives and therefore of CAs is a complex function which depends not only on the average DS but also on the distribution of the acetyl substituents in the AGUs and along and among the cellulose chains [173], minor differences in substituent distribution can result in large differences in solubility in certain cases [174-176].

As can be seen from table 2, only DMSO and N,N-DMAc/LiCl were identified to dissolve all our samples, irrespective of DS.

Table 2: Solubility (+ soluble, +/− partially soluble, − insoluble) of investigated CAs in organic solvents and solvent mixtures evaluated at 25 °C, 55 °C and 90 °C.

Solvent	Sample 2 (DS = 1.59)			Sample 4 (DS = 1.72)			Sample 9 (DS = 2.09)			Sample 16 (DS = 2.60)			Sample 17 (DS = 2.92)		
	25 °C	55 °C	90 °C	25 °C	55 °C	90 °C	25 °C	55 °C	90 °C	25 °C	55 °C	90 °C	25 °C	55 °C	90 °C
Acetic acid	–	–	–	+	+	+	–	+/–	+	+	+	+	–	–	–
Acetone	–	–	–	–	–	–	–	–	–	+	+	+	–	–	–
Acetone/water (1:1)	–	–	–	+	+	+	–	–	–	–	–	–	–	–	–
Acetonitrile	–	–	–	–	–	–	–	–	–	+	+	+	–	–	–
2-Butoxyethanol	–	–	–	–	–	–	–	–	–	–	–	–	–	–	–
Chloroform	–	–	–	–	–	–	–	–	–	–	–	–	+	+	+
DCM	–	–	–	–	–	–	–	–	–	–	–	+/–	+	+	+
1,4-Dioxane	–	–	–	–	–	–	–	–	–	+	+	+	+/–	+/–	+
N,N-DMAc/LiCl	+	+	+	+	+	+	+	+	+	+	+	+	+	+	+
DMF	–	–	–	+	+	+	+	+	+	+	+	+	–	–	–
DMF/water (1:1)	–	–	–	–	+/–	+	–	–	–	+/–	+/–	+/–	–	–	–
DMSO	+	+	+	+	+	+	+	+	+	+	+	+	+	+	+
Ethanol	–	–	–	–	–	–	–	–	–	–	–	–	–	–	–
Ethyl acetate	–	–	–	–	–	–	–	–	–	–	–	–	–	–	–
n-Hexane	–	–	–	–	–	–	–	–	–	–	–	–	–	–	–
MEK	–	–	–	–	–	–	–	–	–	+/–	+	+	–	–	–
Methanol	–	–	–	–	–	–	–	–	–	–	–	–	–	–	–
2-Methoxyethanol	–	–	–	+	+	+	–	+/–	+/–	+/–	+	+	–	–	–
2-Propanol	–	–	–	–	–	–	–	–	–	–	–	–	–	–	–
1,2,4-TCB	–	–	–	–	–	–	–	–	–	–	–	–	–	–	–
Tetrachloroethylene	–	–	–	–	–	–	–	–	–	–	–	–	–	–	–
THF	–	–	–	–	–	–	–	–	–	–	–	–	–	–	–
THF/water (1:1)	–	–	–	+/–	+/–	+	–	–	–	–	+/–	+/–	–	–	–
Toluene	–	–	–	–	–	–	–	–	–	–	+/–	+/–	–	–	–
Water	–	–	–	–	–	–	–	–	–	–	–	–	–	–	–
Xylene	–	–	–	–	–	–	–	–	–	–	–	–	–	–	–

4.2. Development of chromatographic methods for the characterization of CA

Chemical structure and molecular size are the two most important parameters determining the performance of a polymer in a specific application. This is also true for cellulose derivatives for which molar mass and molar mass distribution, the degree of substitution (DS) and the substitution pattern have to be determined in order to elucidate structure-property relations. For the characterization of polymers chromatographic separation techniques are highly valuable. SEC has become a standard method for the determination of molar mass distributions, whereas methods of interaction chromatography can provide information on the chemical composition distribution. However, the analysis of complex copolymers like CA which actually consist of eight different comonomers (differently substituted AGUs) is highly challenging due to the influence of molar mass, DS and the different substitution pattern of the AGUs on the chromatographic behaviour of the copolymer.

4.2.1. Development of an SEC method for CA

One of the molecular parameters that influence the application performance of CA is molar mass. In contrary to other cellulose derivatives such as cellulose nitrate or cellulose tricarbanilate, the importance of molar mass characterization by SEC is connected to its own commercial production rather than to investigate the molecular properties of the cellulose itself [177-181]. In this chapter, the attempts made to determine molar mass averages and -distributions of CA by SEC-MALLS are discussed. Since the samples can be dissolved in DMSO and DMAc/LiCl, it is possible in principle to run SEC in these solvents.

4.2.1.1. SEC of CA in DMSO

CAs of different DS were first analyzed by SEC-MALLS/RI in pure DMSO to characterize the molar mass and the molar mass distribution. Examples of the chromatograms obtained for the samples of the lowest DS (sample 1, DS = 1.53) and the highest DS (sample 17, DS = 2.92) are illustrated in figure 11. The difference in the RI peak areas is due to the

difference in the refractive index increment (dn/dc) of these samples (see later in figure 13). The RI peaks of both samples are composed of a small peak (prehump) at low elution volume (high molar masses) and a main broad peak thereafter. This prehump is probably due to strong aggregations between the polymer chains, since the higher the number of hydroxyl groups, i.e. the lower DS, the higher is the probability of intermolecular interactions.

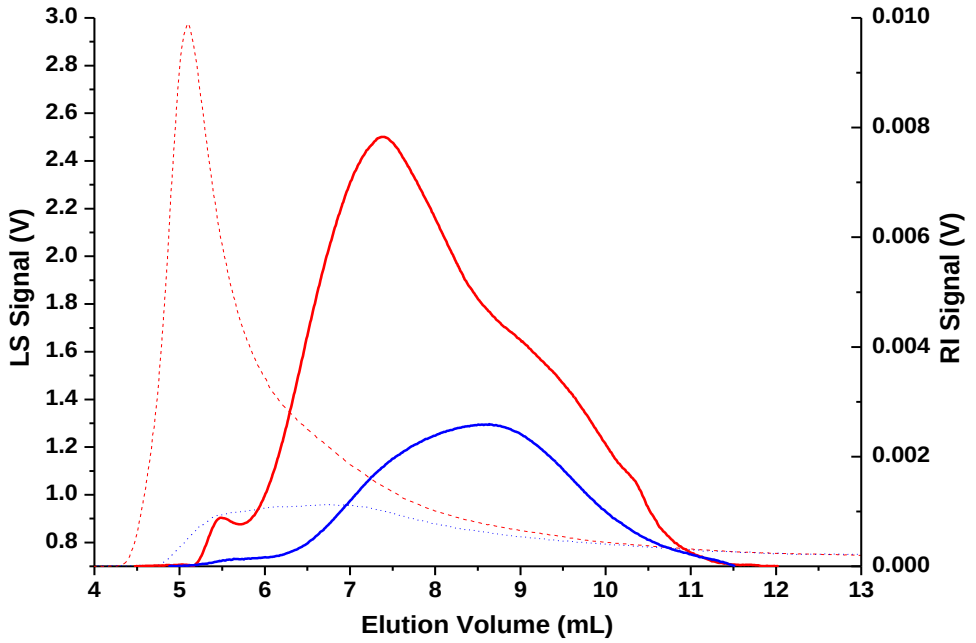

Figure 11: RI- (solid) and corresponding LS-traces (broken lines) of CA dissolved in DMSO; Injection volume: 100 µL (conc. = 3.0 g/L); Eluent: pure DMSO; Column: PSS-GRAM Linear XL (30 cm × 0.8 cm I.D., 10 µm) at 35 °C; RI temperature: 35 °C; Flow rate: 1.0 mL/min; Detector: RI and MALLS. Samples: Sample 1 (DS = 1.53) (red) and sample 17 (DS = 2.92) (blue).

The assumption of aggregates is further supported by the LS-traces. As can be seen, despite the low concentration of the prehump in the RI-peak a tremendous scattering intensity in the LS-peak is observed, indicating structures of very high masses.

Complete suppression of aggregates is a prerequisite to ensure true molar mass determination of the individual chains from light scattering [182, 183]. It has been reported that the addition of an inorganic salt, such as LiCl or LiBr prevents aggregation of the polymer molecules [184-187]. Therefore, experiments with different concentrations of LiCl in DMSO were accomplished in order to test whether the addition of salt has a positive effect and to identify the amount of salt required to obtain aggregate-free chromatograms in RI and LS. The resulting RI- and the corresponding LS-chromatograms at salt concentrations of 50, 100, 150, 200, and

250 mmol/L are shown for three representative samples (sample 2, DS = 1.59; sample 10, DS = 2.16 and sample 17, DS = 2.92) in figure 12.

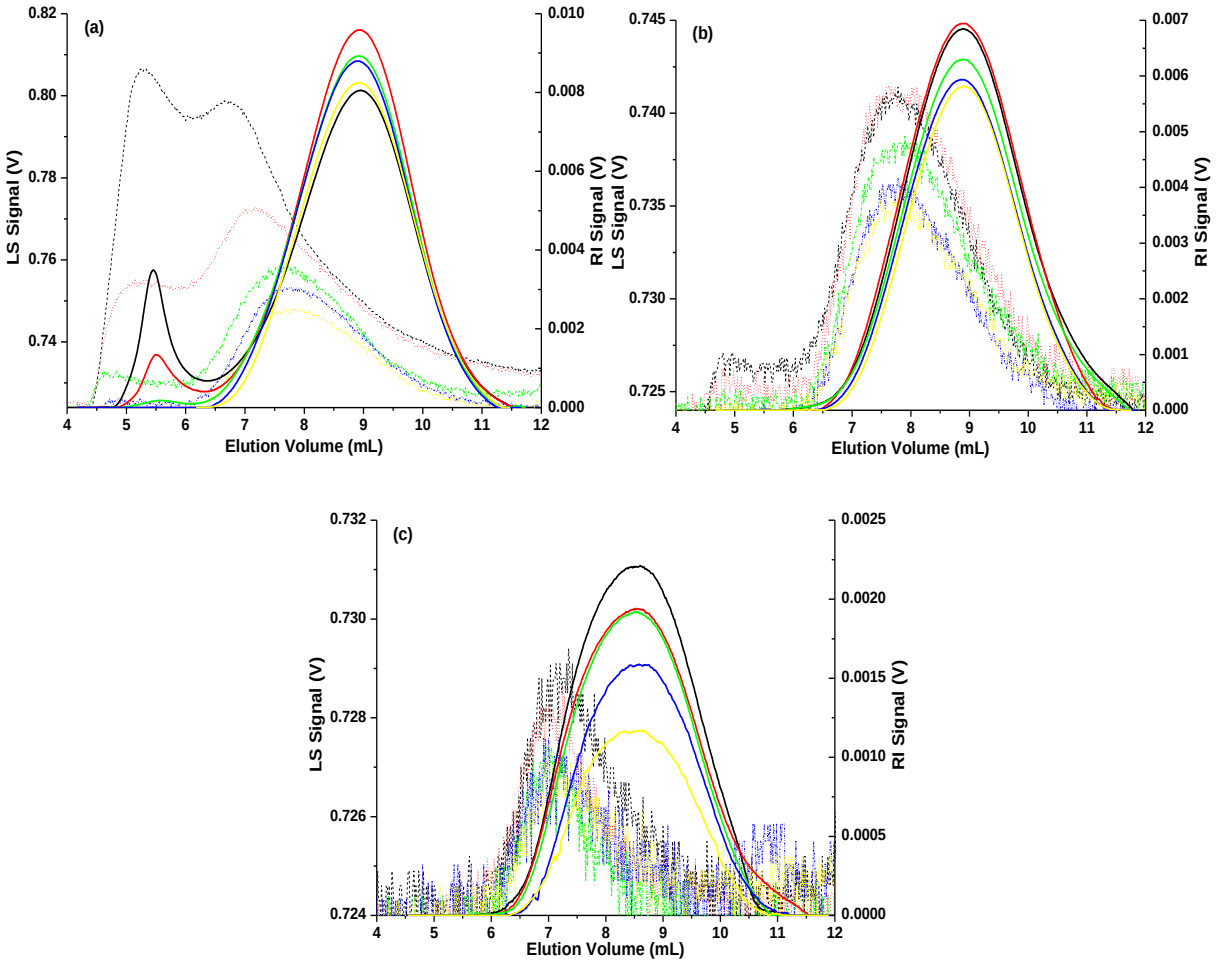

Figure 12: Overlays of RI- (solid) and LS-traces (broken lines) for sample 2 (DS = 1.59) (a), sample 10 (DS = 2.16) (b) and sample 17 (DS = 2.92) (c) at different LiCl salt concentrations; Injection volume: 100 µL (conc. = 3.0 g/L); Sample solvent and Eluent: DMSO + X mmol/L LiCl (X = 50 (black), 100 (red), 150 (green), 200 (blue) and 250 (yellow) mmol/L); Column: PSS-GRAM Linear XL (30 cm × 0.8 cm I.D., 10 µm) at 35 °C; RI temperature: 35 °C; Flow rate: 1.0 mL/min; Detector: RI and MALLS.

At a concentration of 50 mmol/L, clearly bimodal RI and LS peaks are observed for the low DS (sample 2, DS = 1.59) whereas only the LS peak of the middle DS (sample 10, DS = 2.16) gives an indication of remaining aggregates in the sample. However, due to the very low S/N-ratio of the LS peak of the high DS sample (sample 17, DS = 2.92), it is hard to judge whether the sample is completely deaggregated or not. At least no indication for aggregates is observed in the RI-trace. The situation was further improved by increasing the concentration of LiCl until monomodal chromatograms were observed in the LS- and RI-trace for all samples. In fact, the study revealed that a quite high LiCl concentration (250 mmol/L) is

required before aggregation cannot be observed any longer especially for samples of low DS. The disappearance of the prepeaks is an evidence of having no aggregates. Another interesting observation is that salt concentrations higher than 50 mmol/L did not influence the elution position of the main peaks in RI. Except for the lowest DS (sample 2, DS = 1.59), the LS peaks of the other samples remained almost identical in position if the salt concentration exceeds 50 mmol/L. Shifting the main LS peak of the low DS to the higher elution volumes demonstrates the change in aggregation.

In order to obtain the molar masses from light scattering measurements, the dn/dc for the analyzed CA samples in this particular eluent system (DMSO + 250 mmol/L LiCl) must be known, since dn/dc enters by a power of 2 into the Rayleigh-Debye equation. This means that any minor change in dn/dc causes a large deviation in molar mass. So far, no data concerning the dn/dc for CA in DMSO/LiCl is available in literature.

For some cellulose derivatives such as cellulose nitrate and cellulose xanthate it has been established that dn/dc varies with DS [188, 189]. In order to check whether dn/dc depends on DS for the CAs under investigation, dn/dc was calculated based on the intensity of the RI peak area of the samples taken at 250 mmol/L LiCl. The details of the calculation are given in 5.5.2. Figure 13 depicts the dependence of dn/dc of CA on DS in DMSO/LiCl. As can be seen, CAs of different DS have different dn/dc. The values of dn/dc were found to range from dn/dc = 0.009 cm^3/g for the sample of highest DS (sample 17, DS = 2.92) to dn/dc = 0.033 cm^3/g for the sample of lowest DS (sample 1, DS = 1.53).

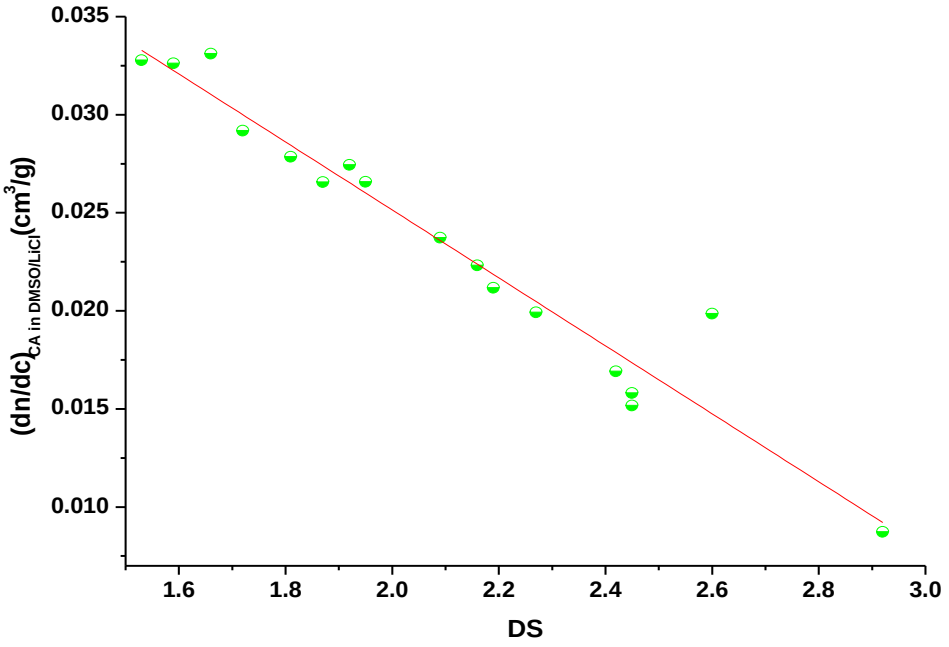

Figure 13: dn/dc of CA in DMSO\LiCl as a function of DS.

The nearly linear variation of dn/dc with DS in DMSO/LiCl can be described by the following equation:

$$\left(\frac{dn}{dc}\right)_{CA\ in\ DMSO/LiCl} = (0.06 - 0.017 \times DS)\ cm^3/g \qquad \textbf{Equation 25}$$

Although a stable SEC method was established, our attempts to determine molar masses by SEC-LS experiments in DMSO/LiCl failed, due to the low dn/dc-values leading to very noisy LS-signals (low S/N-ratio), resulting in very poor reproducibility of the molar masses determined.

4.2.1.2. SEC of CA in DMAc

Since the very low dn/dc of CAs in DMSO/LiCl did not allow obtaining reproducible and reliable molar masses, DMSO was replaced by DMAc. Similarly to DMSO, the application of pure DMAc as eluent resulted in bimodal peaks. Figure 14 shows the RI- and LS-traces of three CA samples of different DS (sample 1, DS = 1.53; sample 14, DS = 2.45 and sample 17, DS = 2.92) in pure DMAc as the eluent.

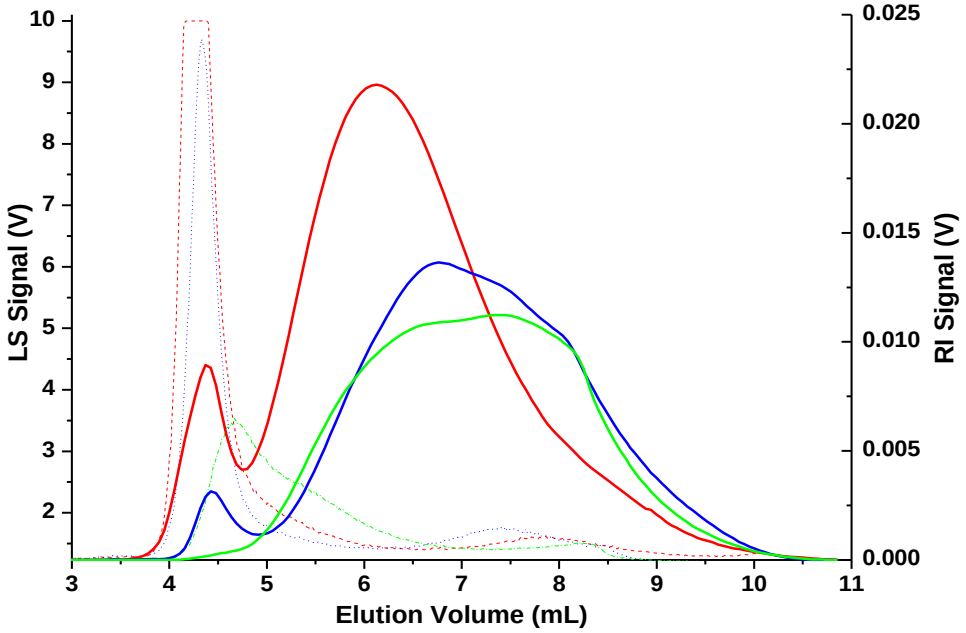

Figure 14: RI- (solid) and corresponding LS-traces (broken lines) of CA dissolved in DMAc; Injection volume: 100 µL (conc. = 3.0 g/L); Eluent: pure DMAc; Column: PSS-GRAM Linear XL (30 cm × 0.8 cm I.D., 10 µm) at 35 °C; RI temperature: 35 °C; Flow rate: 1.0 mL/min; Detector: RI and MALLS. Samples: Sample 1 (DS = 1.53) (red), sample 14 (DS = 2.45) (blue) and sample 17 (DS = 2.92) (green).

The difference in the RI peak areas is due to the difference in the dn/dc of these samples (see later in figure 16). As can be seen, two of the samples (sample 1, DS = 1.53 and sample 14, DS = 2.45) show a prehump at around 4.4 mL in the RI-trace before the main peak. The relative intensity of the prehump seems to correlate with DS. In general, the lower the DS, the more pronounced is the prehump at low elution volume. The assumption of the small prepeak resulting from chain aggregations is further supported by the LS-traces, where a very high signal intensity is observed despite the low concentration of the prehump in the RI. Even sample 17 having the highest DS (DS = 2.92), for which no evidence for aggregation is observed in the RI-trace, shows a clear bimodality in the LS-signal. Analogous to the DMSO system, attempts were undertaken to suppress chain aggregation by the addition of LiCl. Indeed, the addition of 250 mmol/L LiCl in the sample solvent and eluent was found to destroy the aggregation.

The resulting monomodal RI- and LS-peaks for the selected samples are shown in figure 15. No prepeaks are observed proving that the samples are free from aggregates.

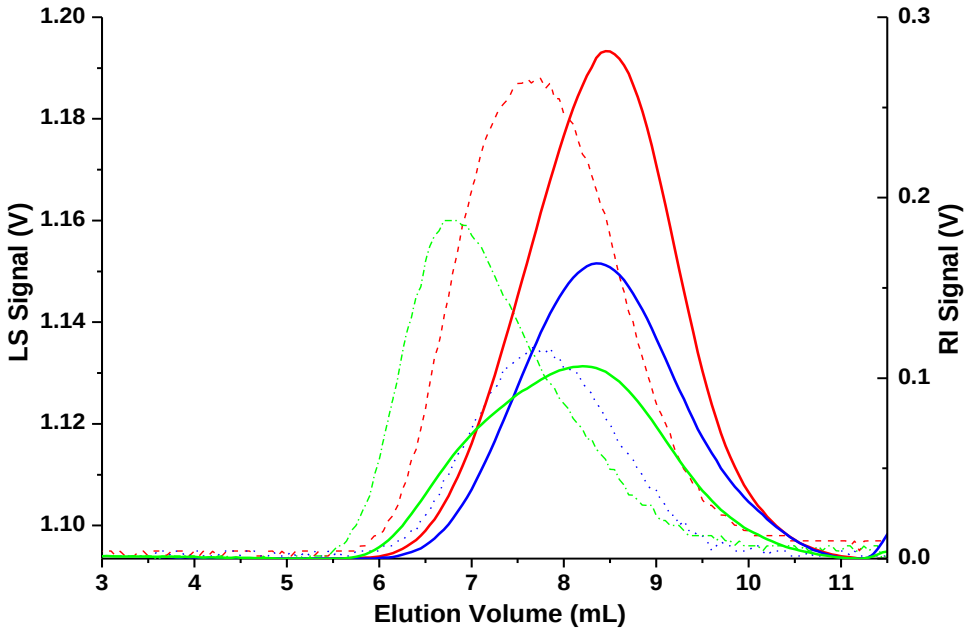

Figure 15: RI- (solid) and corresponding LS-traces (broken lines) of CA dissolved in DMAc + 250 mmol LiCl/L; Injection volume: 100 µL (conc. = 3.0 g/L); Eluent: DMAc + 250 mmol LiCl/L; Column: PSS-GRAM Linear XL (30 cm × 0.8 cm I.D., 10 µm) at 35 °C; RI temperature: 35 °C; Flow rate: 1.0 mL/min; Detector: RI and MALLS. Samples: Sample 1 (DS = 1.53) (red), sample 14 (DS = 2.45) (blue) and sample 17 (DS = 2.92) (green).

The dn/dc-values of the samples in DMAc/LiCl were determined from the RI peak areas (for details see 5.5.2). The evaluation revealed significantly higher dn/dc-values as compared to DMSO/LiCl, which, however, followed the same trend as in the DMSO/LiCl system. Figure 16 represents the determined dn/dc-values of CA in DMAc/LiCl as a function of DS. Despite some scattering clearly dn/dc systematically decreases from dn/dc = 0.044 cm^3/g for DS = 2.92 (sample 17) to dn/dc = 0.09 cm^3/g for the sample of lowest DS = 1.53 (sample 1).

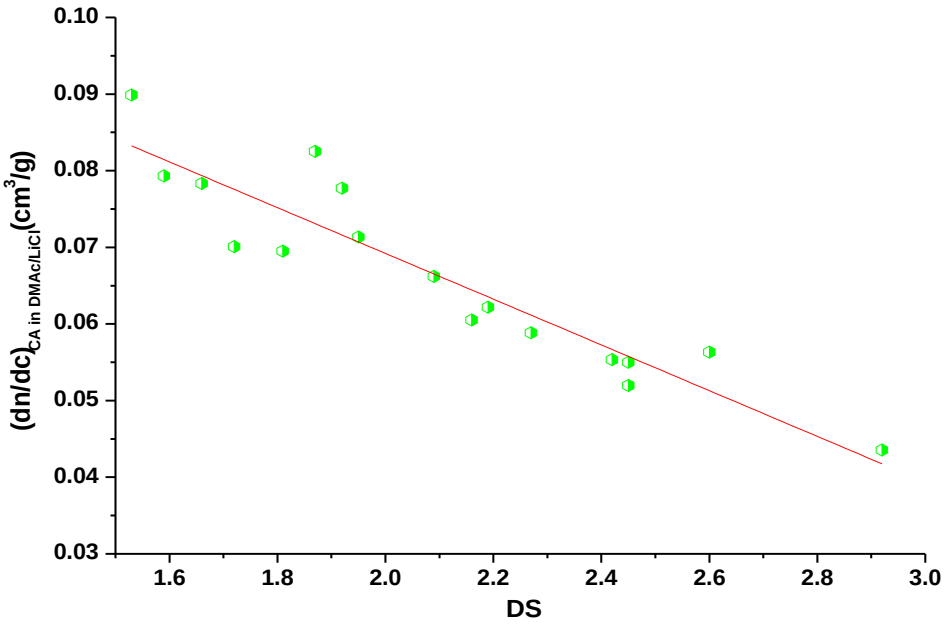

Figure 16: dn/dc of CA in DMAc\LiCl as a function of DS.

The linear variation of dn/dc with DS in DMAc/LiCl can be described by the following relation:

$$\left(\frac{dn}{dc}\right)_{CA\ in\ DMAc/LiCl} = (0.129 - 0.030 \times DS)\ cm^3/g \qquad \textbf{Equation 26}$$

A comparison with literature data on dn/dc for samples of different DS in pure DMAc supports our observation of decreasing dn/dc with increasing DS [190-192]. However, a direct comparison of the absolute values is not possible due to the different wavelengths and salt concentrations.

Although dn/dc-values in DMAc/LiCl were found to be significantly higher than in DMSO/LiCl, rather high polymer concentrations were required to obtain a suitable S/N-ratio for the light scattering signal. However, SEC is known to be prone to easy column overloading, especially for high molar mass samples. Column overloading results in variations of peak position with concentration, which in turn will lead to concentration dependent molar masses, when evaluating the chromatograms using a calibration curve [193-195]. Another concern is a loss of resolution by column overloading. Therefore, concentration dependent experiments were performed on three representative samples of different DS. Figure 17 shows the resulting chromatograms.

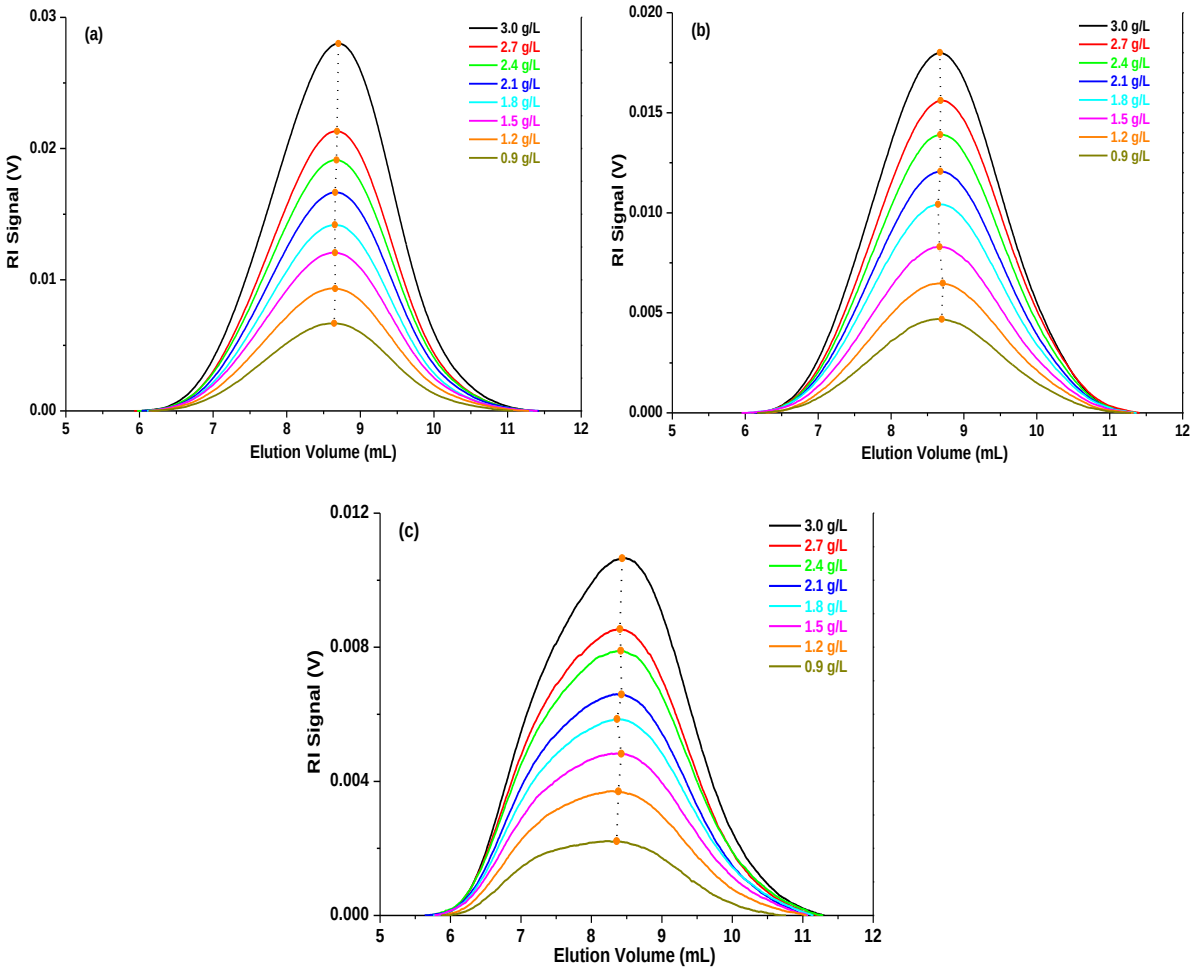

Figure 17: Overlays of RI elugrams at different concentrations for sample 1 (DS = 1.53) **(a)**, sample 10 (DS = 2.16) **(b)** and sample 17 (DS = 2.92) **(c)**; Experimental conditions see figure 15.

No significant and systematic variations in peak positions were observed when the concentration was increased from 0.9 to 3.0 g/L. Thus, a concentration of 3.0 g/L was chosen to prepare the sample solutions as the best compromise between a sufficiently intense LS-signal and position stability.

After the SEC conditions have been optimized, SEC-LS experiments were performed to determine absolute weight average molar masses (M_w) and to determine the dependence of molar mass on elution volume for all industrial and synthesized CA samples. The M_w and the calculated weight average degrees of polymerization (DP_w) of all samples are listed in table 3.

Table 3: Absolute molar masses of CAs obtained from LS (absolute M_w) and calculated DP_w. The industrial samples are marked in grey.

Sample name	DS	LS-M_w [g/mol]	DP_w
Sample 1	1.53	57600	254
Sample 2	1.59	72700	318
Sample 3	1.66	73500	317
Sample 4	1.72	44600	190
Sample 5	1.81	68100	286
Sample 6	1.87	64900	269
Sample 7	1.92	63200	260
Sample 8	1.95	76400	313
Sample 9	2.09	70700	283
Sample 10	2.16	71900	284
Sample 11	2.19	71000	279
Sample 12	2.27	74400	289
Sample 13	2.42	64400	244
Sample 14	2.45	64700	244
Sample 15	2.45	93300	352
Sample 16	2.60	69800	257
Sample 17	2.92	175000	613

The DP_w values were calculated from M_w using the following equation, which takes into account the change in the molar mass of a monomer unit (anhydroglucose unit) due to the different DS:

$$DP_w = \frac{(M_w)_{CA}}{(M)_{AGU}}$$ **Equation 27**

where $(M)_{AGU}$ is the molar mass of an substituted AGU in the CA samples and can be calculated using the following equation:

$$(M)_{AGU} = 159 + DS \times 43 + (3 - DS)$$ **Equation 28**

All samples prepared in this study are based on the same parent material. If the cellulose backbone was not altered by the saponification reaction, the degree of polymerization (DP) should remain constant. However, the molar mass should decrease with decreasing DS, due to the lower molar mass of a repeating unit at lower DS. Indeed, despite some scattering, the DP_w values were found to be fairly constant $DP_w = 284$ with a standard deviation (STD) of

STD = ±23. Therefore, within the accuracy of the LS experiments, the calculated average DP can be regarded as being constant and it can thus be concluded that the chain length distribution of the cellulose backbone was not altered significantly by the saponification reaction. This is in contrast to the acidic saponification of CA under acidic conditions, as acidic saponification severely reduces the degree of polymerization of the cellulosic backbones during hydrolysis [36, 196]. Therefore, alkaline saponification is a better choice for deacetylation of a high DS CA.

Since SEC-MALLS allows determination of molar masses for each elution volume, the dependences of molar mass on elution volume (calibration curves) can be determined. Figure 18 shows calibration curves together with the corresponding RI chromatograms. As expected for a SEC separation, the molar masses decrease with increasing elution volume. All samples are broadly distributed with molar masses covering at least two orders of magnitude ($10^4 – 10^6$ g/mol). The scattering of the data at the high and low molar mass end of the chromatograms are typical for SEC-LS measurements and are attributed to the different sensitivities and dependences on molar mass of the LS- and RI-detectors.

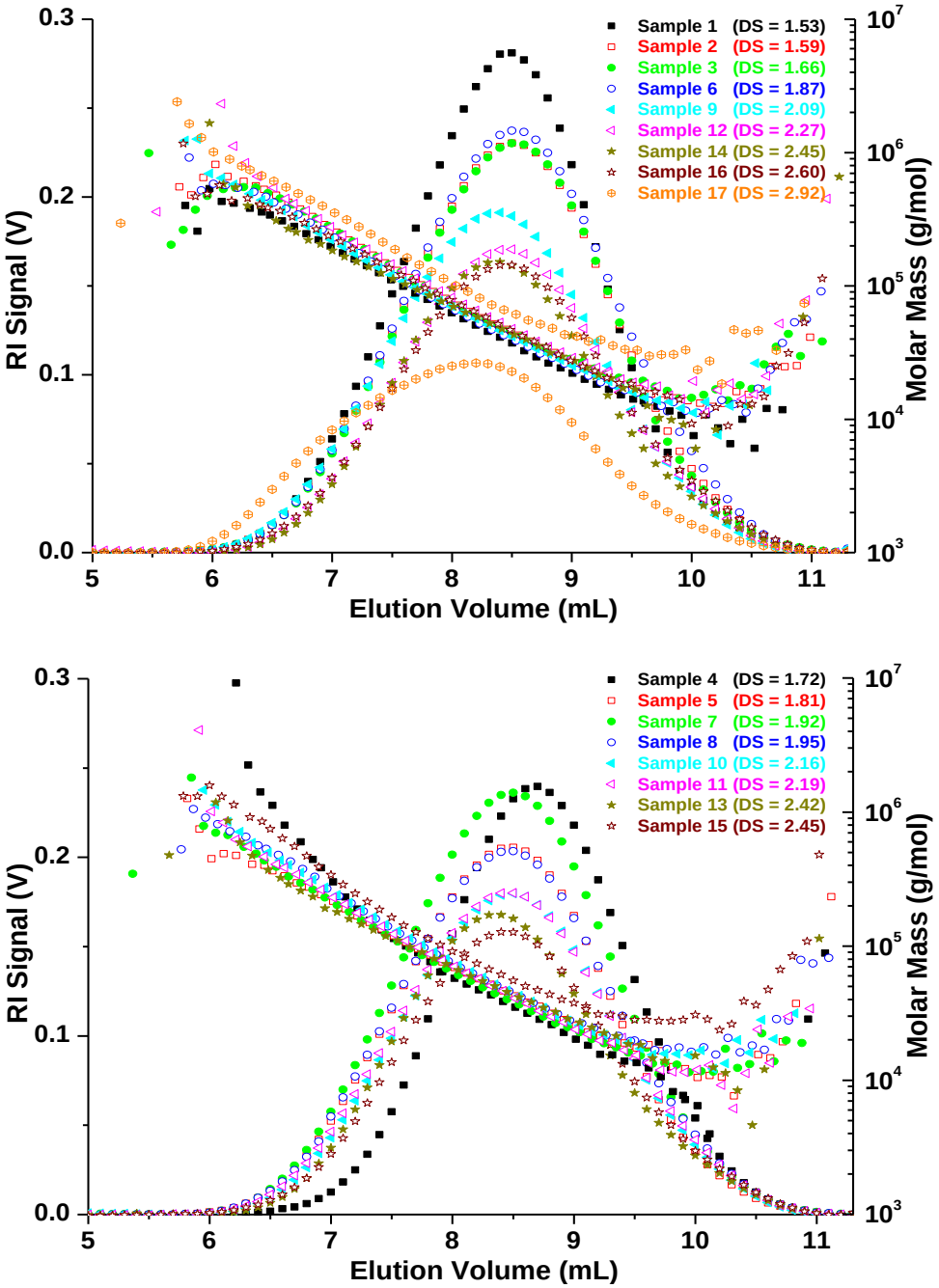

Figure 18: RI-traces and dependences of molar mass on elution volume for CA of different DS. Experimental conditions see figure 15.

With the exception of two of the industrial samples (sample 15, DS = 2.45 and sample 17, DS = 2.92), the dependences of molar mass on elution volume for all samples are very close to each other, despite the differences in average DS and the different origins of the samples. The reason for the deviations of the sample 15 and sample 17 is unclear yet. Since both deviate to higher molar masses, branching might be an explanation. At a given elution volume the molar masses scatter by approximately ±10% relative, which is in the order of the

uncertainty of LS measurements anyway. In addition, it has to be kept in mind that the molar mass varies with DS. However, no systematic dependence of the molar masses with DP at a given elution volume was observed. As a result, it can be concluded that the variation of DS within the range given in this investigation does not alter significantly the hydrodynamic volume. As a consequence, the molar masses of CAs in the DS-range investigated can be determined using the same calibration curve.

Furthermore, the samples prepared in this study which are based on the same parent material exhibit nearly identical elution profiles as shown in figure 19 (chromatogram of the precursor, sample 16, DS = 2.60 is also included). This indicates that the variation of DS does not change the hydrodynamic volume considerably.

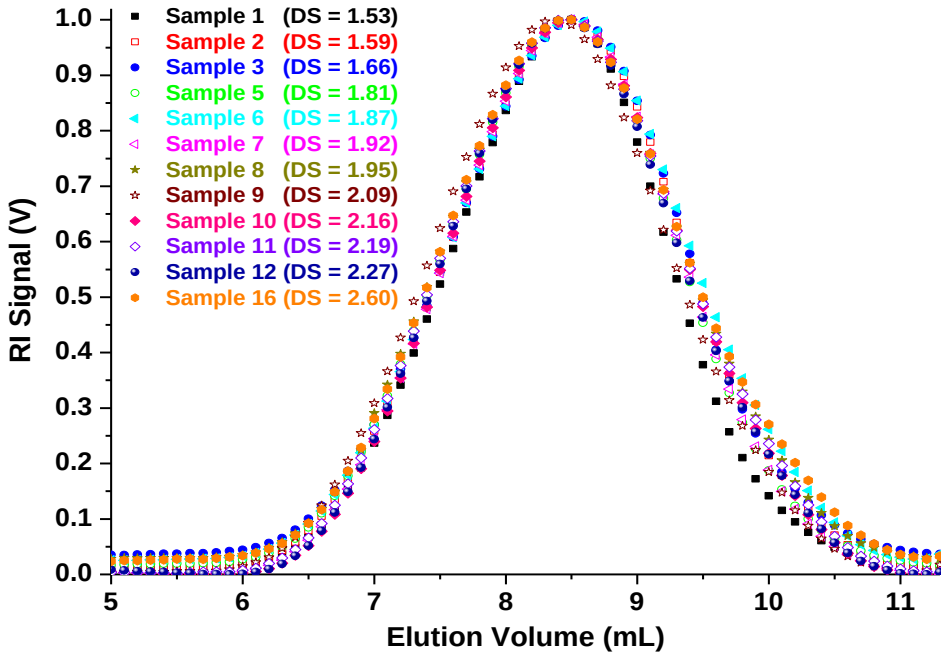

Figure 19: Normalized RI chromatograms of synthesized samples including the precursor (sample 16, DS = 2.60). Experimental conditions see figure 15.

SEC-LS provides a sophisticated way for determination of absolute molar masses. However, the price and the higher complexity usually prevent to use SEC-LS as a routine method. SEC for molar mass determination with respect to a calibration curve based on standards is still the method of choice in many laboratories. However, one of the major problems of molar mass analysis of CAs by SEC is the lack of proper CA standards as primary calibrants. CAs of low molar mass heterogeneity are not commercially available. Therefore, the suitability of other calibrants, such as PMMA, was examined. For this purpose, a set of well-defined PMMA

standards was run under the same SEC conditions to compare the PMMA-equivalent molar masses of the CAs with the absolute molar masses determined by SEC-LS.

The PMMA-equivalent molar masses of the CA samples obtained from the PMMA calibration curve are given in table 4 in comparison to the absolute M_w derived by LS (see third column of table 4).

Table 4: Comparison of absolute M_w of CAs measured by SEC-LS and relative molar masses determined by SEC with PMMA calibration (PMMA-equivalent M_w). The samples marked in grey are industrial samples.

Sample name	DS	LS-M_w [g/mol]	PMMA-equivalent M_w [g/mol]
Sample 1	1.53	57600	223000
Sample 2	1.59	72700	224000
Sample 3	1.66	73500	224000
Sample 4	1.72	44600	131000
Sample 5	1.81	68100	218000
Sample 6	1.87	64900	215000
Sample 7	1.92	63200	214000
Sample 8	1.95	76400	222000
Sample 9	2.09	70700	219000
Sample 10	2.16	71900	217000
Sample 11	2.19	71000	220000
Sample 12	2.27	74400	220000
Sample 13	2.42	64400	211000
Sample 14	2.45	64700	212000
Sample 15	2.45	93300	210000
Sample 16	2.60	69800	220000
Sample 17	2.92	175000	387000

As can be seen, the PMMA-equivalent molar masses exceed the true ones by approximately a factor of 3 revealing the differences in the hydrodynamic volumes of PMMA and CA at a given molar mass. This indicates that a calibration curve constructed using PMMA standards cannot be applied directly for the determination of true molar masses of CA. Therefore, the PMMA calibration curve has to be corrected. In other words, the PMMA calibration curve has to be converted into a CA calibration curve from which the molar masses of CAs can be recalculated using their chromatograms. That is why correction factors were aimed for, allowing calculating a CA calibration based on a PMMA calibration curve.

In order to derive suitable correction factors, the concept of broad calibration was applied [197]. For this purpose, a set of narrowly distributed standards having arbitrary chemical structures and at least either two average molar masses (e.g. M_n and M_w) of one broadly distributed sample and its chromatogram or two average molar masses of two significantly different samples and their chromatograms of the same chemical and topological structure as analyte are required. The SEC chromatograms of these broadly distributed samples and the conventional standard calibration have to be established under the same experimental conditions.

In the present case, a set of narrowly distributed PMMA standards and the LS-M_w values of CA samples together with their chromatograms were used as calibrant and broadly distributed samples, respectively. If both, the broadly distributed sample and the calibrant obey the universal calibration principle, the following equation holds true at any elution volume [198, 199]:

$$M_2 = \left(\frac{K_1 \times M_1^{a_1+1}}{K_2} \right)^{\frac{1}{a_2+1}} \qquad \textbf{Equation 29}$$

where M_2 is molar mass of the broadly distributed sample (here CA), M_1 molar mass of the calibrant (here PMMA) and K and a are the Mark-Houwink constants for the corresponding polymers in the respective solvent and at the respective temperature. The above equation can be simplified as written in the logarithmic form:

$$\log M_2 = B \times \log M_1 + \log A \qquad \textbf{Equation 30}$$

where $A = (K_1 / K_2)^{\frac{1}{a_2+1}}$ and $B = \frac{a_1 + 1}{a_2 + 1}$ are the so far unknown correction factors.

Variations in the parameters A and B lead to a parallel shift and a change in the slope of the calibration curve, respectively, relative to the base (PMMA) calibration curve. From equation 30 and the chromatograms of the broadly distributed samples, their average molar masses can be calculated, which, however, depend on the actual selection of the yet unknown parameters A and B. However, using suitable fitting algorithms the parameters A and B are varied until the calculated average molar masses of the CAs closely agree with the given set values. The so obtained A and B parameters should allow calculating a CA calibration curve. In the present thesis different sets of combinations of the CA samples were used together with the PMMA base calibration. The resulting A and B parameters given in table 5 were obtained.

Table 5: A & B parameters calculated by broad calibration approach using samples of different chromatograms measured in DMAc/LiCl system and absolute molar masses from LS; the samples used to establish the calibration curves also included.

Row number	Samples used to setup broad calibration	A	B
1	Samples (2, 4, 7, 8, 9, 11, 14, 17)	0.010	1.406
2	Samples (5, 7, 9, 10, 12, 14, 15, 17)	0.010	1.271
3	Samples (1, 2, 3, 4, 14, 15, 16, 17)	0.033	1.176
4	Samples (2, 4, 6, 8, 10, 12, 14, 16)	1.052	0.907
5	Samples (1, 3, 4, 6, 8, 9, 11, 13)	2.830	0.825
6	Samples (1, 4, 5, 7, 9, 11, 13, 16)	3.032	0.818
7	Samples (1, 2, 3, 4, 5, 6, 7, 8)	3.074	0.818
8	Samples (2, 3, 5, 6, 8, 9, 10, 13)	5.214	0.780
9	Samples (2, 3, 5, 6, 7, 8, 9, 10)	9.024	0.736
10	Samples (1, 3, 5, 7, 10, 12, 14, 16)	12.161	0.709
11	Samples (3, 5, 8, 12, 13, 14, 15, 16)	18.292	0.681
12	Samples (2, 3, 5, 7, 9, 11, 13, 15)	25.339	0.654
13	Samples (1, 3, 5, 7, 9, 11, 13, 15)	34.193	0.627
14	Samples (5, 6, 7, 12, 13, 14, 15, 16)	48.861	0.600
15	Samples (9, 10, 11, 12, 13, 14, 15, 16)	50.447	0.600

The A and B parameters were used to convert the PMMA calibration curve into CA calibration, which was subsequently used to derive the average molar masses of all CA samples based on their chromatograms. Significant deviations of the A and B values, derived using different combinations of CA chromatograms, were observed. These differences in the A and B parameters resulted in strongly differing calibration curves (see figure 20), despite the fact that the fitting procedures to calculate the A and B parameters for sample sets of table 5 showed a good agreement of the recalculated molar masses and the ones from light scattering (typical deviations ±8% except two of the industrial samples (sample 15, DS = 2.45 and sample 17, DS = 2.92), deviations ±35%, which have also shown abnormal behaviour in figure 18). The difference in the A and B parameters is because the M_ws of CAs chosen for the broad calibration are located in a very narrow range. A good agreement for the molar masses to be fitted can therefore be obtained for straight lines of different slope and intercept. Thus, the samples taken to establish broad calibration should be largely different in molar mass. In order to overcome the problem of the limited molar mass range, A and B values were calculated in another way: For five samples of different DS (sample 2, DS = 1.59; sample 6, DS = 1.87; sample 11, DS = 2.19; sample 13, DS = 2.42 and sample 16, DS = 2.60) the logarithm of the true CA molar masses from the respective

SEC-LS experiments were determined at different elution volumes. These molar masses were plotted against the corresponding PMMA-equivalent molar masses at the same elution volume. This procedure allows correlation of PMMA-equivalent molar masses with true CA molar masses over nearly two decades in molar mass. These data were fitted by linear regression as depicted in figure 20. This procedure resulted in the following A and B values:

A = 1.636

B = 0.867

For better comparison, the resulting linear fits from three different sets of A and B correction factors (A = 0.033 & B = 1.176 (red), A = 3.032 & B = 0.818 (green), and A = 48.861 & B = 0.600 (blue)) are included on the same graph.

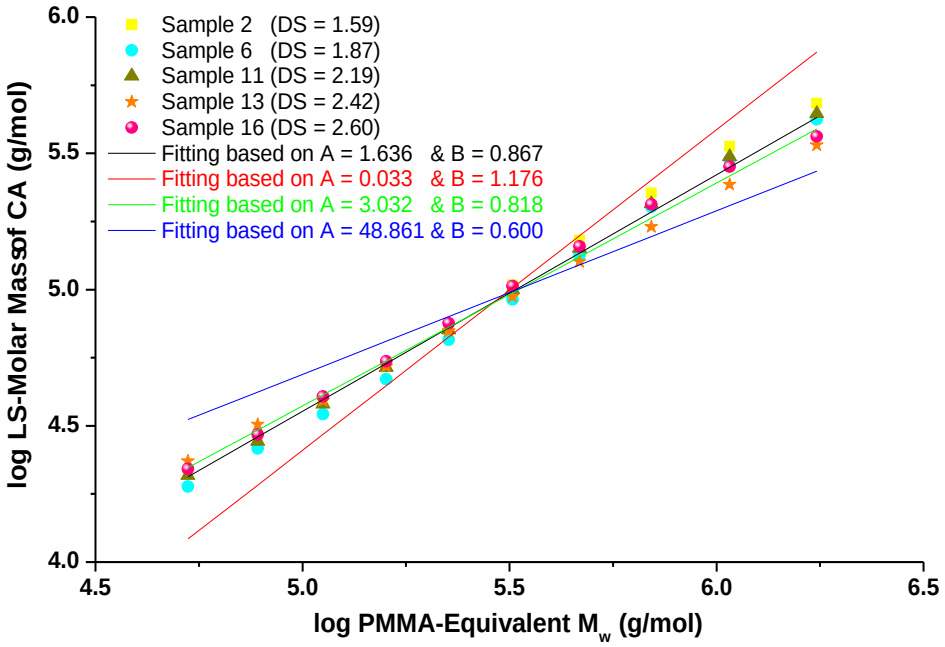

Figure 20: log of true CA molar mass versus log of PMMA-equivalent molar mass taken at different elution volume for samples of different DS. The black solid line shows the resulting linear fit for the respective data (A = 1.636 and B = 0.867) while the other solid lines show the correlations from broad calibration for A = 0.033 & B = 1.176 (red), A = 3.032 & B = 0.818 (green), and A = 48.861 & B = 0.600 (blue) (refer to table 5).

As can be seen, despite the difference in A and B sets of table 5, the resulting linear fits crossed within a very narrow range, corresponding to approx. the (nearly identical) M_ws of the CAs taken to establish the broad calibration (see the red, green and blue lines in figure 20). However, it was found that the linear fit derived from one of the broad calibration set parameters of A = 3.032 and B = 0.818 (green line) closely agrees with the one derived from the new set values of A = 1.636 and B = 0.867 (black line). The deviations of the

CA molar masses between them were less than ±10% across the complete molar mass range. The recalculated M_w derived from the new correction factors (i.e. A = 1.636 and B = 0.867) and their deviations to the absolute molar masses from LS (in %) are listed in the fourth and fifth columns of table 6, respectively. The M_w data from LS are included in this table.

Table 6: Absolute M_w from LS, recalculated M_w of all CAs using correction factors (A = 1.636 and B = 0.867) in DMAc/LiCl and its relative deviation to the absolute LS data. The samples marked in grey are industrial samples.

Sample name	DS	LS-M_w [g/mol]	Recalculated M_w [g/mol]	% Deviation
Sample 1	1.53	57600	67700	18
Sample 2	1.59	72700	67600	-7
Sample 3	1.66	73500	67700	-8
Sample 4	1.72	44600	43200	-3
Sample 5	1.81	68100	66300	-3
Sample 6	1.87	64900	65300	0.6
Sample 7	1.92	63200	65300	3
Sample 8	1.95	76400	67100	-12
Sample 9	2.09	70700	66600	-6
Sample 10	2.16	71900	65900	-8
Sample 11	2.19	71000	66700	-6
Sample 12	2.27	74400	66800	-10
Sample 13	2.42	64400	64900	0.8
Sample 14	2.45	64700	65100	0.6
Sample 15	2.45	93300	64200	-31
Sample 16	2.60	69800	66800	-4
Sample 17	2.92	175000	108000	-38

As can be seen, the highest deviations again arise for the two of the industrial samples (sample 15, DS = 2.45 and sample 17, DS = 2.92) which have also shown abnormal behaviour in figure 18. A good agreement between the molar masses from the above new approach and those from LS for all other samples indicates the reliability of this approach for SEC calibration, in case the broadly distributed samples used for broad calibration are not satisfactory different in their true molar masses.

It is interesting to mention once more that the molar mass conversion from PMMA to CA using the equation 30 is irrelevant to the DS of the analyzed CA sample.

After developing an SEC method for the determination of average molar masses and molar mass distributions of CAs, the next investigation will be dedicated to develop a gradient HPLC method to separate the CA samples with respect to DS. The detailed experimental results will be represented in 4.2.2.

4.2.2. Separation of CA according to DS

The first step in setting up a chromatographic gradient method is to select a suitable stationary phase based on the separation to be established. In addition, at least two suitable solvents differing in eluent strength need to be identified. In normal-phase HPLC, a polar stationary phase is employed together with a gradient whose polarity increases in the course of the chromatographic run. Ideally, the sample is dissolved in a good solvent and then injected into a mobile phase of weak eluent. The solvent should allow for adsorption of the sample to the stationary phase. A complete desorption of the sample components should take place by continuously increasing the eluent strength of the mobile phase. In gradient chromatography of polymers the desorption occurs at different eluent compositions which should correlate with the chemical composition of individual polymer chains in order to result in a separation with respect to chemical composition.

The most common polar columns applied in normal-phase gradient system are packed with bare or polar modified silica. The surface of the silica stationary phase is covered with silanol groups (Si-OH) which enhance polar interactions with the sample molecules resulting in an increase in retention with sample polarity. Since our CA samples contain polar groups, they should interact with the polar groups of the stationary phase resulting in their adsorption. Therefore, a stationary phase consisting of bare silica has been used in the development of a gradient method for separation of CAs according to DS.

In order to identify suitable eluents for gradient chromatography of the CA samples, we take advantage of the solubility results in 4.1.2 on page 41. As already reported in table 2 DMSO and DMAc/LiCl were the only two solvents capable to dissolve all the samples, irrespective of DS. Since the samples are only partially soluble in DMAc without the addition of LiCl and since the use of non-volatile LiCl is incompatible with evaporative light scattering detection (ELSD), the use of DMSO was the preferred choice as a sample solvent. Nevertheless, DMSO could not be used as an initial eluent because it produced an excessively high back pressure and detector noise. In addition, DMSO did not allow the polymer to be adsorbed on the column due to its high solvent strength. Thus, DMSO acts as desorli. Furthermore, the evaporation difficulty due to the high boiling point of this solvent prevented using DMSO as eluent for subsequent LC-FTIR experiments.

Seeking for two solvents to start a gradient run, the following experiments were conducted: 0.1 mL of 1.0 mg/mL solutions of the lowest and highest DS CA (sample 1, DS = 1.53 and

sample17, DS = 2.92, respectively) in DMSO were taken and a second solvent (in this case, DCM) was added dropwise to identify the composition of the eluent mixture at which precipitation occurs. It turned out that the DMSO solutions could be infinitely diluted with DCM without visible precipitation. Interestingly, the CA samples could not be dissolved in DCM directly (see table 2). However, dissolution of the samples in DMSO and subsequent dilution with DCM might provide a suitable way to inject the samples at adsorbing conditions without precipitation. If the CAs are injected into 100% DCM as eluent onto the polar silica stationary phase, they should become adsorbed due to the low polarity of DCM. Thus, another solvent, which has a higher polarity than DCM, should desorb the samples resulting in elution from the column. In order to identify this solvent, 1.0 mL of the lowest and highest DS CA (sample 1, DS = 1.53 and sample 17, DS = 2.92, respectively) were prepared in DMSO/DCM (10/90, v/v) mixtures at a concentration of 0.1 mg/mL, by first dissolving the samples in DMSO and subsequent dissolution using DCM. The mixtures were taken and the third solvent (in this case, MeOH) was added dropwise. It was found that the samples were soluble until the MeOH content reaches 62% for the sample of highest DS and 80% for the lowest DS.

In preliminary chromatographic experiments it now needs to be confirmed that CAs (dissolved in DMSO) adsorb completely from DCM as initial eluent on the silica stationary phase, while the addition of MeOH causes desorption. Therefore, a simple linear 10 min gradient running from 100% DCM to 100% MeOH was applied. The resulting chromatograms along with the eluent composition at the detector are shown for selected samples (sample 1, DS = 1.53; sample 5, DS = 1.81; sample 6, DS = 1.87 and sample 17, DS = 2.92) in figure 21a. The delay of 5.1 mL of the gradient composition reaching the detector is caused by both the dwell volume (V_d), i.e. the volume between the mixing chamber of the instrument and the column head, and the void volume (V_0) of the chromatographic system. This volume shift has to be considered in calculating the eluent composition of the CA samples at the time of elution.

As can be seen, all the peaks elute within the gradient (i.e. at times larger than 5.1 min) but at different elution times, i.e. at different eluent compositions. This means that all the samples are initially adsorbed onto the stationary phase despite the use of the DMSO as sample solvent. Desorption of the low DS samples in the narrow DS-range DS = 1.5 – 1.8 occurs at significantly higher MeOH contents than necessary for the elution of all samples having DS > 1.8. It is obvious that the samples of the DS > 1.8 are not separated but coelute. Furthermore, it is interesting to observe the bimodal characteristics of the eluting peaks

(except for sample 17, DS = 2.92). A narrow sharp peak appears at a low elution volume within the gradient prior to the elution of the main broad sample peak.

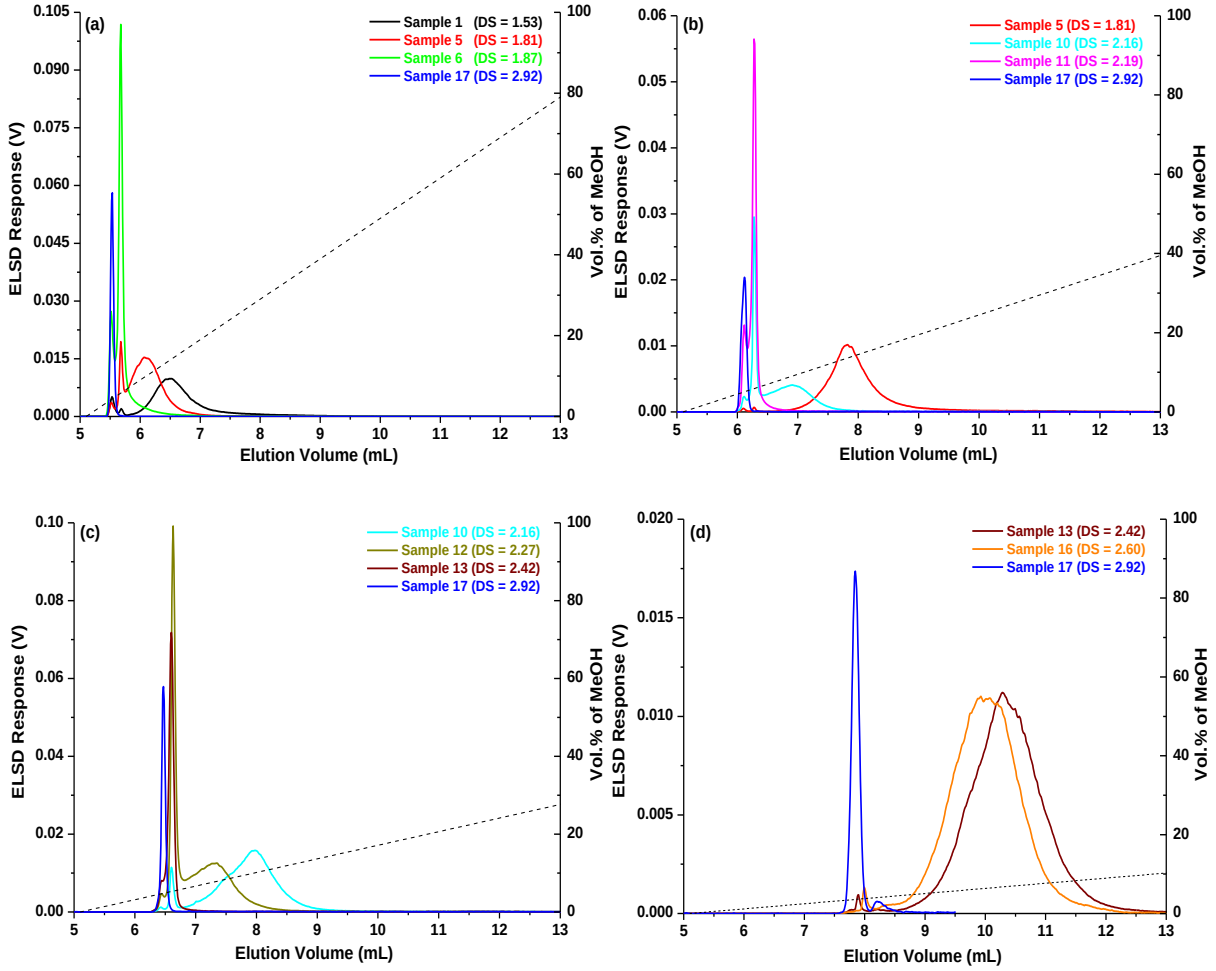

Figure 21: Overlay of chromatograms of CAs having different DS; Sample solvent: DMSO; Injection volume: 15 µL (conc. = 0.15 – 1.5 g/L)*; Gradient program: Linear change from 100% DCM to 100% MeOH **(a)**, 100% DCM to 50% MeOH **(b)**, 100% DCM to 35% MeOH **(c)** and 100% DCM to 13% MeOH **(d)** in 10 min; Column: Nucleosil (25 cm × 0.4 cm I.D., 5 µm) at 35 °C; Flow rate: 1.0 mL/min; Detector: ELSD (nebulization temperature (NEB Temp) = 50 °C, evaporation temperature (EVAP Temp) = 90 °C and gas flow = 1.0 SLM). Dotted lines represent the eluent composition at the detector. (* No column overloading was observed; see figure 26)

Generally, a steep gradient will compress the eluting peaks and often reduces the resolution. Accordingly, lowering the gradient slope may improve the resolution of the high DS samples in the range DS = 1.8 to DS = 2.9. Therefore, the gradient slope was systematically reduced by running linear 10 min gradients from 100% DCM to 50%, 35% and 13% MeOH, respectively. The chromatograms of selected samples are shown in figure 21b-d. As the slope of the gradients becomes more shallow, the peaks of the higher DS samples shift to the higher

elution volume and a better resolution for the higher DS samples is obtained. However, with the final MeOH content decreasing from 100% MeOH to 50%, 35%, and 13% MeOH, the lower DS samples might be partially desorbed or completely retarded by the column when the gradient slope is reduced. Again, bimodal chromatograms are observed. The origin of which will be investigated in further experiments.

More detailed information about the influence of gradient slope on the DS-range possible to be separated is collected in table 7.

Table 7: Relation between the gradient and the separation and/or coelution of a DS-range.

Linear gradient		**Resolved approx. DS-range**	**Coeluted approx. DS-range**
t = 0 min	t = 10 min		
100% DCM	100% MeOH	DS = 1.5 to DS = 1.8	DS > 1.8
100% DCM	50% MeOH	DS = 1.8 to DS = 2.2	DS > 2.2
100% DCM	35% MeOH	DS = 2.2 to DS = 2.4	DS > 2.4
100% DCM	13% MeOH	DS = 2.4 to DS = 2.9	–

From table 7 it becomes clear that within each gradient a particular DS-range can be separated while the samples of lower DS may not be desorbed and those possessing a higher DS may coelute. This indicates that none of these linear gradients within the gradient run time is capable of separating the samples for the whole DS-range.

In the next experiments, the reproducibility of all chromatograms and the recovery of the samples (sample 1, DS = 1.53; sample 5, DS = 1.81; sample 10, DS = 2.16 and sample 13, DS = 2.42 seen in figure 21a-d, respectively) at each gradient step were tested. Figure 22 shows the resulting reproducibility of all eluting chromatograms. As can be seen, all the traces are well overlaid indicating good reproducibility.

It is known that the eluent composition at the time of elution in gradient chromatography is very close or equal to the critical one determined by isocratic experiments, at which the polymer molecules can elute from the column [132, 200, 201]. Therefore, to determine the recovery, the eluent composition at the time of elution for each sample was calculated from the gradient. At the so determined compositions, isocratic experiments were carried out. The details of the recovery experiments for one of the sample (sample 1, DS = 1.53) are exemplified here. First, the eluent composition at the time of elution for this sample was estimated to be 86/14 (v/v DCM/MeOH) from the retention volume (V_R) of a 10 min gradient

varying from 100% DCM to 100% MeOH using the following equation (Modified from equation 14):

$$\%MeOH = (V_R - V_0 - V_d) \times \frac{\Delta\%MeOH}{F \times t_G} \qquad \textbf{Equation 31}$$

where V_0 is the column void volume, V_d the dwell volume, Δ%MeOH the total change in composition of MeOH during the gradient, t_G the gradient time, and F the flow rate. Using the calculated eluent composition (86/14, v/v DCM/MeOH), 15 µL of sample 1 with a concentration of 1.5 g/L were injected onto and collected after the column in a well-defined elution range (i.e. cover the elution range of the sample).

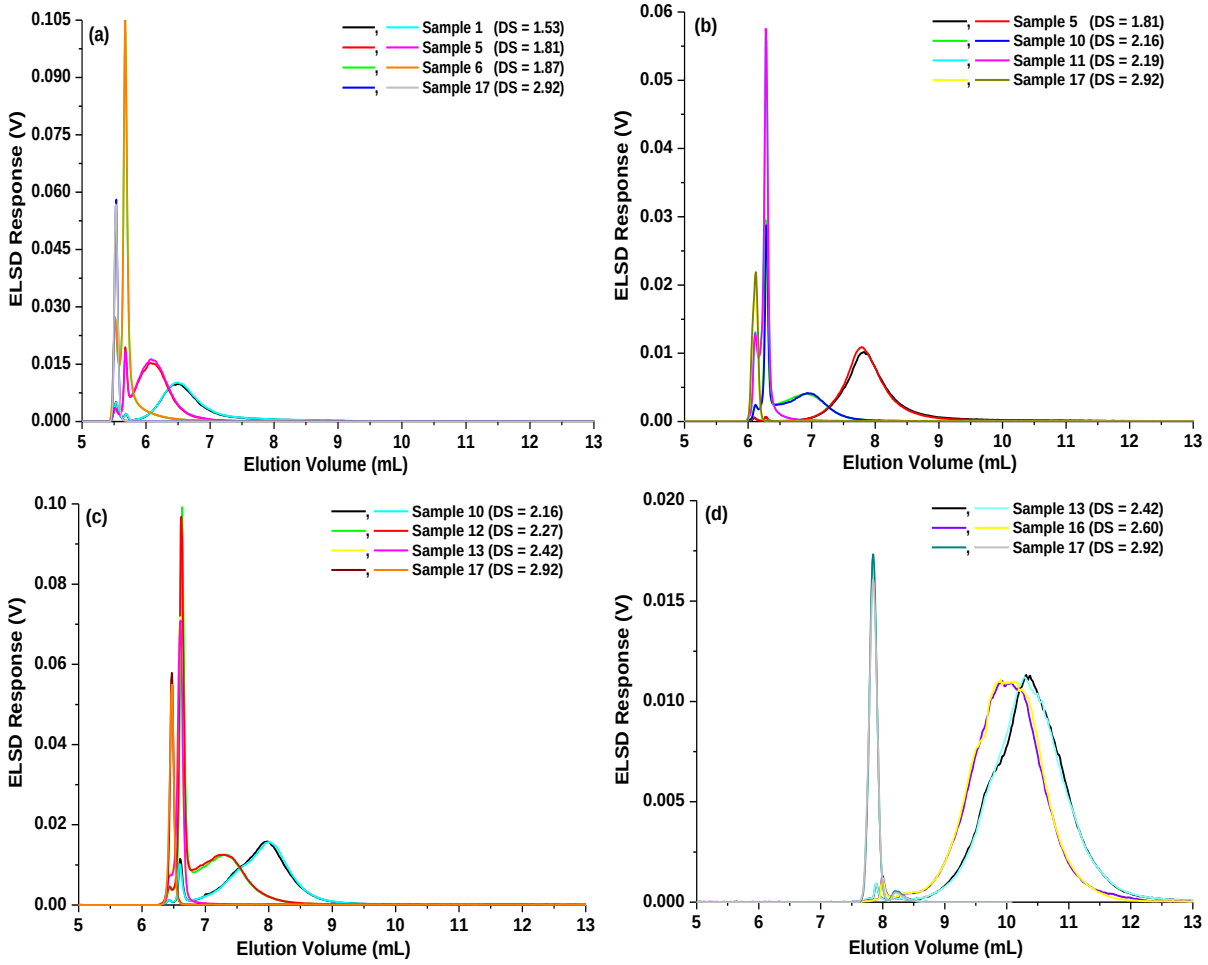

Figure 22: Reproducibility of overlaid chromatograms of CAs having different DS; Gradient program: Linear change from 100% DCM to 100% MeOH **(a)**, 100% DCM to 50% MeOH **(b)**, 100% DCM to 35% MeOH **(c)** and 100% DCM to 13% MeOH **(d)** in 10 min; Experimental conditions see figure 21.

In order to determine the concentration of the collected sample, a calibration curve was constructed by injecting known amounts of the sample with the given eluent without column and plotting the resulting peak area versus injected mass as seen in figure 23. The concentration of the collected sample was then determined from this calibration curve by injecting the collected sample without column as well. By this procedure a sample recovery of nearly 96% was obtained, which can be regarded to be quantitative with the accuracy of the method.

Following the same representative procedure, recoveries of 98% for sample 5, 96% for sample 10 and 99% for sample 13 from a linear gradient step of 100% DCM to 50% MeOH, 100% DCM to 35% MeOH and 100% DCM to 13% MeOH, respectively, were obtained.

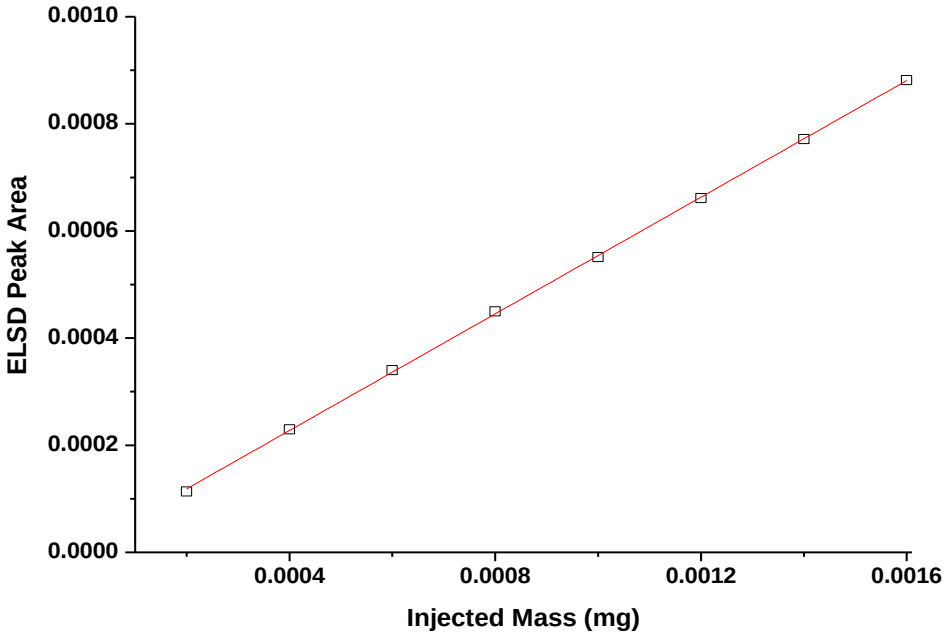

Figure 23: Peak area of ELSD as a function of injected mass; Sample 1 (DS = 1.53) dissolved in DMSO; Injection volume range: 5 µL – 40 µL (conc. = 0.04 g/L); Eluent: 86% DCM + 14% MeOH; Without column; Flow rate: 1.0 mL/min; Detector: ELSD (NEB Temp = 50 °C, EVAP Temp = 90 °C and gas flow = 1.0 SLM).

In order to investigate the origin of the sharp peaks at low retention times seen in figure 21a-d and in order to minimize or to avoid these early eluting peaks, the influence of experimental parameters such as injected amount of sample, injection volume and type of the sample solvent, additional isocratic and gradient elution steps were investigated. Meanwhile, the special emphasis is laid on the sample-size parameter for its effect on sample retention.

In all cases, the linear gradient program from 100% DCM to 13% MeOH in 10 min and a sample eluting in this range (e.g. sample 15, DS = 2.45) were selected. The first experiments were dedicated to study the influence of injection volume of the sample solvent (DMSO) on the occurrence of peak bimodality. For this purpose, approximately the same amount (0.03 mg) of the sample 15 (DS = 2.45) was injected by varying the injection volume in the range 20 µL – 55 µL. The resulting chromatograms along with the eluent composition at the detector are shown in figure 24.

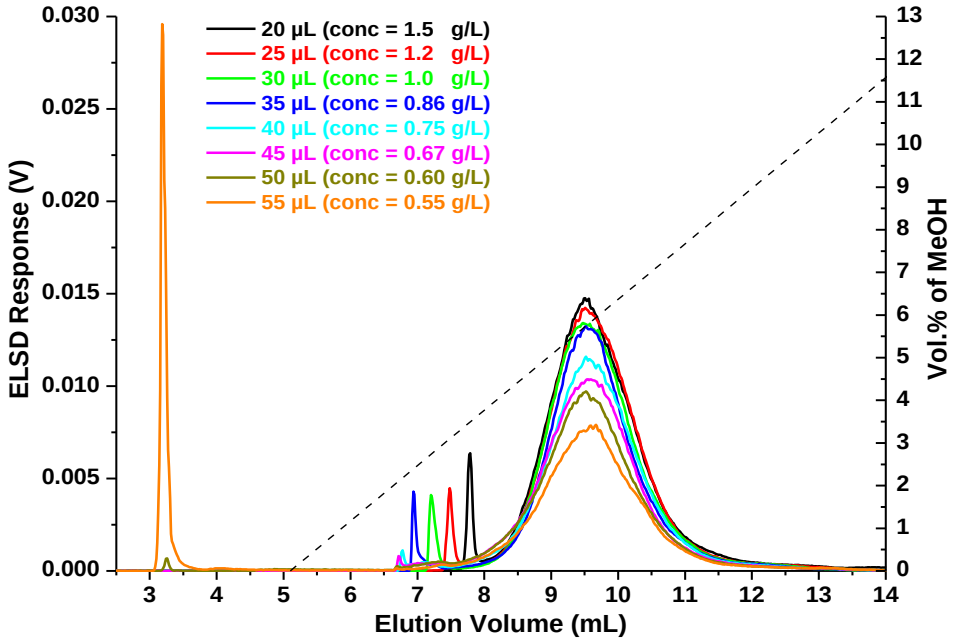

Figure 24: Influence of injection volume at constant injected sample mass on the elution behaviour of CA; Sample 15 (DS = 2.45) dissolved in DMSO; Gradient program: Linear change from 100% DCM to 13% MeOH in 10 min. Experimental conditions see figure 21. Dotted line represents the eluent composition at the detector.

Each chromatogram is composed of a broad sample peak covering an elution volume range from 8.0 – 12.0 mL and a narrow sharp peak (prepeak). By increasing the injection volume the peak area of the broad peak decreases, however its elution position remains unchanged. On the other hand the narrow prepeak apparently shifts to lower elution volumes until an unretained peak is observed around 3.0 – 3.5 mL for injection volumes $\geq$ 50 µL. This unretained peak appears at the elution volume of the solvent peak and is apparently caused by the elution of a part of the sample. According to the definition given in 3.2.1 on page 31 such elution peaks called breakthrough peak and resulted from a significant difference in eluent strength between the DCM and DMSO.

Jiang et al. investigated the parameters which cause the breakthrough phenomenon and stated that if a polymer dissolved in a thermodynamically strong eluent is injected into a weak eluent breakthrough peaks might appear [202]. In the present case, the CAs were dissolved in DMSO, which is a strong eluent, and were injected into the weak initial solvent DCM. Therefore, the breakthrough peak at high injection volume was observed. In order to avoid breakthrough peaks injection volume should be kept small. Therefore, the injection volume was restricted to ≤ 20 µL in the following experiments, where pure DMSO was used as the sample solvent.

It is already mentioned that the samples in DMSO can infinitely be diluted by DCM without precipitation. Accordingly, an attempt was given to reduce the eluent strength of the initial solvent DMSO by the addition of DCM. For example, a series of 1.5 g/L of the sample 15 (DS = 2.45) prepared in DMSO with 10, 30, 50, 70, and 92% DCM was injected into the linear gradient (100% DCM to 13% MeOH in 10 min). All chromatograms along with the eluent composition at the detector are represented in figure 25.

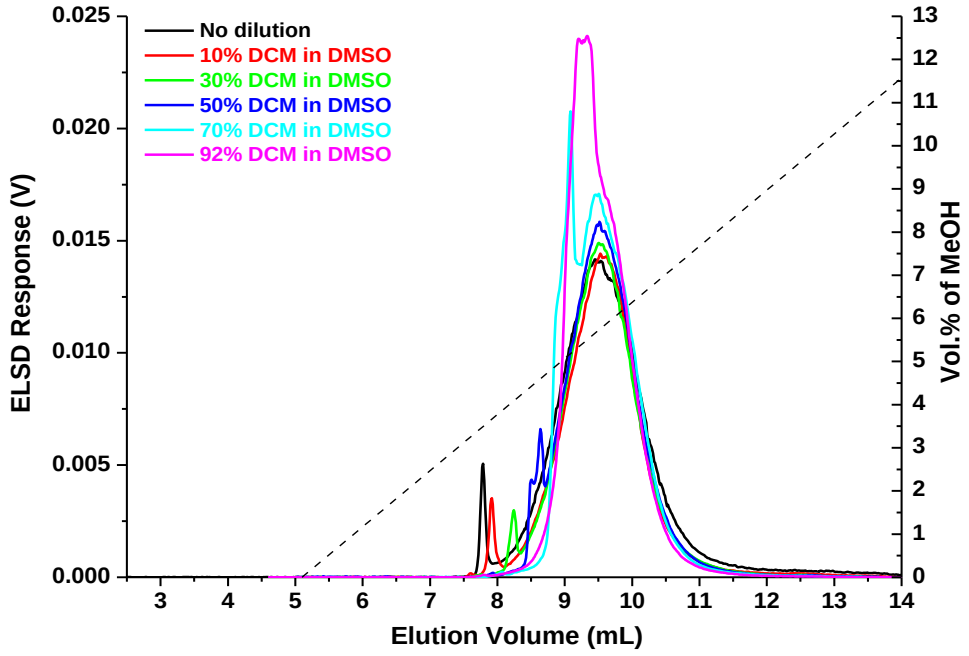

Figure 25: Influence of initial solvent strength on the elution behaviour of CA; Sample 15 (DS = 2.45) in DMSO diluted with 10, 30, 50, 70, and 90% DCM; Injection volume: 20 µL (conc. = 1.5 g/L); Gradient program: Linear change from 100% DCM to 13% MeOH in 10 min. Experimental conditions see figure 21. Dotted line represents the eluent composition at the detector.

It is obvious that the prepeak shifts to the higher elution volume with increasing amount of DCM in DMSO while the sample elution position remains nearly unchanged. At the highest

amount of DCM, the remaining DMSO has still a large impact on elution behavior of the sample, as the peak loses its Gaussian peak shape. Several other weak solvents were examined but the results were pretty similar. Therefore, dilution of the samples with a weaker eluent cannot completely eliminate the effect of DMSO on the elution behavior of the sample molecules.

For the adsorption-controlled systems, it has been generalized that the retention volume decreases with increasing sample load on the column when the adsorption isotherms become non-linear (the column is overloaded) [74, 203, 204]. Since the sample-size criterion is general and can be applied to HPLC of polymers as well, it was checked, whether the injected sample amount influences the retention volume. Therefore, different masses ranging from 0.012 to 0.054 mg of sample 15 (DS = 2.45) were injected using the same linear gradient system (100% DCM to 13% MeOH in 10 min). Figure 26 shows the chromatograms along with the eluent composition at the detector.

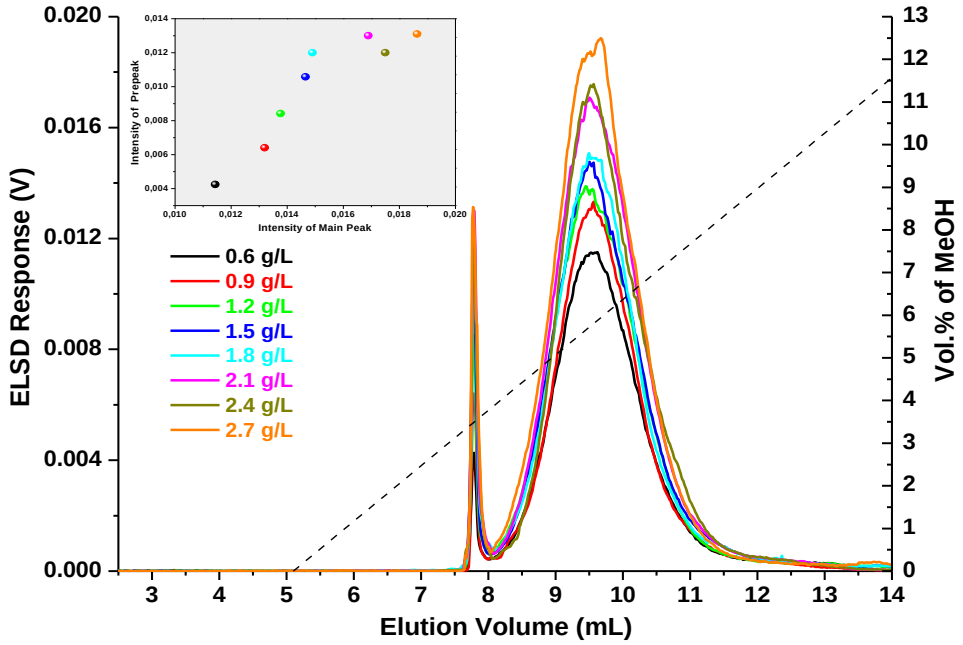

Figure 26: Influence of injected mass at constant injection volume on the elution behaviour of CA; Sample 15 (DS = 2.45) dissolved in DMSO; Injection volume: 20 µL with varied concentrations; Gradient program: Linear change from 100% DCM to 13% MeOH in 10 min. Experimental conditions see figure 21. Dotted line represents the eluent composition at the detector. (The small window depicts variation in intensity of prepeak to intensity of main peak)

The prepeak becomes more pronounced at an unshifted position with increasing the sample-size. In addition, no notable shift in elution position of the main sample peak is

observed. Finally, nearly constant relative intensities between the prepeak and main peak are seen for the injected mass range of 0.012 – 0.054 mg. Thus, no effects of column overloading are observed.

So far, it has not been understood whether the occurrence of the prepeaks is caused by the solvent of DMSO or not. A possible way to clarify this point is by displacing the sample solvent with a lower polar one. Fortunately, the solubility studies described in 4.1.2 on page 41 revealed the possibility to use 1,4-dioxane to dissolve the high DS CAs. Unfortunately, this solvent cannot be applied for the entire system since it does not dissolve the lower DSs. The polarity index of 1,4-dioxane is much lower than the one of DMSO, but in-between the ones of DCM and MeOH. It was therefore tested, whether the sample preparation in mixtures of DMSO and 1,4-dioxane was possible to eliminate the prepeaks. However, these experiments failed similar to the sample preparation in mixtures of DMSO and DCM (see figure 25).

Figure 27 shows the comparison of the chromatograms along with the eluent composition at the detector for the sample 15 (DS = 2.45) dissolved in 1,4-dioxane and DMSO, individually, and injected into the linear gradient system (100% DCM to 13% MeOH in 10 min).

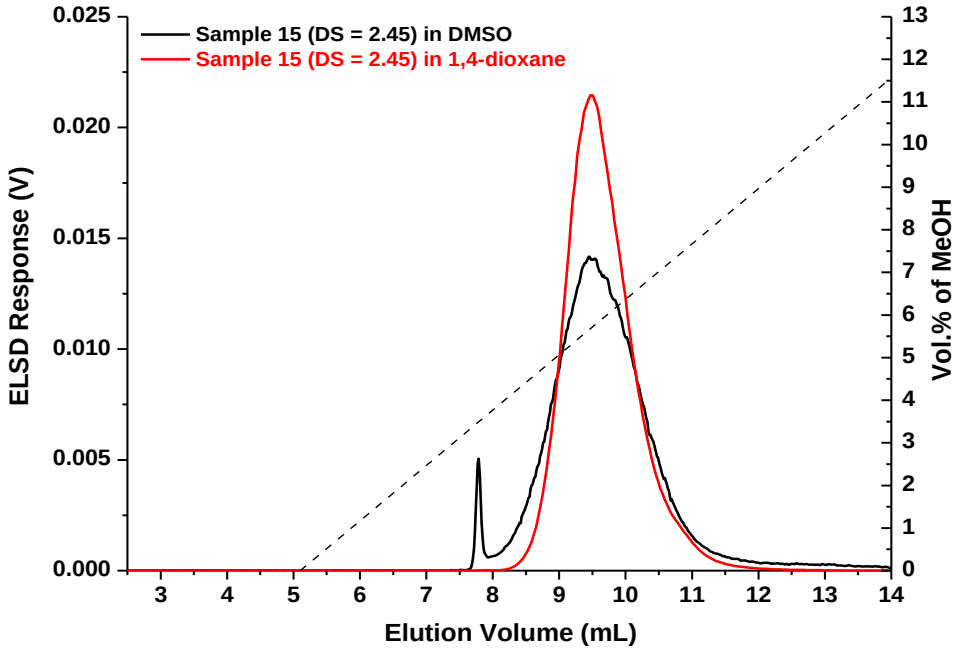

Figure 27: Effect of sample solvent on prepeaks; Injection volume: 20 µL (conc. = 1.5 g/L); Gradient program: Linear change from 100% DCM to 13% MeOH in 10 min. Experimental conditions see figure 21. Dotted line represents the eluent composition at the detector.

As can be seen, the prepeak which usually is observed when dissolving the sample in DMSO disappeared when 1,4-dioxane was used as the sample solvent, resulting in a monomodal peak. Therefore, it is reasonable to deduce that the solvent of DMSO is the main cause of an early eluting part of the sample.

It can be hypothesized that DMSO can also adsorb to the polar silica surface similar to the sample molecules. Since the elution order is based on polarity in normal-phase gradient chromatography, fractions of high DS within a single sample, which will be adsorbed only weakly, compete with DMSO. The CAs of high DS might have a lower affinity to the silica than DMSO and will therefore elute from the silica surface. As a result, a prepeak is observed. This assumption paves the way to modify the gradient by addition of another elution step to avoid the prepeaks. This can be either an isocratic or a gradient step. Within this additional step, DMSO may be washed off while the polymer molecules should remain adsorbed on the column. In the subsiding second step solvent-free sample molecules (i.e. free from DMSO) may start eluting. To examine the workability of the modified gradients, an isocratic step of 100% DCM for 5 min and 10 min as well as a 10 min linear gradient step of 0 – 1% MeOH, respectively, were added as the first step before the gradient step of 0 – 13% MeOH. The effect on the elution of sample 15 (DS = 2.45) in these gradients was examined. Figure 28a-d shows the resulting chromatograms along with the eluent compositions at the detector. The corresponding gradient programs are summarized in table 8.

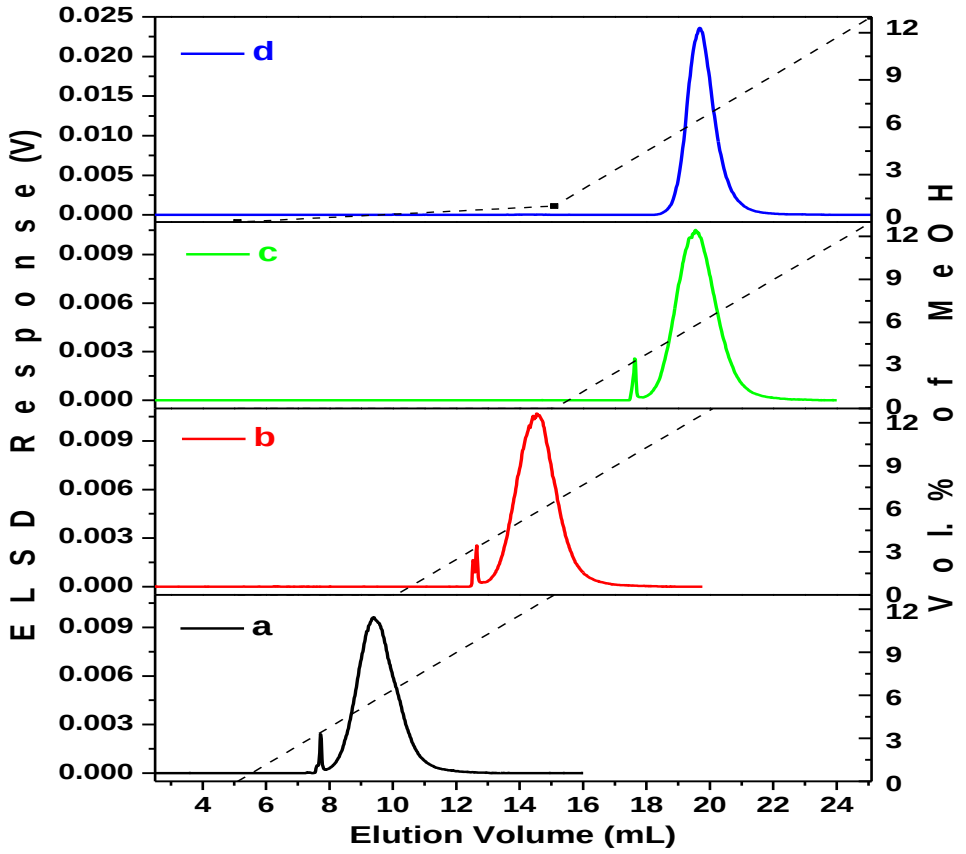

Figure 28: Effect of additional isocratic or gradient step on prepeaks; Sample 15 (DS = 2.45) dissolved in DMSO; Injection volume: 20 µL (conc. = 1.5 g/L); Eluent program: Refer to table 8; Experimental conditions see figure 21. Dotted lines represent the eluent composition at the detector.

Table 8: Description of mobile phase programs to study the effect of additional isocratic or gradient on prepeaks.

Experiment	Mobile phase program	
	t (min)	% MeOH
a	0	0
	10	13
b	0	0
	5	0
	15	13
c	0	0
	10	0
	20	13
d	0	0
	10	1
	20	13

As can be seen, the prepeaks could not be eliminated by the addition of an isocratic step in pure DCM. The peaks are shifted to the higher elution volume by 5 mL and 10 mL,

which correspond to the run times of the additional isocratic steps (b and c, respectively, relative to a in figure 28). However, the prepeak remains. This means that pure DCM cannot desorb DMSO from the column surface. In contrast, a very shallow linear gradient of just 0 – 1% MeOH was enough to completely suppress the activity of the DMSO, resulting in a monomodal peak for the sample (d relative to a in figure 28). This was somehow unexpected since the prepeaks eluted at eluent compositions of around 3% MeOH. An explanation for this slight discrepancy is hard to give. However, the gradient step for the elimination of the prepeak needs to be implemented in a final optimized gradient.

Since it was not possible to separate CA samples over the complete DS-range in one single 10 min linear gradient and since a very shallow gradient of 0 – 100% MeOH for a long period of time might cause detection problems due to a decrease in sample concentration by dilution, a multi-step gradient suitable to separate samples of the complete DS-range was developed by combining the different gradients. The final optimized gradient is given in table 9 and the resulting chromatograms obtained in this gradient along with the eluent compositions at the detector are shown in figure 29.

Table 9: Gradient profile of the multi-step gradient from DCM to MeOH.

t (min)	0	10	20	30	40	50	50.01
% MeOH	0	1	4.5	13	35	70	0

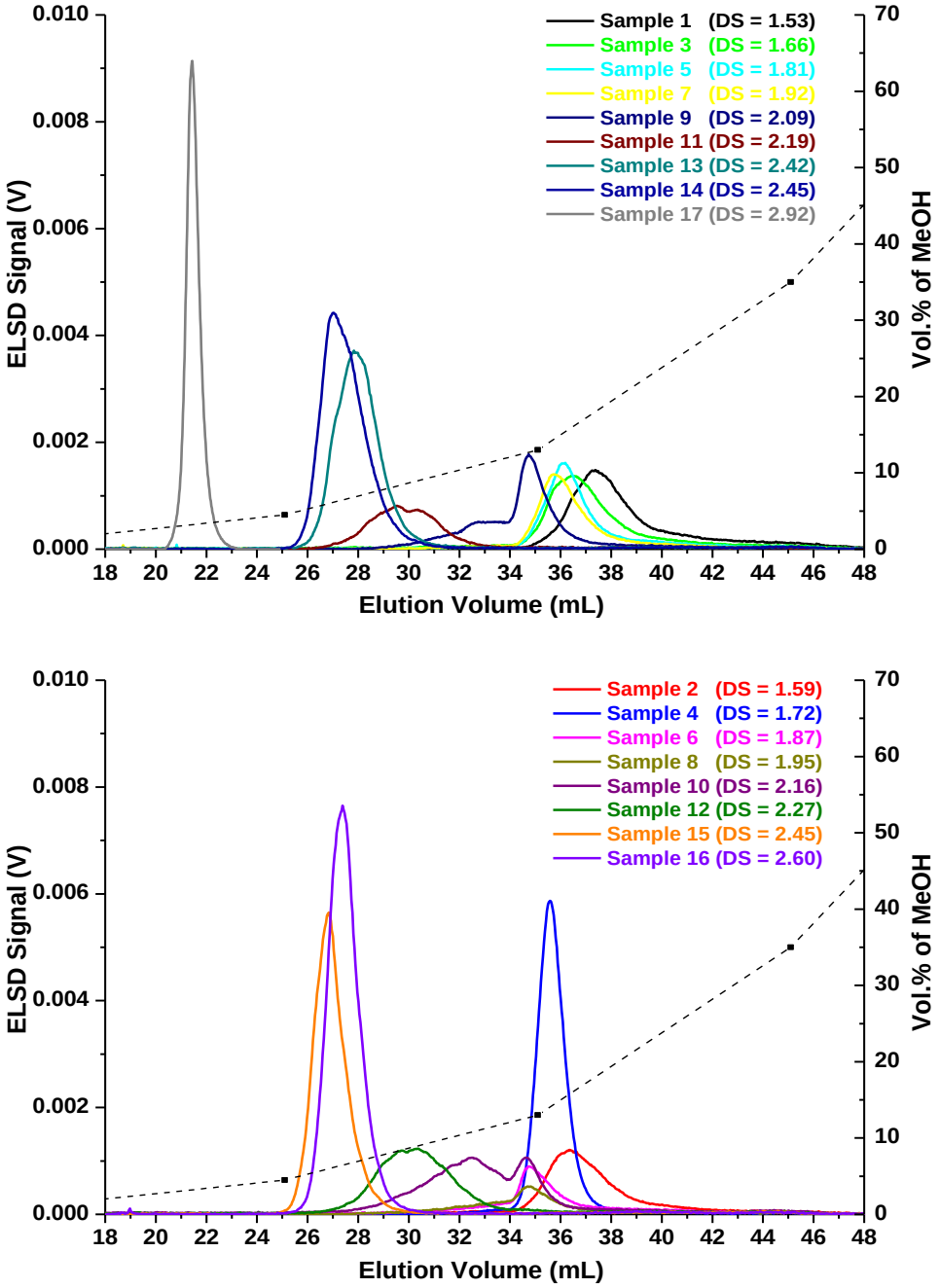

Figure 29: Superimposed chromatograms of CAs having different DS in the multi-step gradient; Samples dissolved in DMSO; Injection volume: 15 µL (conc. = 1.5 g/L); Gradient program: Refer to table 9; Experimental conditions see figure 21. Dotted lines represent the eluent composition at the detector.

As can be seen, CAs of different DS elute at different retention times without any prepeaks. The peak maxima are observed at MeOH contents of less than 20%. However, some peaks of low DSs extend to MeOH contents of up to 40%. The less polar the CA i.e. the higher the DS, the lower is the MeOH content required for desorption. The MeOH range required for desorption is much lower than the MeOH content required for the precipitation

determined before (MeOH content of 62% for the sample of highest DS and 80% for the lowest DS, see page 64). It can therefore be concluded that the separation of CAs in the developed gradient is based on adsorption-desorption mechanism rather than on precipitation-redissolution.

As it is known that interaction chromatography might be affected by chemical composition and molar mass, it is appropriate to have a closer look on both parameters. Starting with chemical composition (DS), the elution volume at peak maximum (V_{apex}) for all samples taken from figure 29 was plotted versus average DS in figure 30. The industrial samples are indicated by a black rectangle (■) and those synthesized in this work including the precursor (sample 16, DS = 2.60) by a green one (■).

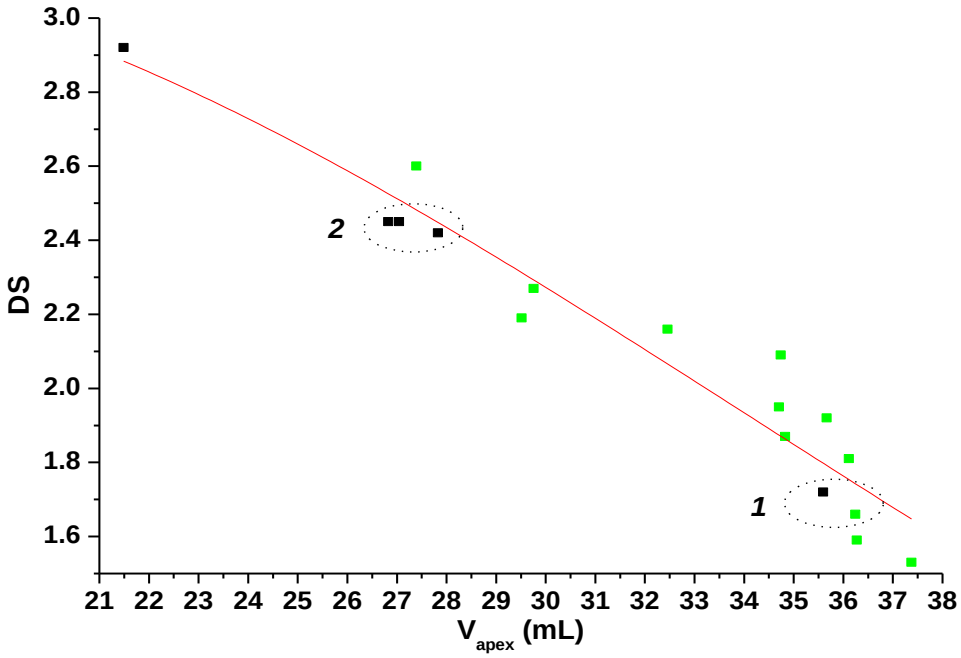

Figure 30: Chromatographic retention as a function of DS for the optimized gradient given in table 9. ■: Industrial samples ■: Samples synthesized and the precursor.

Despite some scattering, the samples (including the precursor) elute clearly from highest to lowest DS. The LS data of these samples (see table 3) revealed that they are very similar in their weight average DP (DP_w) and DP_w-distribution. Thus, from figure 30 it can be concluded that a separation with regard to DS is realized within the investigated DS-range for samples of identical DP.

The mechanism of the separation with regard to the chemical composition (DS) can be explained as follows: In the beginning of the gradient from DCM to MeOH, the composition of DCM in the eluent is large enough to allow adsorbing the CAs onto the stationary phase

through enthalpic interactions between the active sites of the stationary phase and the hydroxyl groups of CAs. By gradually increasing the polarity of the eluent (or eluent strength) i.e. increasing MeOH content, the polymer molecules will be desorbed with respect to their polarity. Less polar (higher substituted) molecules elute earlier followed by stronger polar (lower substituted) ones. This is because of the weaker interaction strength of the higher DS than the lower DS. Furthermore, this elution sequence of CAs on silica is in agreement with the general rule in normal-phase chromatography. As a result, the separation according to increasing polarity and thus according to decreasing DS has been obtained.

To elucidate the molar mass contribution of the separation process under these conditions, samples of similar DS but varying DP are required. However, these kinds of samples were not available. In order to get at least some indication on the influence of molar mass on the separation, two data sets 1 and 2 having nearly similar DS but distinct difference in molar mass are considered in figure 30 (i.e. set 1: sample 3, DS = 1.66, Mw = 73500 and sample 4, DS = 1.72, Mw = 44600; set 2: sample 13, DS = 2.42, Mw = 64400; sample 14, DS = 2.45, Mw = 64700 and sample 15, DS = 2.45, Mw = 93300). Despite nearly identical DS, one might speculate from the differences in gradient elution volume that there might be still a small influence of molar mass on the separation. Correlations between the DS and molar mass by two-dimensional separation might help to obtain information on the complete complex distribution functions. The experimental details and related results will be discussed in 4.2.3. The two-dimensional experiments should disclose to which extend the given separation by DS is influenced by molar mass.

Since it is possible to measure compositional distribution in polymers from chromatographic peak width, it is necessary to provide information on the stability or suitability of the gradient separation method. To show if there is any interference in elution behaviour when two or more samples of different DS are mixed, a mixture of three CAs of different DS (sample 4, DS = 1.72; sample 15, DS = 2.45 and sample 17, DS = 2.92) and also each sample separately are injected into the multi-step gradient system. The resulting chromatograms are represented in figure 31.

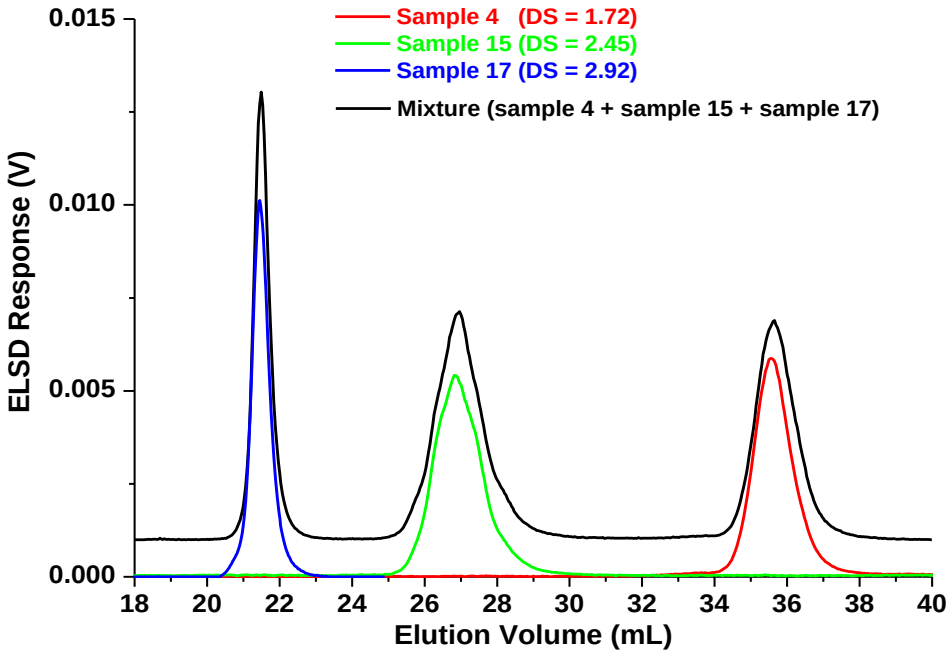

Figure 31: Superimposed chromatograms of sample 4 (DS = 1.72), sample 15 (DS = 2.45) and sample 17 (DS = 2.92), and a mixture of sample 4 + sample 15 + sample 17; Injection volume: 15 µL (conc. = 1.5 g/L for individual samples and concentration of each sample in the mixture); Gradient program: Refer to table 9; Experimental conditions see figure 21.

It is obvious that the mixture produced three peaks at different elution volumes which correspond to the elution volume of the individual component. This means that no interference occurs by mixing different DS. In another experiment, it was checked that the observed peak width is mainly the result of the separation and not of column or instrumental peak broadening. For this purpose, sample 15 (DS = 2.45) was fractionated into 0.65 mL volume slices which were re-injected into the multi-step gradient method. The resulting chromatograms of the original sample along with seven successive fractions are represented in figure 32.

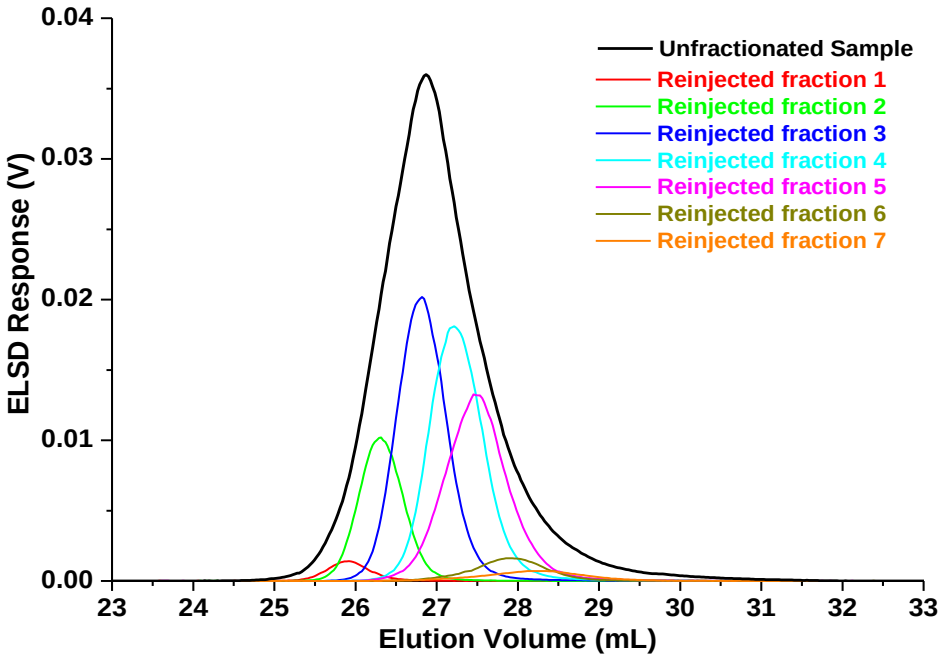

Figure 32: Superimposed chromatograms of sample 15 (DS = 2.45) before and after fractionation; Before fractionation: Polymer in DMSO diluted with 42% DCM; Injection volume: 50 µL (conc. = 5.8 g/L); After fractionation: Fractions re-dissolved in DMSO; Injection volume: 70 µL; Gradient program: Refer to table 9; Experimental conditions see figure 21.

As can be seen, all the fractions are eluted within the elution volume range of the original unfractionated sample, with clear changes in elution volume. Narrower peak widths compared to the original sample are observed. This proves that there is a true separation with only minor influence of peak dispersion.

Therefore, the gradient method developed can be applied to calculate the chemical composition distribution (DS-distribution). In order to calculate the DS-distribution, the dependence of DS on elution volume was fitted by a non-linear regression (see figure 30). For the best fit, the following equation was used:

$$DS_i = \exp(A + B \times V_{e,i} + C \times V_{e,i}^2) \qquad \textbf{Equation 32}$$

where DS_i is the DS at any elution volume of $V_{e,i}$ and A, B and C the adjustable parameters. The normalized DS-distribution, w(DS) was calculated from the ELSD signal using the following equation:

$$w(DS) = \frac{S \times \Delta V}{\Delta DS \times \Sigma(S \times \Delta V)} \qquad \textbf{Equation 33}$$

where S is the detector signal, ΔV the difference of two adjacent data points (volume strip width) and ΔDS the difference of two adjacent DS values calculated at each volume. The product of S and ΔV is, to a first approximation, proportional to the amount of polymer eluting in a volume element of [V, V + ΔV] and this must be equal to the amount of polymer within the DS-range of [DS, DS + ΔDS].

However, the ELSD's response curve is non-linear in concentration and has been reported to depend on several variables such as nature of the mobile phase, nature of the solute and the detector set conditions…etc. [205-207]. Therefore, the proportionality between detector signal and concentration is only an approximation. Since the chemical structure is one factor influencing ELSD response, it is interesting to know how the detector response varies with the DS of the sample. To eliminate the effect of changing mobile phase composition, the experiments were carried out without column by injecting the same sample mass (injection volume = 15 µL with a concentration of 2.0 g/L) under identical isocratic condition in pure DCM. The detector peak area of all of the samples as a function of average DS is shown in figure 33.

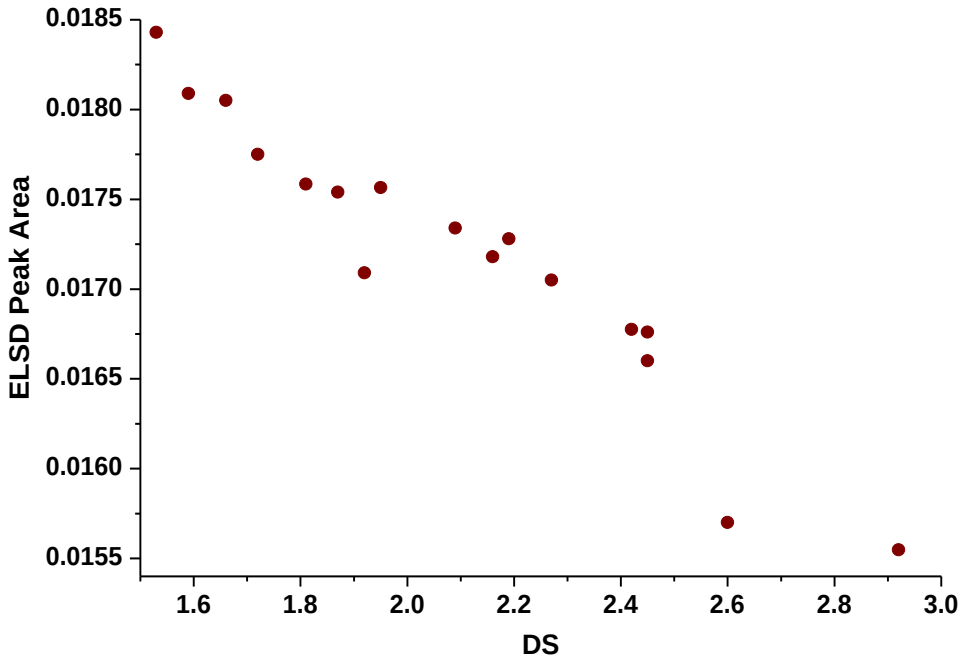

Figure 33: Dependence of ELS peak area on DS for CAs; Samples dissolved in DMSO; Injection volume: 15 µL (conc. = 2.0 g/L); Eluent program: A 2 min isocratic DCM; No column used; Flow rate: 1.0 mL/min; Detector: ELSD (NEB Temp = 50 °C, EVAP Temp = 90 °C and gas flow = 1.0 SLM).

As can be seen, the detector peak area decreases slightly with DS by approximately 15% over the DS-range from DS = 1.5 to DS = 2.9. When this procedure was repeated for different

concentrations the same dependence of peak area on DS can be observed as shown in figure 34. However, the detector response in terms of concentration is linear till the injected mass of approx. 0.03 mg. After that the response deviates from linearity for each DS.

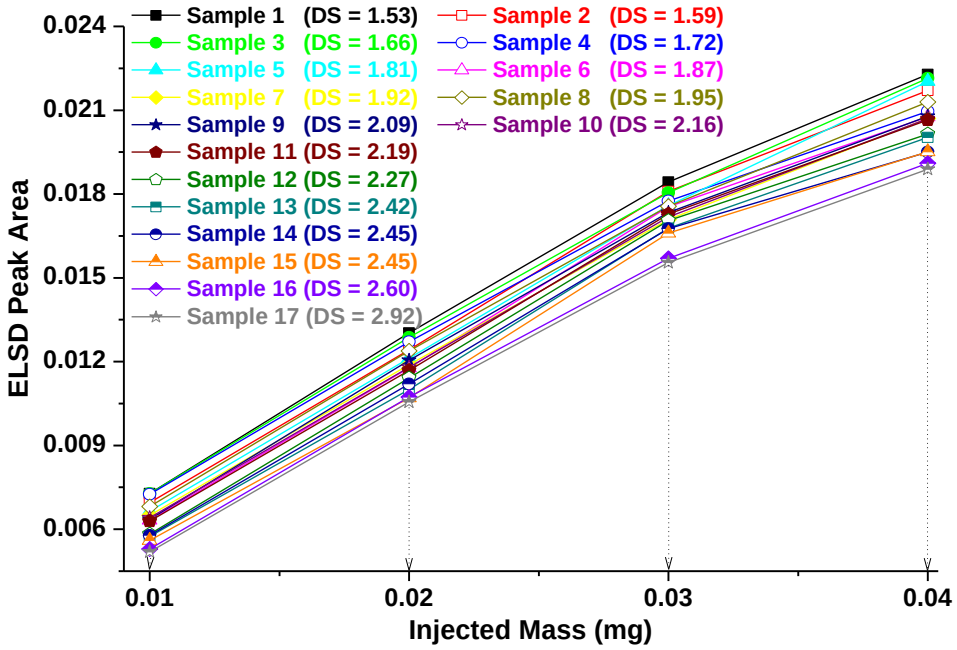

Figure 34: Dependence of ELS peak area on DS for CAs at different concentrations; Samples dissolved in DMSO; Injection volumes: 5 µL – 20 µL (conc. = 2.0 g/L); Eluent program: A 2 min isocratic DCM; No column used; Flow rate: 1.0 mL/min; Detector: ELSD (NEB Temp = 50 °C, EVAP Temp = 90 °C and gas flow = 1.0 SLM).

Since the overall change of detector response with DS is rather low, the ELSD signals for the calculation of DS-distribution were used without correction.

From equation 33 the DS-distribution for all of the CA samples was determined and the results are represented in figure 35.

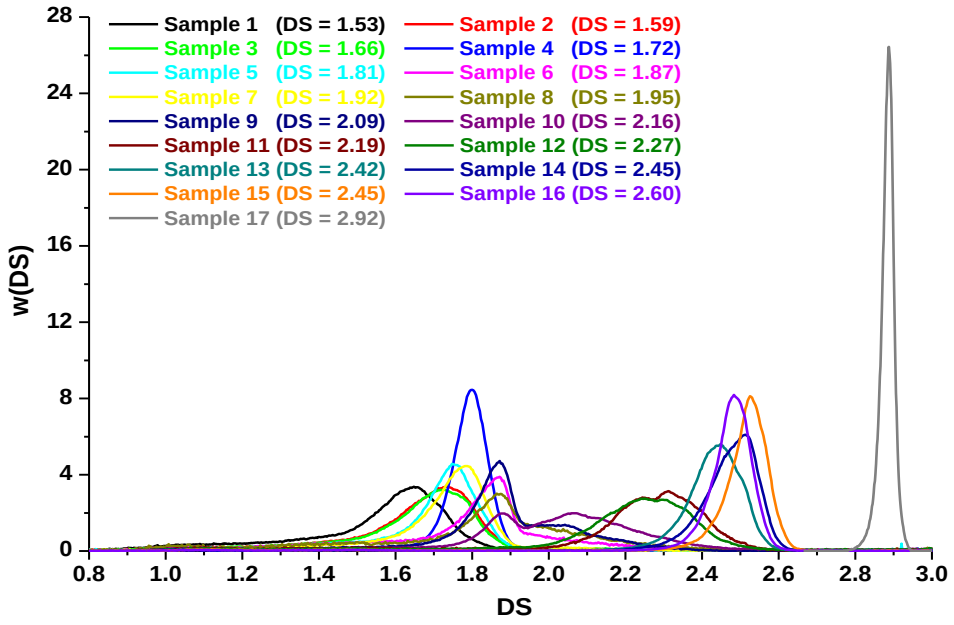

Figure 35: DS-Distribution of CAs of different DS calculated from equation 33.

Samples of different average DS possess different width, i.e. a different degree of chemical heterogeneity, with the highest DS sample (sample 17, DS = 2.92) being fairly uniform in DS while the sample of lowest DS (sample 1, DS = 1.53) contains polymer chains ranging from DS = 0.8 to DS = 1.9. However, there is no a systematic increase in degree of heterogeneity in going from the highest to the lowest DS.

An advantage of the chromatographic separation method as compared to NMR is that chromatography does not allow only calculating the weight average degree of substitution (DS_w)

$$DS_w = \frac{\Sigma w(DS) \times \Delta DS \times DS}{\Sigma w(DS) \times \Delta DS} \qquad \textbf{Equation 34}$$

but the DS variance (σ^2) as well

$$\sigma^2 = \frac{\Sigma w(DS) \times \Delta DS \times (DS - DS_w)^2}{\Sigma w(DS) \times \Delta DS} \qquad \textbf{Equation 35}$$

The variance gives a quantitative measure of the width of the DS-distribution. The calculated values for both the DS_w and the variances of the CAs are given in table 10.

Table 10: Weight average DS (DS_w) calculated from DS-distribution and variance of the DS-distribution peaks; the samples marked in grey are industrial samples.

Sample name	^{1}H-NMR DS	DS_w	σ^2
Sample 1	1.53	1.54	0.05
Sample 2	1.59	1.65	0.06
Sample 3	1.66	1.70	0.12
Sample 4	1.72	1.78	0.01
Sample 5	1.81	1.73	0.11
Sample 6	1.87	1.82	0.12
Sample 7	1.92	1.75	0.09
Sample 8	1.95	1.83	0.12
Sample 9	2.09	1.87	0.05
Sample 10	2.16	2.04	0.14
Sample 11	2.19	2.19	0.11
Sample 12	2.27	2.20	0.13
Sample 13	2.42	2.39	0.07
Sample 14	2.45	2.42	0.06
Sample 15	2.45	2.46	0.08
Sample 16	2.60	2.44	0.05
Sample 17	2.92	2.88	0.0007

As expected, the DS values determined by NMR and DS_w values calculated from DS-distribution are quite close to each other. The large difference in the value of variance for the highest and lowest DS affirms our previous observation of the difference in degree of heterogeneity between these two samples. A comparison among samples from different origin can be made based on the variance. The industrially based sample 4 (DS = 1.72) has a smaller variance $\sigma^2 = 0.01$ than the ones synthesized in our laboratory (sample 5, DS = 1.81 to sample 12, DS = 2.27) which have variances in the range of $\sigma^2 = 0.05 – 0.14$. This means that the sample 4 is more homogeneous in chemical composition compared to others. The rest of industrial based samples (i.e. sample 13, DS = 2.42 to sample 17, DS = 2.92) have quite small variances and thus are homogeneous in DS.

There is a relation between modification process and chemical structure (i.e. substituent distribution). Homogeneous derivatization should result in a random substituent distribution along and among the cellulose chains while heterogeneous derivatization can result in a non-random substituent distribution. Therefore, there might be a difference in the synthetic route between the industrial and our laboratory derived samples based on the differences in variance between two different sample origins.

A mixture of CAs differing in DS usually will cover a much larger DS-range than the range of chemical heterogeneity expected for a single sample. In order to be able to determine the degree of substitution distribution of a single sample, it has to be checked that the separations according to DS can be established even across the peak of a single sample. In order to prove this, the CA samples have to be fractionated in terms of DS and the DS of each fraction has to be determined. The low sample-sizes obtained after the chromatographic fractionation, which are typically in the µg-range, require highly sensitive analytical means to characterize the DS of the fractions. For such polymer characterizations, hyphenation of liquid chromatography and ^{1}H-NMR, which can be performed online or off-line, is highly informative. In the present case, online hyphenation was not suitable, because of the interference of proton signals of MeOH, DCM and water with the proton signals of the CA units. Elimination of these solvent signals by solvent suppression techniques was not possible due to the gradient elution [208]. Off-line ^{1}H-NMR on the polymer fractions obtained might provide an alternative since DCM and MeOH can easily be evaporated. However, to obtain reasonable S/N-ratio costly and time demanding repeated fractionations would be required.

As already discussed in 4.1.1, the small amounts of material required in conjunction with the amount of information that can be gained by FTIR experiments make FTIR an ideal detection device. However, typical eluents like MeOH and DCM used in chromatography are strong IR absorbers which would hide the absorbances of the analytes. This drawback of solvent absorption bands can be overcome if the solvent is removed from the eluting fractions. The most effective way is using an LC-Transform interface, which allows hyphenation of chromatography and FTIR. In this interface the eluent is evaporated upon passing through a heated nozzle. A high temperature and an inert gas flow (compressed air) are used to perform this evaporation. As a result, the non-volatile CA fractions corresponding to different retention times are deposited at different positions on a Germanium disc, which moves below the nozzle, thereby creating a track of a thin polymer film. Afterwards, the disc is placed in the FTIR spectrometer and the spectra of the polymer track are automatically recorded at regular intervals.

The lower surface of the Germanium disc is coated with aluminium, rendering it reflective. By using a small optical device, the infrared beam is directed from the FTIR source onto the sample deposit. The laser beam passes through the deposit and the Germanium and is

reflected from the aluminium coated surface through the sample and further to the FTIR detector. The result is a double-pass transmission measurement of the sample.

In order to get useful polymer deposits optimization of evaporation conditions (i.e. an appropriate temperature and a gas pressure) is necessary. If the nozzle temperature is too low the mobile phase cannot be evaporated completely, which results in redissolution of the previously deposited fraction. This in turn will result in broad tracks with loss of resolution. If the temperature is too high, partial precipitating of the sample in the nozzle capillary might occur. Under these conditions a uniform polymer track cannot be obtained. Therefore, different evaporation conditions were experimentally tested. The optimum conditions were found using a nozzle temperature gradient changing from 130 °C at the start of injection point to 140 °C at the end of the ramp time (i.e. the sum of delay start and deposition duration), a gas pressure of 30 psi and a disc velocity of 5 mm/min at a mobile phase flow rate of 0.5 mL/min. Due to the change in flow rate, the multi-step gradient was adjusted as given in table 11 for the FTIR experiments.

Table 11: Optimized gradient profile of the multi-step gradient from DCM to MeOH for LC-FTIR.

t (min)	0	10	30	50	70	90	90.01
% MeOH	0	1	4.5	13	35	70	0

The DS of an unknown CA fraction can be determined from its FTIR spectrum only after suitable calibration, e.g. by using a set of CAs which have been well characterized in terms of their average DS, e.g. by ^{1}H-NMR (refer to 4.1.1 on page 37). It should be mentioned that the calibration derived by FTIR/ATR technique (given in 4.1.1 on page 40) cannot be applied to the LC-FTIR experiments, due to the different FTIR techniques used. Therefore, the spectra of original CA samples were acquired by injecting and depositing the different samples of known average DS. Since a direct injection and deposition of the samples without column was not possible due to difficulty in evaporation of DMSO under the conditions applied, the samples were deposited by running the samples through the HPLC column, however without performing an HPLC separation by DS. For this purpose, the mobile phase was programmed as follows: A 0 – 1% MeOH gradient in 5 min was used to elute the DMSO while the polymer molecules stayed adsorbed on the column. This step was followed by a 5 min isocratic elution at 100% MeOH to allow the molecules being desorbed. A concentration of 5 g/L and an injection volume of 10 µL were used. A nozzle temperature of 190 °C, a gas

pressure of 30 psi and the lowest possible disc velocity of 0.5 mm/min at a mobile phase flow rate of 1.0 mL/min were applied for the calibration experiments. In analogy to 4.1.1 on page 40, the calibration curves were constructed based on the average DS of each sample determined by NMR. The spectral band area of each C=O stretching (1600 – 1880 cm^{-1}), C-H deformation (1340 – 1405 cm^{-1}) and C-O stretching (1186 – 1305 cm^{-1}) of the acetyl groups were divided by the band area of C-O skeletal stretching (967 – 1145 cm^{-1}). The baseline settings were set identical to the integration limits. Thus, calibrations 1, 2 and 3 correspond to average DS versus area ratios of C=O acetyl/C-O skeleton, C-H acetyl/C-O skeleton, and C-O acetyl/C-O skeleton, respectively.

The calibrations could be well described by the following equations:

$$DS_1 = -0.97 + 3.7 \times \frac{A_{(C=O)Acetyl}}{A_{(C-O)Skeleton}}$$ **Equation 36**

$$DS_2 = -0.13 + 14.5 \times \frac{A_{(C-H)Acetyl}}{A_{(C-O)Skeleton}}$$ **Equation 37**

$$DS_3 = -1.5 + 4.4 \times \frac{A_{(C-O)Acetyl}}{A_{(C-O)Skeleton}}$$ **Equation 38**

where A is the FTIR peak areas of respective spectral bands of acetyl and anhydroglucose units.

For the determination of DS from the FTIR spectra the DS values calculated from the different band ratios were averaged:

$$DS = (DS_1 + DS_2 + DS_3)/3$$ **Equation 39**

These equations were directly utilized for the DS determination by LC-FTIR experiments after chromatographic separation by DS using the gradient given in table 11.

As a test for the applicability of the LC-FTIR strategy, two CA samples of different DS (sample 5, DS = 1.81 and sample 13, DS = 2.42) were analyzed. The dependences of DS on elution volume and their reproducibility are shown in figure 36.

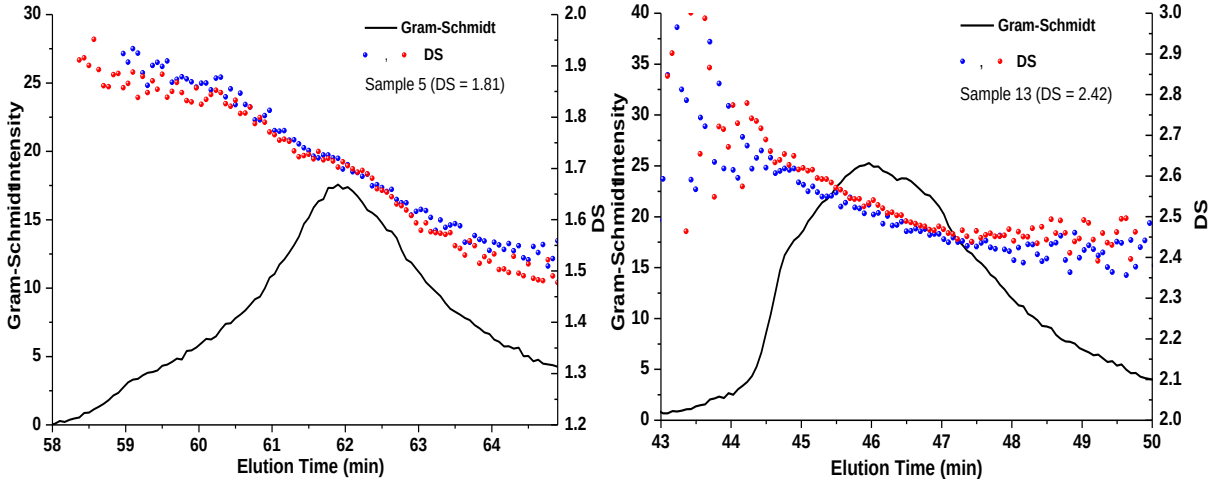

Figure 36: DS as a function of elution time determined by LC-FTIR; Sample solvent: DMSO; Injection volume: 20 µL (conc. = 1.5 g/L); Multi-step gradient program: Refer to table 11; Flow rate: 0.5 mL/min; Other experimental conditions see figure 21. FTIR resolution: 0.333 mm/spectral file.

For both samples a good reproducibility of the DS values calculated for the different elution volumes was found, confirming the reliability of the method. Across the sample chromatograms decreasing DS with increasing elution volume is clearly observed, except in those regions where only very little sample amounts were deposited. For sample 5 (DS = 1.81) DS varies from approx. DS = 1.45 to DS = 1.95 and therefore is more pronounced than the DS variation of sample 13 (DS = 2.42) which varies from approx. DS = 2.35 to DS = 2.65. However, the range of the DS variation for both samples is approx. twofold smaller than that calculated from HPLC method (see figure 35): Here DS varied from DS = 1.0 to DS = 2.10 for sample 5 (DS = 1.81) and from DS = 1.80 to DS = 2.60 for sample 13 (DS = 2.42). One reason might be that the concentrations at the peak starts and peak ends of the chromatograms are too low to result in a good S/N-ratio for the FTIR spectra. As a result, many scattered DS values on both ends of the chromatograms in LC-FTIR experiments can be observed.

It was possible to calculate DS_w and variance from the Gram-Schmidt intensities and the DS values determined from LC-FTIR data using equation 34 and equation 35, respectively. For sample 5 (DS = 1.81) and sample 13 (DS = 2.42) the DS_w and variance values are compiled in table 12.

Table 12: Weight average DS (DS_w) and variance (σ^2) calculated from the DS-distribution obtained by LC-FTIR experiments. Two values of DS_w and σ^2 for each sample indicate reproducibility of LC-FTIR experiments (refer to figure 36).

Sample name	^{1}H-NMR DS	DS_w	σ^2
Sample 5	1.81	1.71	0.013
		1.69	0.012
Sample 13	2.42	2.50	0.006
		2.52	0.007

As expected again, both DS values determined by NMR and DS_w values calculated from DS-distribution of LC-FTIR experiments are quite close to each other. The difference in the value of variance for sample 5 and sample 13 indicate the higher heterogeneity level for the former sample as compared to the latter one. However, variances from LC-FTIR are nearly 10-fold smaller than that from HPLC ($\sigma^2 = 0.11$ for sample 5 and $\sigma^2 = 0.07$ for sample 13; see table 10). One reason might be related to the resolution of eluting fractions detected by the ELSD or collected by the LC-Transform [140, 209-211]. Every system has its own instrumental band broadening. By increasing the band broadening, the resolution decreases and variance should decrease. In the present case, the peak width in LC-Transform is larger than that in ELSD by approx. a factor of 3 (variance has a square root, σ^2). This might be due to the larger instrumental band broadening of LC-Transform compared to ELSD, which reduces the resolution of eluting fractions. As a result, the variance decreases.

Nevertheless, it can be concluded from LC-FTIR experiments that separations according to DS were achieved even within a single sample.

In another experiment LC-FTIR was dedicated to analyze a mixture of CAs having different DS. The dependence of DS on elution volume for the mixture composed of [sample 1 (DS = 1.53) + sample 9 (DS = 2.09) + sample 12 (DS = 2.27) + sample 15 (DS = 2.45) + sample 17 (DS = 2.92)] is depicted in figure 37.

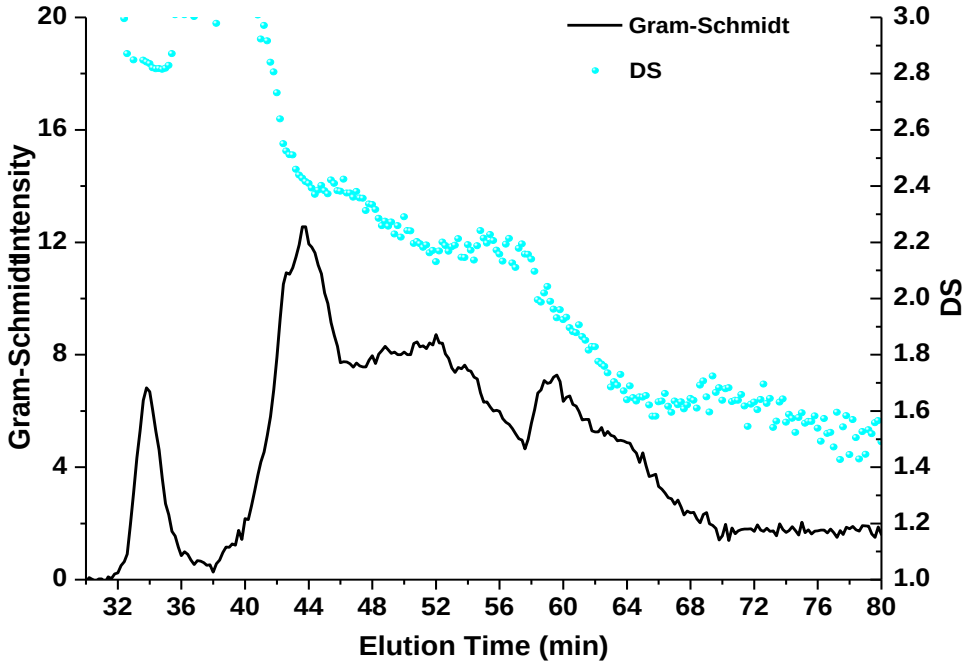

Figure 37: DS as a function of elution time determined by LC-FTIR; Sample mixture: sample 1 (DS = 1.53) + sample 9 (DS = 2.09) + sample 12 (DS = 2.27) + sample 15 (DS = 2.45) + sample 17 (DS = 2.92); Sample solvent: DMSO; Injection volume: 20 µL (conc. of each sample in the mixture = 1.5 g/L); Multi-step gradient program: Refer to table 11; Flow rate: 0.5 mL/min; Other experimental conditions see figure 21. FTIR resolution: 1.0 mm/spectral file.

Similar to the peaks of the single samples, a decrease of DS with increasing elution volume can be seen except in the regions of very low sample concentrations. These observations confirm once more the chromatographic separation by DS not only for samples of different average DS (see figure 29) but also within a single sample (see figure 36).

After an SEC method for the characterization of molar mass distributions (MMD) and a gradient HPLC method for the characterization of degree of substitution distributions (DS-distribution) were developed, it was of great interest to combine both methods in a two-dimensional liquid chromatographic system (2D-LC) in order to correlate MMD and DS-distribution. A major advantage of 2D-LC separations is the differentiation between samples which show identical chromatograms in the first and second dimensions. A distinct additional advantage of the 2D systems is to elucidate whether the separation in gradient HPLC is mainly influenced by DS and/or molar mass. Therefore, the next chapter is dedicated to the experimental attempts given to combine SEC and gradient HPLC.

4.2.3. Two-dimensional liquid chromatography (Gradient LAC × SEC): Correlation of CCD and MMD of CA

It is well known that a single chromatographic separation either by SEC or by gradient HPLC cannot provide the full heterogeneity information of CAs. However, coupling of gradient HPLC with SEC should provide simultaneous information on both, chemical composition and molar mass distribution. An important factor of a 2D chromatographic separation is the order in which the separations are carried out. Gradient HPLC in the first dimension is most often used. Following the reasons given in 3.2.1 on page 31, it would be beneficial to use the gradient method developed in 4.2.2 as the first dimension and the SEC method developed in 4.2.1.2 as the second dimension.

However, in order to get a proper online 2D system, the experimental conditions had to be readjusted. In general, to match the collection time of a fraction in the first dimension with the analysis time of the previous fraction in the second dimension, a slow first dimension and a fast second dimension are required. Other important features are a high sample load in order to obtain chromatograms with high S/N-ratio in the second dimension as well as a detector being compatible with the second dimension eluent.

According to the optimized SEC conditions (see figure 17) every fraction injected into the second dimension should contain at least approx. 0.3 mg material as a compromise between a sufficiently intense detector signal and stable elution volumes if RI should be applied for detection. However, the maximum injected mass for the gradient method was found to be approx. 0.35 mg even after some additional optimization attempts (dilution of the samples with DCM and/or repeated injections prior to the start of the gradient). At higher injected masses reappearance of the breakthrough peak was observed. At such injected masses in the first dimension, the concentrations in the second dimension would become too low for good detection. Therefore, RI-detection was not an option for the online 2D separation to be performed in this study.

Due to the higher sensitivity evaporative light scattering detection (ELSD) seems to be a better choice. However, the use of a non-volatile salt is incompatible with this detector. Therefore, the DMAc/LiCl method developed in 4.2.1.2 could not be applied as the second dimension (SEC) for online 2D separations. Thus, attempts were undertaken to develop an SEC method being compatible with ELSD.

From the gradient experiments it was known that DCM with a sufficient amount of MeOH was capable of eluting CAs from a polar stationary phase. The eluent composition at the time

of elution is close to the critical one. A further increase in eluent strength leads to a deviation from critical conditions to a molar mass dependent elution in SEC mode. Therefore, compositions of increasing MeOH content should change the chromatographic mode from LAC over LC-CC to SEC. To check this, a solvent mixture of 30% MeOH in DCM was applied on a GRAM column. Figure 38a shows the resulting chromatograms for CA of different DS (sample 1, DS = 1.53; sample 8, DS = 1.95 and sample 17, DS = 2.92). Bimodal chromatograms were observed. The first peaks on low elution volume scale were believed to be due to the presence of aggregates in the samples. Therefore, 50 mmol ammonium acetate (CH_3COONH_4) were added to the mobile phase as ELSD-compatible salt, to suppress potential aggregates. However, the bimodalities remained (figure 38b) and could not be removed even when increasing the salt concentration. Therefore, no further attempts were undertaken using DCM/MeOH mixtures.

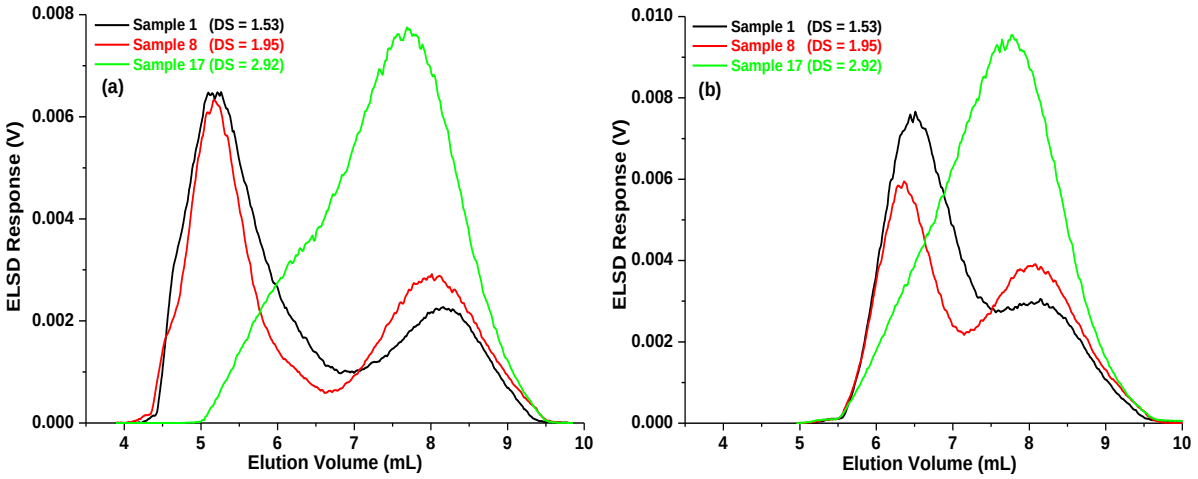

Figure 38: Overlay of chromatograms of CAs having different DS; Sample solvent: DMSO; Injection volume: 50 µL (conc. = 2.0 g/L); Eluent: Mixture of 30% MeOH in DCM **(a)** and mixture of 30% MeOH in DCM + 50 mmol/L CH_3COONH_4 **(b)**; Column: PSS-GRAM Linear XL (30 cm × 0.8 cm I.D., 10 µm) at 35 °C; Flow rate: 1.0 mL/min; Detector: ELSD (NEB Temp = 50 °C, EVAP Temp = 90 °C and gas flow = 1.0 SLM).

Similarly, when the CA samples (sample 1, DS = 1.53; sample 8, DS = 1.95 and sample 17, DS = 2.92) were run in pure DMSO multimodal peaks were observed as represented in figure 39a. The early eluting peaks before the main peak are due to the presence of aggregates. This eluting behaviour of CA samples in DMSO is similar to the behaviour observed in figure 11where pure DMSO was applied as eluent and RI for detection. Complete deaggregation in DMSO was there achieved by adding LiCl salt (see figure 12). However, since LiCl cannot be evaporated in ELSD the LiCl was replaced by ammonium acetate.

Indeed, the aggregates were completely suppressed by an addition of 50 mmol/L ammonium acetate. The resulting monomodal peaks are shown in figure 39b. However, when using normal SEC concentrations, the ELSD signal was very noisy even after optimizing the nebulization (NEB) and evaporation (EVAP) temperature of the ELSD. The reason for the low S/N-ratio is the high boiling point of DMSO, which makes DMSO difficult to evaporate. This would be even worse when running an online 2D experiment, where high flow rates need to be applied in the second dimension. Therefore, it was tried to decrease the DMSO content in the mobile phase by adding 1,4-dioxane.

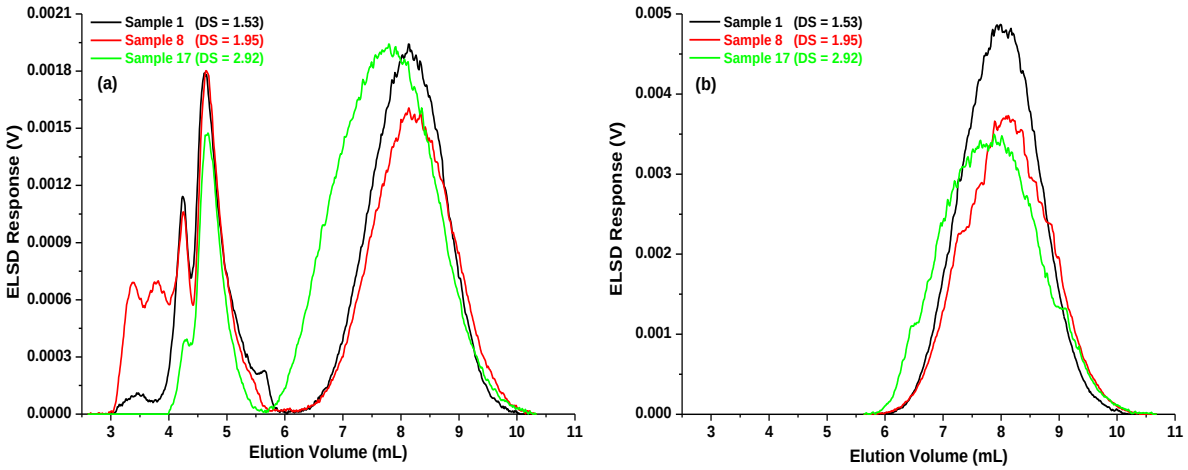

Figure 39: Overlay of chromatograms of CAs having different DS; Sample solvent: DMSO; Injection volume: 50 µL (conc. = 2.0 g/L); Eluent: DMSO **(a)** and DMSO + 50 mmol/L CH_3COONH_4 **(b)**; Column: PSS-GRAM Linear XL (30 cm × 0.8 cm I.D., 10 µm) at 35 °C; Flow rate: 1.0 mL/min; Detector: ELSD (NEB Temp = 150 °C, EVAP Temp = 270 °C and gas flow = 1.5 SLM).

After optimizing the eluent composition and the ELSD conditions the best eluent with respect to ELSD S/N-ratio was found to be a mixture composed of 45% DMSO and 55% 1,4-dioxane which contains 50 mmol/L ammonium acetate using a nebulization temperature NEB Temp = 170 °C and an evaporation temperature EVAP Temp = 295 °C at a gas flow of 1.6 SLM. The resulting chromatograms for the CA samples (sample 1, DS = 1.53; sample 8, DS = 1.95 and sample 17, DS = 2.92) under these conditions are depicted in figure 40.

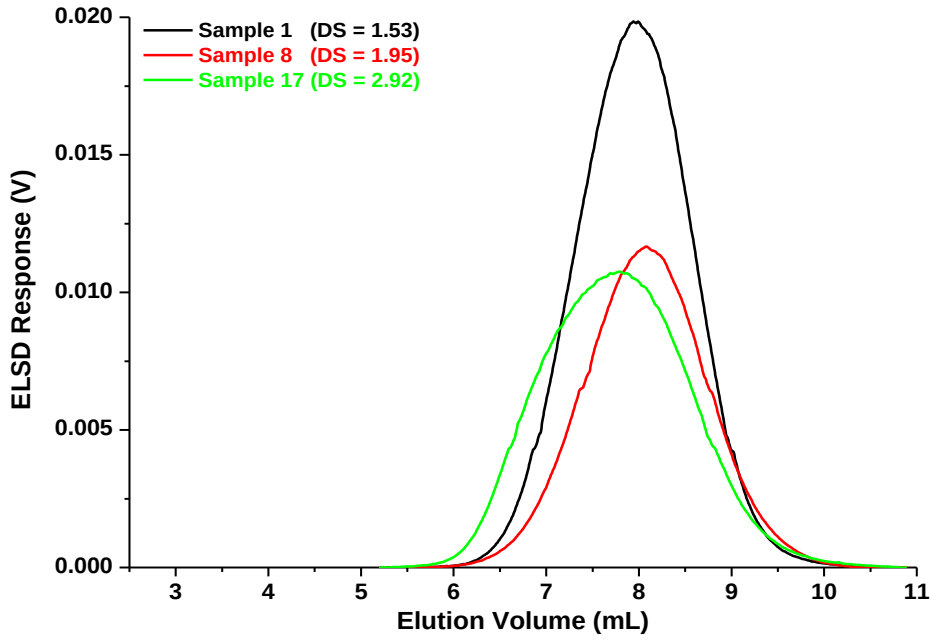

Figure 40: Overlay of chromatograms of CAs having different DS; Sample solvent: DMSO; Injection volume: 50 µL (conc. = 2.0 g/L); Eluent: 45% DMSO + 55% 1,4-dioxane + 50 mmol/L CH_3COONH_4; Column: PSS-GRAM Linear XL (30 cm × 0.8 cm I.D., 10 µm) at 35 °C; Flow rate: 1.0 mL/min; Detector: ELSD (NEB Temp = 170 °C, EVAP Temp = 295 °C and gas flow = 1.6 SLM).

Once more, the injections with 0.35 mg (see page 91) did not result in a sufficient ELSD S/N-ratio for this new SEC method. Since suitable conditions for online 2D separation could not be identified despite all efforts, the 2D separations were carried out off-line. Using a fraction collector, fractionations were repeatedly performed in the first dimension (gradient chromatography), in order to collect sufficient amounts of each fraction. Since the solvents (DCM and MeOH) could be easily evaporated, high concentrations could be obtained upon redissolution of the material in a small volume of DMAc/LiCl or pure DMSO.

However, the application of DMAc/LiCl with RI as the second dimension would not produce sufficient RI S/N-ratio compared to the new SEC method (45% DMSO + 55% 1,4-dioxane + 50 mmol/L CH_3COONH_4) when ELSD uses for detection. This is because RI is less sensitive than ELSD. Accordingly, the latter was employed as the second dimension.

The experimental conditions used for the 2D-LC can be summarized as follows:

Table 13: 2D-LC experimental conditions.

1st Dimension	Column:	Nucleosil (25 cm × 0.4 cm I.D., 5 µm)
	Sample solvent:	42% DCM in DMSO
	Sample conc.:	5.8 g/L
	Injection volume:	45 µL
	Flow rate:	1.0 or 2.0 mL/min
	Gradient:	Refer to table 9
2nd Dimension	Column:	PSS-GRAM Linear XL (30 cm × 0.8 cm I.D., 10 µm)
	Sample solvent:	DMSO
	Injection volume:	70 µL
	Flow rate:	1.0 mL/min
	Mobile phase:	45% DMSO + 55% 1,4-dioxane + 50 mmol/L CH_3COONH_4
	Detection:	ELSD (NEB Temp = 170 °C, EVAP Temp = 295 °C and gas flow = 1.6 SLM)

CAs of different DS were analyzed using the 2D-LC method. The resulting normalized SEC chromatograms of 15 consecutive fractions for three samples (sample 9, DS = 2.09; sample 12, DS = 2.27 and sample 16, DS = 2.60) and reproducibility for the last two samples are exemplified in figure 41. The chromatograms of sample 12 and sample 16 show a good reproducibility. Three different types of correlations between molar mass and gradient elution volume can be distinguished. For sample 12 (DS = 2.27) the chromatograms of fraction 1 to 7 shift to the lower SEC elution volume (i.e. higher molar mass) with increasing fraction number (i.e. gradient elution volume, i.e. lower DS). At higher gradient elution volume the SEC elution volumes become nearly constant (fraction 7 to 15). This type of correlation will be denoted form 1 in the following. For sample 9 (DS = 2.09) and sample 16 (DS = 2.60) a similar decrease in SEC elution volume with 1st dimension fraction number can be observed up to fraction 7. However, contrasting to sample 12, the SEC elution volumes continue to decrease for the fractions 11 to 15 of sample 9 (termed form 2) while a clear increase in elution volumes is observed for the fractions 11 to 15 of sample 16 (termed form 3).

In gradient chromatography, the correlation types of form 1 and form 2 would be expected for a chemically homogeneous polymer but heterogeneous in molar mass [212]. In contrast, when the chromatograms of the fractions would elute at identical SEC elution volumes (i.e. same molar mass) with increasing fraction number (i.e. gradient elution volume, i.e. lower DS), this type of correlation would be expected for a sample which contains chemically different components having the same MMD. Since neither of these cases is similar to form 3, the elution behaviours of the fractions 11 to 15 for the sample 16 cannot be explained by a simple MMD or DS-distribution.

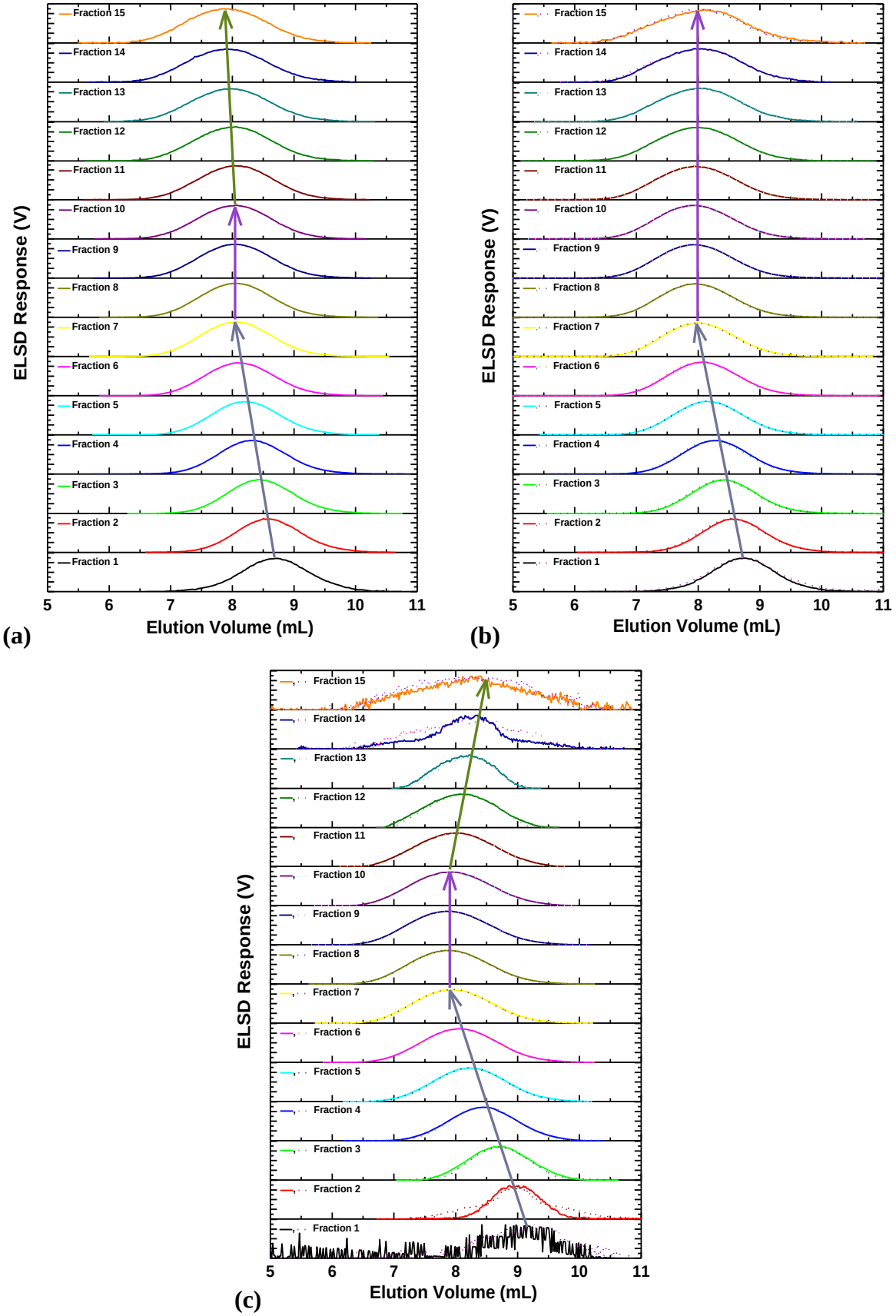

Figure 41: Normalized SEC chromatograms of 15 fractions collected in 1st dimension (gradient chromatography) and subsequently injected into 2nd dimension (SEC); Samples: Sample 9, DS = 2.09 **(a)**, sample 12, DS = 2.27 **(b)** and sample 16, DS = 2.60 **(c)**; Experimental conditions see table 13.

All samples could be assigned to one of the abovementioned three correlation forms between molar mass and gradient elution volume. The assignments for each CA sample are listed in table 14.

Table 14: Assignments of the correlation between molar mass and gradient elution volume to the samples. The samples marked in grey are industrial samples.

Sample name	DS	Correlation form of molar mass and gradient elution volume
Sample 1	1.53	form 2
Sample 2	1.59	form 2
Sample 3	1.66	form 2
Sample 4	1.72	form 3
Sample 5	1.81	form 2
Sample 6	1.87	form 2
Sample 7	1.92	form 2
Sample 8	1.95	form 2
Sample 9	2.09	form 2
Sample 10	2.16	form 1
Sample 11	2.19	form 1
Sample 12	2.27	form 1
Sample 13	2.42	form 3
Sample 14	2.45	form 3
Sample 15	2.45	form 3
Sample 16	2.60	form 3
Sample 17	2.92	form 1

From the correlation forms it becomes clear that the differences in the correlations between molar mass and gradient elution volume arise from fraction 11 to fraction 15. Interestingly, the industrial samples (marked in grey in table 11) except sample 17 (DS = 2.92) and the precursor (sample 16, DS = 2.60) display the same correlation form (form 3) while the laboratory synthesized samples exhibit either correlations of form 1 or form 2. For the laboratory samples those of larger DS (DS = 2.1 – 2.3) have correlations of form 1 while those with an average DS < 2.1 show correlations of form 2. The reason for the variations is yet unknown, but one might speculate that it might result from differences in the microstructure (i.e. arrangements of differently substituted AGUs along the CA chains). The microstructure of a polymer can strongly influence the physical properties which in turn govern the application of this material in industrial performance.

Further experiments were performed to investigate the reason for the different elution patterns in form 3. For this purpose, the samples were fractionated multiple times in the first dimension and the fractions were characterized by ^{1}H-NMR. There were small differences in the ^{1}H-NMR spectra of these fractions. However, due to the low spectral resolution it was not possible to interpret this difference. Unfortunately, ^{13}C-NMR spectra could not be acquired on these fractions due to the low amounts of sample obtained even after multiple fractionations. An alternative could be the degradation of these fractions and characterization of the resulting degraded products by the techniques such as HPAEC-PAD, CE-UV, GLC-MS, etc. In this way, the information about second order heterogeneity might be obtained.

To determine the molar masses of the 2D fractions, the 2nd dimension (SEC) was calibrated with a set of well-defined PMMA standards under the same chromatographic conditions. However, the PMMA calibration curve cannot be used directly for the determination of the molar masses of CAs, due to the difference in hydrodynamic volume between PMMA and CA as revealed in 4.2.1.2 on page 57. Therefore, the PMMA calibration curve had to be converted into a CA calibration curve using appropriate correction factors A and B. For the determination of the parameters A and B the chromatograms of unfractionated CA samples obtained under the SEC conditions of the 2D experiments (see table 13) as well as their absolute molar masses (absolute M_w) from light scattering (see table 3) were used. The procedure used is described in 4.2.1.2 on page 59.

The information on DS and molar mass data can be represented in a contour plot. The Y-axis of the contour plot corresponds to the elution volume of the first dimension (gradient) which separates mainly according to DS. On the X-axis the molar masses corresponding to the elution volumes in the second dimension (SEC) are given. The contour plots of the three samples (sample 9, DS = 2.09; sample 12, DS = 2.27 and sample 16, DS = 2.60) and reproducibility for the last two samples are represented in figure 42.

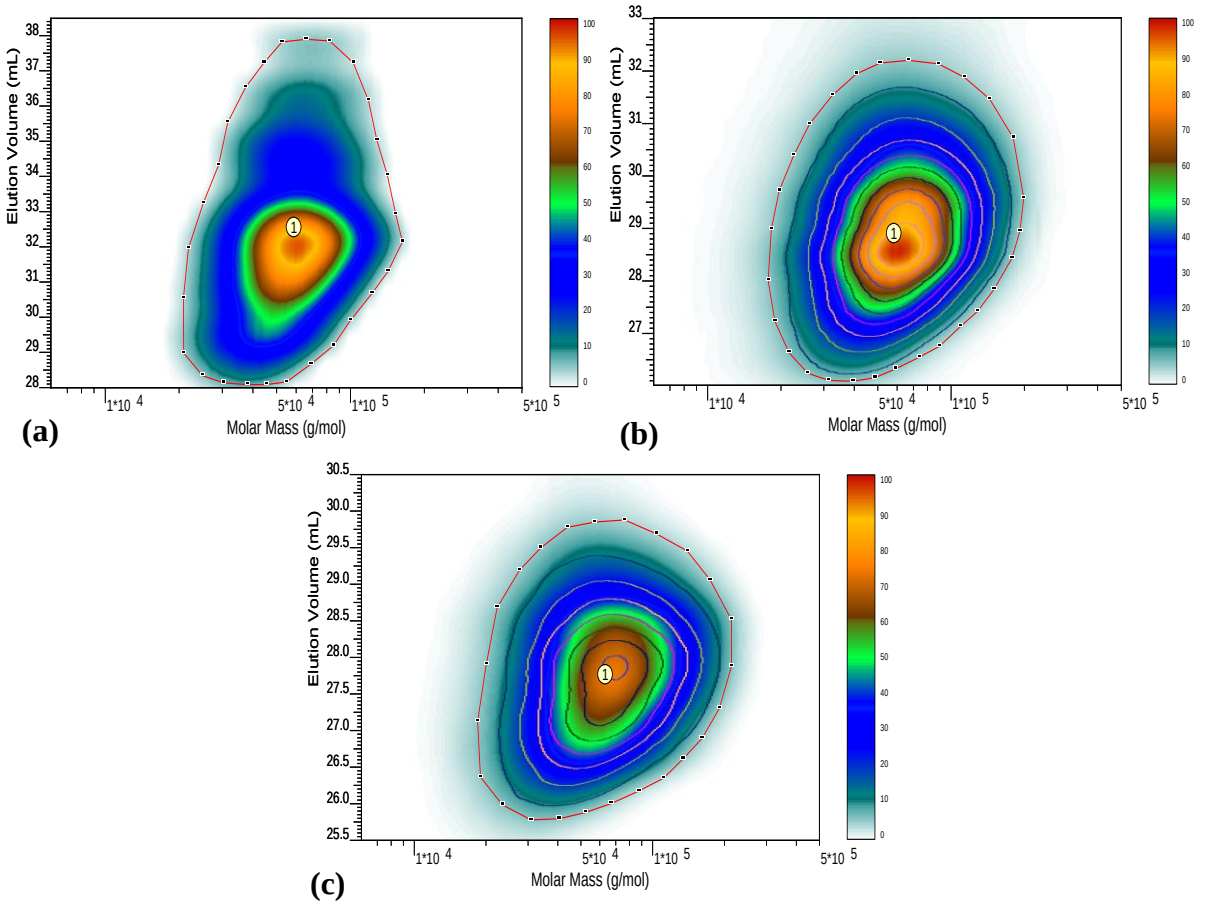

Figure 42: 2D-LC contour plot of sample 9, DS = 2.09 **(a)**, sample 12, DS = 2.27 **(b)** and sample 16, DS = 2.60 **(c)**; For each sample, 15 fractions collected in 1st dimension (gradient chromatography) and subsequently injected into 2nd dimension (SEC); Experimental conditions see table 13. The coloured isolines in the overlay of **b** and **c** contour plots indicate the reproducibility of the experiments.

Quite good reproducibility can be seen for sample 12, DS = 2.27 and sample 16, DS = 2.60 (figure 42b and c, respectively). For all samples the molar mass of the fractions ranged from about 20000 to 200000 g/mol indicating nearly similar heterogeneity with respect to molar mass. Weight average molar masses of M_w = 60000, 66000 and 70000 g/mol for sample 9, 12 and 16, respectively, were obtained from the contour plots. These values are slightly lower than the absolute molar masses derived from light scattering (see table 3). However, keeping in mind that the response curve of ELSD used in the 2D experiments is non-linear in concentration. In addition, the ELSD intensity might vary with molar mass which makes molar mass determination in both ELSD and RI systems different.

In contrast to the molar masses, the degree of substitution distribution varies among the samples. First of all, as expected, every sample elutes within a gradient elution range comparable to that of the simple gradient adsorption method (refer to figure 29). The sample with the lowest DS (i.e. sample 9, DS = 2.09) elutes within an approx. 10 mL gradient

elution range (figure 42a) whereas the sample with the highest DS (i.e. sample 16, DS = 2.60) covers an approx. 5 mL range (figure 42d), indicating a higher chemical heterogeneity for the former sample, in agreement with the results on the variance in table 10. It should be mentioned that the large elution range is not in any case an indication of large chemical heterogeneity.

All the samples show only one peak. The shape of the contour plot of sample 12 (b) and sample 16 (c) resembles to each other while the shape of the contour plot of sample 9 appears to be different.

In addition, only weak correlations between molar mass and DS can be identified from the contour plots in figure 42. By increasing molar mass the gradient elution volume (i.e. DS) slightly increases. However, this weak correlation does not allow clarifying whether the gradient separation is influenced by DS only, or whether there is an effect of molar mass as well. In order to definitely clarify this point it would be necessary to have some samples of identical DS but largely different molar masses. The contour plots in figure 42 do not reveal at first glimpse the curved dependences of molar mass on gradient elution volume for the chromatograms of fraction 11 to 15 identified in figure 41. To check whether this is a real loss of information, or merely a question of the representation, the elugrams corresponding to a particular gradient elution volume were normalized and a contour plot was constructed from the normalized chromatograms. The resulting plots are represented in figure 43.

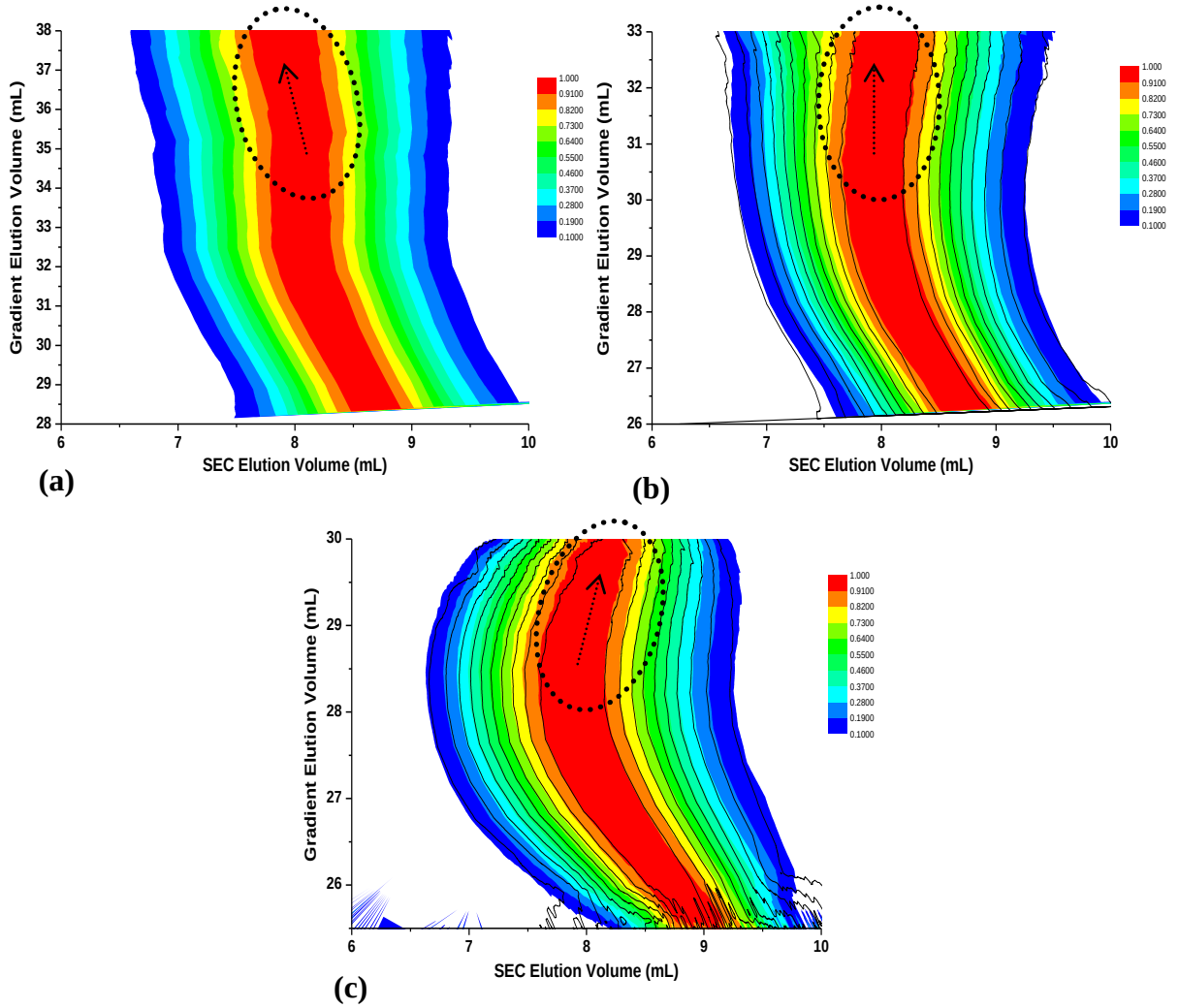

Figure 43: Normalized 2D-LC contour plot of sample 9, DS = 2.09 **(a)**, sample 12, DS = 2.27 **(b)** and sample 16, DS = 2.60 **(c)**; Experimental conditions see table 13.

It is obvious that the SEC elution volume remains nearly unchanged for the last 5 fractions (fraction 11 to fraction 15) of sample 12 (figure 43b) whereas it decreases (i.e. molar mass increases) for sample 9 (figure 43a) and it increases (i.e. molar mass decreases) for sample 16 (figure 43c). Thus, the informational content of the normalized contour plots is blurred by the different intensities in the non-normalized contour plots.

To show the potential of 2D chromatography for the characterization of complex CA mixtures, a mixture of two samples differing in DS was analysed by 2D-LC. The 2D contour plot of a mixture of sample 4 (DS = 1.72) and sample 15 (DS = 2.45) [1:1] is shown in figure 44.

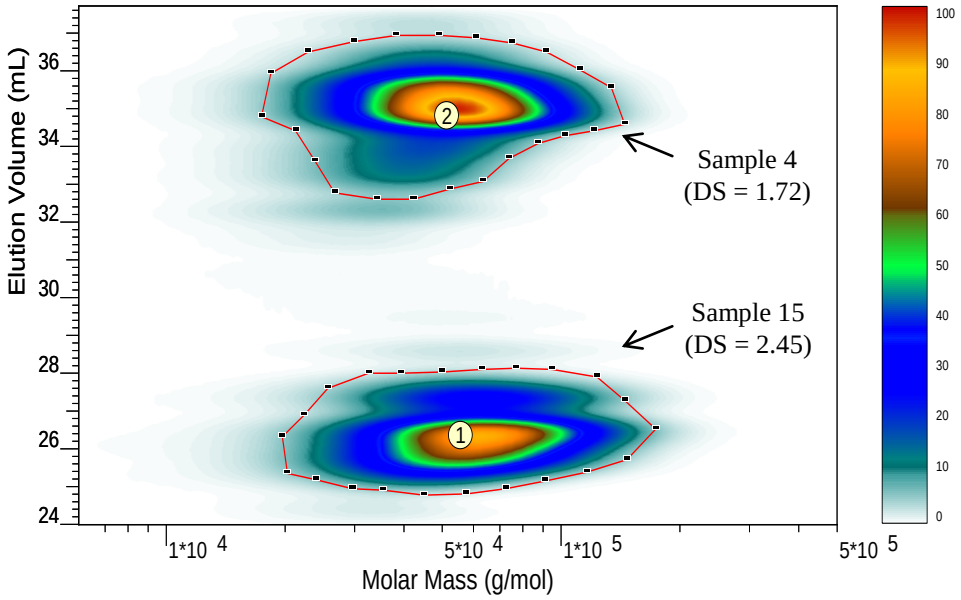

Figure 44: 2D-LC contour plot of a mixture composed of sample 4 (DS = 1.72) and sample 15 (DS = 2.45) [1:1]; Experimental conditions see table 13.

As expected the plot consists of two peaks. The first peak appearing in the elution volume range 25 – 29 mL belongs to the high DS sample (i.e. sample 15, DS = 2.45) while the second peak in the elution range 32 – 38 mL corresponds to the one of lower DS (i.e. sample 4, DS = 1.72). The heterogeneity with respect to molar mass for both samples is nearly identical, as expected, comparing to Figure 18. The M_w values were 63000 g/mol for sample 15 and 50000 g/mol for sample 4. If only a separation by size (SEC) would be performed, the resulting chromatograms of sample 4 and sample 15 would overlap, without indication of chemical heterogeneity. Similarly, a separation by gradient chromatography would reveal two distinct peaks, however without indication of the heterogeneity with respect to molar mass. Thus, only the 2D approach can reveal the heterogeneity in both dimensions.

A major advantage of 2D experiments is that the separation capacities of each HPLC and SEC dimension can be multiplied, offering a high peak capacity to resolve samples of great complexity. It has been shown that 2D chromatography is capable to separate complex CA mixtures into their individual components. In addition, the 2D-LC results on individual samples revealed some unexpected features that could not be observed in a single chromatographic run, neither by gradient HPLC nor by SEC. These unexpected features indicated that apart from molar mass and DS, other molecular characteristics such as second

order heterogeneities or distribution of substituents within AGUs influence the elution behaviour of CAs.

5. Experimental Section

5.1. Chemicals and solvents

Dichloromethane (DCM), dimethyl sulfoxide (DMSO), 1,4-Dioxane and methanol (MeOH) (VWR, Darmstadt, Germany) and N,N-dimethyl acetamide (DMAc) (MERCK, Hohenbrunn, Germany) were of HPLC grade and used as received. Water was obtained by deionization through a Milli-Q system (Millipore water). Lithium chloride (LiCl) and sodium hydroxide (NaOH) pellets were purchased from MERCK (Darmstadt, Germany). Ammonium acetate (CH_3COONH_4) was obtained from VWR (Haasrode, Belgium).

5.2. Cellulose acetate (CA) samples

CA samples with average DS ranging from DS = 1.5 to DS = 2.9 were used. Five of the CA samples (sample 4, DS = 1.72; sample 13, DS = 2.42; sample 14, DS = 2.45; sample 15, DS = 2.45 and sample 17, DS = 2.92) were obtained from an industrial source (Rhodia Acetow GmbH, Freiburg im Breisgau, Germany). The others were prepared in our laboratory by partial saponification of a commercial high DS sample (sample 16, DS = 2.60, Acetati, Italy).

A typical protocol for the saponification was as follows: 9.18 g of sample 16 were dissolved in 255 mL of 1,4-dioxane (36 g/L). The required amounts of NaOH, calculated based on the theoretical DS and given in table 15, were added as an aqueous solution under stirring at room temperature. The mixture was allowed to stand for one hour at room temperature. Afterwards, the polymer was precipitated by dropwise addition into deionized water. The precipitates were washed twice with deionized water and dried in vacuum oven at 80 °C.

Table 15: Required amounts of NaOH added to a stock solution of sample 16 (9.18 g in 255 mL 1,4-dioxane; conc. = 36 g/L) calculated based on theoretical DS.

Sample name	Theoretical DS	Amount and concentration of NaOH added
Sample 1	1.55	142 mL (conc. = 0.25 M ≈ 35.5 mmol)
Sample 2	1.64	65 mL (conc. = 0.50 M ≈ 32.5 mmol)
Sample 3	1.73	59 mL (conc. = 0.50 M ≈ 29.4 mmol)
Sample 5	1.85	101 mL (conc. = 0.25 M ≈ 25.4 mmol)
Sample 6	1.90	47 mL (conc. = 0.50 M ≈ 23.7 mmol)
Sample 7	1.95	65 mL (conc. = 0.34 M ≈ 22.0 mmol)
Sample 8	2.05	37 mL (conc. = 0.50 M ≈ 18.6 mmol)
Sample 9	2.15	45 mL (conc. = 0.34 M ≈ 15.2 mmol)
Sample 10	2.20	54 mL (conc. = 0.25 M ≈ 13.5 mmol)
Sample 11	2.26	23 mL (conc. = 0.50 M ≈ 11.5 mmol)
Sample 12	2.35	50 mL (conc. = 0.17 M ≈ 8.5 mmol)

5.3. Determination of DS by ^{1}H-NMR spectroscopy

5 – 10 mg of each polymer were dissolved homogeneously in 1.0 mL of DMSO-d_6 at 60 °C. The DSs of the samples were determined by ^{1}H-NMR spectroscopy using the signals at δ = 2.2 – 1.6 ppm (acetyl protons) and δ = 5.5 – 2.8 ppm (cellulosic protons), upon subtracting the integral intensity of the sharp peak arising from residual water protons (δ = 3.14 ppm). The ^{1}H-NMR spectra were acquired on a 400 MHz (9.4 Tesla) Mercury-VX (Varian Inc., Sao Palo, USA) NMR spectrometer equipped with a 5 mm inverse-probe. ^{1}H measurements were executed using a 90° pulse, 2.6 s acquisition time (32 k data points, 16 ppm spectral width), 10 s relaxation delay, 64 – 256 accumulated scans depending on the analyte concentration, simple zero addition and exponential multiplication with lb = 0.3 Hz, respectively. The ^{1}H-NMR spectra were recorded at 60 °C and processed and evaluated using ACD 11 Software (Advanced Chemistry Development Inc., Toronto, Canada).

5.4. FTIR/attenuated total reflectance (ATR)-spectroscopy

The FTIR spectra of CA powders were acquired using a Thermo Nicolet NEXUS 670 FTIR spectrometer equipped with a temperature-stabilized deuterated tryglycine sulfate (DGTS) detector and a single-bounce ATR. 32 scans were accumulated at a spectral resolution

of 4 cm^{-1}. For data acquisition and evaluation the OMNIC Software version 7.3 (Thermo Electron, Waltham, USA) was applied.

5.5. SEC-MALLS

5.5.1. Chromatographic system and conditions

SEC-MALLS experiments were performed in DMSO and DMAc as solvents at different concentrations of LiCl using a TOSOH Bioscience (Tokyo, Japan) EcoSEC Micro-SEC-System with build-in RI-detector. A MALLS detector (DAWN DSP, Wyatt Technology, Santa Barbara, USA) was attached between the column and the RI-detector.

A single PSS-GRAM Linear XL column (10 µm particle size, 30 cm × 0.8 cm I.D., PSS Polymer Standards Service GmbH, Mainz, Germany) was applied at a flow rate of 1.0 mL/min. The samples were prepared by adding the DMSO/LiCl or DMAc/LiCl to the polymer and allowing to stand overnight at room temperature. For both eluents a sample concentration of 3.0 g/L and an injection volume of 100 µL were used, if not stated otherwise.

SEC calibration was performed using poly(methyl methacrylate) (PMMA) standards (PSS Polymer Standards Service GmbH, Mainz, Germany) having molar masses ranging from 3600 to 1.2×10^6 g/mol. For data acquisition and evaluation PSS WinGPC Unity version 7.0 (PSS Polymer Standards Service GmbH, Mainz, Germany) and ASTRA version 4.90.08 (Wyatt Technology, USA) Software were used.

The LS-detector was calibrated using pure toluene assuming a Rayleigh ratio of 9.78×10^{-6} cm^{-1} at 633 nm. The refractive index increments (dn/dc) of the samples in both DMSO/LiCl and DMAc/LiCl eluents were determined from the responses of the RI-detector presuming complete sample recovery (see the details in 5.5.2).

The RI-detector was calibrated using PMMA in THF assuming a dn/dc-value of 0.089 cm^3/g [213]. No attempts were undertaken to correct for the differences in the wavelengths between the RI-detector (white light) and the one of the light scattering instrument (633 nm).

5.5.2. Determination of refractive index increment (dn/dc)

No data on dn/dc for CA in the DMSO/LiCl or DMAc/LiCl are available in literature. Therefore the dn/dc of all CA samples was determined as follows:

A set of PMMA standards having molar masses ranging from 3600 to 1.2×10^6 g/mol was run in THF, in DMSO/LiCl and in DMAc/LiCl. In each case, PMMA concentrations of 1.0 g/L and an injection volume of 100 µL were used. The values of dn/dc for PMMA in DMSO/LiCl and DMAc/LiCl were calculated using the following equation:

$$\frac{A_1}{A_2} = \frac{k_{inst} \times conc_1 \times \left[\frac{dn}{dc}\right]_1}{k_{inst} \times conc_2 \times \left[\frac{dn}{dc}\right]_2} \qquad \textbf{Equation 40}$$

where A_1 and A_2 are the RI peak area of PMMA in the THF and DMSO/LiCl or DMAc/LiCl, respectively, k_{inst} RI instrument constant, $conc_1$ and $conc_2$ concentrations of PMMA in g/mL for THF and DMSO/LiCl or DMAc/LiCl, respectively, and $(dn/dc)_1$ and $(dn/dc)_2$ the specific refractive index increments of PMMA in THF (0.089 cm^3/g) [213] and DMSO/LiCl or DMAc/LiCl, respectively. The values of dn/dc of PMMA in the DMSO/LiCl and DMAc/LiCl were found to be 0.024 (±15%) cm^3/g and 0.058 (±4%) cm^3/g, respectively.

After all CA samples were measured in the DMSO/LiCl and DMAc/LiCl, their dn/dc-values were calculated via the following relation:

$$\frac{A_2}{A_3} = \frac{k_{inst} \times conc_2 \times \left[\frac{dn}{dc}\right]_2}{k_{inst} \times conc_3 \times \left[\frac{dn}{dc}\right]_3} \qquad \textbf{Equation 41}$$

where A_3 is the RI peak area, $conc_3$ the concentration and $(dn/dc)_3$ the specific refractive index increment of the CAs in the DMSO/LiCl or DMAc/LiCl system.

5.6. Gradient LAC

5.6.1. Chromatographic system and conditions

For the chromatographic separations of CAs according to DS a Shimadzu HPLC system consisting of a DGU-14A degasser, a FCV-10ALvp solvent mixing chamber, a LC-10ADvp pump and a SIL 10ADvp auto sampler was used. For detection an evaporative light scattering detector (ELSD, model PL-ELS 1000, Polymer Laboratories, UK) was added. The detector was operated at a nebulization temperature of 50 °C, an evaporation temperature of 90 °C and a gas flow of 1.0 SLM. The flow rate of the mobile phase was 1.0 mL/min unless mentioned otherwise. Data collection and processing was performed using 'WinGPC Software version 7.0' (Polymer Standards Service GmbH, Mainz, Germany).

The experiments were performed on a pure silica stationary phase Nucleosil, 5 µm particle size, 100 Å pore diameter, 25 cm × 0.4 cm I.D. (Macherey-Nagel GmbH, Düren, Germany). The column temperature was kept constant at 35 °C using a column oven K 4 (Techlab GmbH, Erkerode, Germany). The injected sample volume was 15 – 20 µL with concentrations of 0.15 – 2.0 g/L. DMSO was used as a sample solvent. The eluents were DCM as a weak eluent and MeOH as a displacer.

The void volume (V_0) of the column was estimated by injecting a low molar mass polystyrene standard (M_w of PS = 410 g/mol) using pure tetrahydrofuran (THF) as eluent. The resulting V_0 was 2.8 mL. The dwell volume (V_d) of the chromatographic system was determined to be 2.3 mL by subtracting the void volume from the onset of the increasing UV-signal due to a linear gradient starting from pure THF and running to THF containing 0.3% acetone.

5.7. Two-dimensional gradient LAC × SEC

Gradient LAC in the 1st dimension and SEC in the 2nd dimension were applied for the characterization of CAs. In the 1st dimension a Shimadzu system consisting of a DGU-14A degasser, a FCV-10Alvp solvent mixing chamber, a LC-10Advp pump and a SIL 10Advp auto sampler was used. The separations were performed on a pure silica stationary phase Nucleosil, 5 µm particle size, 100 Å pore diameter, 25 cm × 0.4 cm I.D. (Macherey-Nagel GmbH, Düren, Germany). The column was kept in a column oven K 4 (Techlab GmbH,

Erkerode, Germany) at 35 °C. The injected sample volume was 45 µL with concentrations of 5.8 g/L. 42% DCM in DMSO was used as a sample solvent. The eluents were DCM as poor eluent and MeOH as strong eluent. The flow rate of the mobile phase was 1.0 or 2.0 mL/min unless mentioned otherwise.

An Advantec SF 2120 Fraction collector (Advantec MFS, Inc., Dublin, CA, USA) was used to collect the fractions in the 1st dimension. 10 - 24 fractions were collected from the 1st dimension. To get sufficient concentrations of the fractions, the experiments were repeated 10 - 22 times. The solvents (DCM and MeOH) were vaporized in open-air at room temperature and the residues were subsequently re-dissolved in 106 µL DMSO. 70 µL of each fraction were re-injected into the 2nd dimension using the same chromatographic instrument as used to fractionate the samples in the 1st dimension. A mixture composed of 45% DMSO and 55% 1,4-dioxane containing 50 mmol/L ammonium acetate was used as mobile phase at a flow rate of 1.0 mL/min. The stationary phase in the second dimension was a single PSS-GRAM Linear XL column (10 µm particle size, 30 cm × 0.8 cm I.D., PSS Polymer Standards Service GmbH, Mainz, Germany). For detection an evaporative light scattering detector (ELSD, model PL-ELS 1000, Polymer Laboratories, UK) was utilized. The detector was operated at a nebulisation temperature of 170 °C, an evaporation temperature of 295 °C and a gas flow of 1.6 SLM. The SEC calibration was performed using PMMA standards (PSS Polymer Standards Service GmbH, Mainz, Germany) having molar masses ranging from 3600 to 1.2×10^6 g/mol. Data collection and processing was performed using 'WinGPC Software version 7.0' (Polymer Standards Service GmbH, Mainz, Germany).

5.8. LC-FTIR interface and FTIR spectroscopy

For obtaining information on the chemical composition of the eluting fractions the ELSD was replaced by a LC-Transform FTIR Interface, Series 600xy (Lab Connections, Marlborough, USA). The interface consists of a spraying device which eliminates the solvent by evaporation while the non-volatile polymer fractions are deposited on a rectangular Germanium plate (55 mm × 55 mm) placed on a movable stage below a heated nozzle. To get an ideal shape for the deposited track, an optimized nozzle temperature gradient from 130 °C at the start of injection point to 140 °C at the end of ramp time (i.e. the sum of delay start and deposition duration) was applied to account for the change in eluent composition over time from low boiling to higher boiling solvents used in the gradient. The gas pressure of the LC-Transform

system was set to 30 psi. For the LC-Transform experiments the flow rate of the mobile phase was changed to 0.5 mL/min. The solvent gradient was adjusted accordingly (see table 11). The motion velocity of the Germanium plate was 5 mm/min.

After the chromatographic experiment the FTIR analyses of the deposited polymer samples were performed by placing the Germanium plate on a motor driven optical device within a Nicolet Protégé 460 FTIR spectrometer (Thermo Electron, Waltham, USA), equipped with a DGTS-detector. The optical device consists of a number of mirrors directing the FTIR beam from the FTIR source onto the sample deposit. The laser beam passes through the deposit and the Germanium and is reflected from the aluminium coated surface back through the sample and further to the FTIR detector. Hereby the FTIR spectra for every position are obtained after the laser beam passed twice through the sample deposits.The motor of the device allowed the movement of the plate, such that the fractions at the different positions can be positioned automatically in the FTIR beam. FTIR spectra were recorded every 0.333 mm in the spectral region of 700 to 4000 cm^{-1} using 32 scans. Each spectrum corresponded to a different elution time of the chromatographic separation. For data collection and processing, Omnic Software version 7.3 (Thermo Electron, Waltham, USA) was used.

6. Summary and Conclusions

In the framework of this study it was shown that partial saponification using sodium hydroxide (NaOH) is a suitable method for preparing cellulose acetates (CA) of different average degree of substitution (DS) without altering the degree of polymerization (DP). The comparison of the theoretical average DS values with the ones determined by ^{1}H-NMR showed that the deacetylation reaction can be well controlled by the amount of NaOH added.

Due to the need of a large amount of sample as well as the use of costly instrumentations for the characterization by NMR techniques, an alternative straightforward method based on FTIR/ATR for a fast estimation of average DS was represented. In addition, since the FTIR/ATR correlations proved profitable to determine DS with very low amounts of sample, they made it possible to characterize chromatographic fractions with respect to DS.

In the solubility investigations, only dimethyl sulfoxide (DMSO) and Dimethylacetamide (DMAc)/lithium chloride (LiCl) were identified as suitable solvents to dissolve the CA samples in the DS-range of DS = 1.5 – 2.9, irrespective of their DS. Therefore, these two solvents were utilized for the chromatographic experiments.

SEC-light scattering investigations in DMSO and DMAc revealed aggregates which could be completely suppressed by the addition of LiCl. However, the significantly lower refractive index increment (dn/dc) of CA in DMSO as compared to DMAc made DMAc the preferred choice for SEC experiments. Samples differing in DS but being prepared from the same parent material showed nearly the same elution profile and nearly identical calibration curves, indicating that variations of the DS within the range of DS = 1.5 – 2.9 do not alter remarkably the hydrodynamic volume. As a consequence, all the CA samples can be evaluated based on the same calibration curve, irrespective of their DS. The comparison of the true molar masses obtained by light scattering with PMMA-equivalent molar masses revealed that the PMMA-equivalent molar masses overestimated the absolute ones significantly. Therefore, correction factors (i.e. A and B values) were determined using the broad calibration approach. However, the deviation between the A/B sets was found to be large. This was explained by the weight average molar mass (M_w) of CAs chosen for the broad calibration, which were located in a very narrow range of M_w. Therefore, the correlation between absolute molar mass

from light scattering and the corresponding PMMA-equivalent molar mass at the same elution volume was used to determine the correction parameters A and B. The finally obtained equation is as follows:

$$\log M_{CA} = 0.867 \times \log M_{PMMA} + 0.214$$ **Equation 42**

After establishing a suitable SEC method, a normal-phase gradient liquid chromatography method capable to separate CAs with respect to DS was developed. The separation was based on an adsorption-desorption mechanism rather than precipitation-redissolution using a multi-step gradient of dichloromethane (DCM) and methanol (MeOH) on silica gel as the stationary phase. Applicability of the developed multi-step gradient allowed separating CA within the DS-range of DS = 1.5 – 2.9. This DS-range of CA is the target for most of its applications.

LC-FTIR was employed in order to prove that a separation by DS was achieved not only for samples clearly differing in their average DS values, but also within a single sample. Thus, the developed method for the first time allowed determination of the DS-distribution (heterogeneity of the first order) of intact cellulose acetate chains.

However, we were not able to fully visualize if the gradient separation is governed purely by DS or has got a contribution of molar mass. To clarify this question, samples varying in molar mass but of identical DS are required, which were not available.

Both, gradient HPLC and SEC were combined to determine the correlations between the molar mass and DS. However, since the use of non-volatile LiCl salt is incompatible with evaporative light scattering detection (ELSD), the DMAc/LiCl method developed could not be applied as the second dimension (SEC). Thus, attempts were undertaken to develop another SEC method being compatible with ELSD. It was found that a mixture composed of 45% DMSO and 55% 1,4-dioxane containing ammonium acetate was the best eluent with respect to ELSD compatibility and signal-to-noise ratio, as well. Therefore, fractions from the gradient HPLC were collected and subsequently injected into the SEC. Interestingly, three different types of correlations between molar mass and DS were observed. These forms were termed form 1, form 2 and form 3.

In form 1, the chromatograms of fraction 1 to 7 shifted to the lower SEC elution volume (i.e. higher molar mass) with increasing fraction number (i.e. gradient elution volume, i.e. lower

DS). At higher gradient elution volume the SEC elution volumes became nearly constant (fraction 7 to 15). In form 2 and form 3, a similar decrease in SEC elution volume with 1st dimension fraction number was observed up to fraction 7. However, contrasting to form 1, the SEC elution volumes continued to decrease for the chromatograms of fraction 11 to 15 (form 2) whereas a clear increase in elution volumes was unexpectedly observed for the chromatograms of fraction 11 to 15 (form 3). These behaviours might be explained by differences in microstructure (i.e. arrangements of differently substituted AGUs along the CA chains) of CAs. Furthermore, differences in the shape of the 2D contour plots were observed. The newly developed techniques are expected to give new insight into the heterogeneity of CAs.

7. List of Abbreviations and Acronyms

σ^2	Variance
δ	Proton NMR Chemical Shift
λ	Wavelength
Φ_0	Initial Mobile Phase Composition
Φ_e	Mobile Phase Composition at Elution Point
ΔG	Free Gibbs Energy Difference
ΔH	Change in Interaction Enthalpy
ΔS	Change in Conformational Entropy
1,2,4-TCB	1,2,4-Trichlorobenzene
2D-LC	Two-Dimensional Liquid Chromatography
A	Peak Area
A_2	Second Virial Coefficient
AGU	Anhydroglucose Unit
ATR	Attenuated Total Reflectance
CA	Cellulose Acetate
CAP	Cellulose Acetopropionate
CCD	Chemical Composition Distribution
CDA	Cellulose Diacetate
CE	Capillary Electrophoresis
CH_3COONH_4	Ammonium Acetate
CMC	Carboxymethyl Cellulose
conc.	Concentration
CTA	Cellulose Triacetate
CX	Cellulose Xanthate
DCM	Dichloromethane
DGTS	Temperature-Stabilized Deuterated Tryglycine Sulfate
$Đ_M$	Molar Mass Dispersity
DMAc	N,N-Dimethylacetamide
DMF	Dimethylformamide
DMSO	Dimethyl Sulfoxide

dn/dc	Refractive Index Increment
DP	Degree of Polymerization
DP_w	Weight Average Degree of Polymerization
DS	Average Degree of Substitution
DS_w	Weight Average Degree of Substitution
ELSD	Evaporative Light Scattering Detector
ESI	Electrospray Ionization
EVAP Temp	Evaporation Temperature
F	Mobile Phase Flow Rate
FID	Flame Ionization Detector
FTD	Functionality Type Distribution
FTIR	Fourier Transform Infra Red
G	Mobile Phase Gradient Slope
G(L)C	Gas (Liquid) Chromatography
AEC	Anion-Exchange Chromatography
H_2SO_4	Sulfuric Acid
$HClO_4$	Perchloric Acid
(^{1}H)-NMR	(Proton)-Nuclear Magnetic Resonance
HPLC	High Performance Liquid Chromatography
HPC	Hydroxypropyl Cellulose
HPMC	Hydroxypropyl Methylcellulose
I.D.	Column Internal Diameter
K_d	Distribution (or Partition) Coefficient
k_{inst}	Refractive Index Instrument Constant
K_{LAC}	Contribution of Adsorption to K_d
K_{SEC}	Contribution of Size Exclusion to K_d
LAC	Liquid Adsorption Chromatography
LALLS	Low Angle Laser Light Scattering
LC	Liquid Chromatography
LC-CC	Liquid Chromatography at Critical Conditions
LiCl	Lithium Chloride
MALDI	Matrix Assisted Laser Desorption/Ionization
MALLS	Multi-angle Laser Light Scattering
MC	Methyl Cellulose

MEK	Methyl Ethyl Ketone
MeOH	Methanol
min	Minute
MMD	Molar Mass Distribution
M_n	Number Average Molar Mass
MS	Average Molar Substitution
MS	Mass Spectrometry
M_w	Weight Average Molar Mass
N_A	Avogadro's Number
NaOH	Sodium Hydroxide
NEB Temp	Nebulization Temperature
NPLC	Normal-Phase Liquid Chromatography
$P(\theta)$	Particle Scattering Factor
PAD	Pulsed Amperometric Detection
PMMA	Poly(Methyl Methacrylate)
ppm	Parts Per Million
PS	Polystyrene
psi	Pound-force per Square Inch
R	Gas Constant
R_θ	Rayleigh Ratio
R_f	Retardation Factor
R_g	Radius of Gyration
RI	Refractive Index Detector
RPLC	Reverse-Phase Liquid Chromatography
SEC	Size Exclusion Chromatography
S/N-ratio	Signal-to-Noise-Ratio
STD	Standard Deviation
t	Time
T	Absolute Temperature
TBAF	Tetrabutylammonium Fluoride
t_G	Gradient Time
THF	Tetrahydrofuran
TLC	Thin Layer Chromatography
ToF	Time-of-Flight

t_R	Retention Time
UV	Ultraviolet Detector
V_0	Dead (Hold-up) Volume of the System
V_{apex}	Elution Volume at Peak Maximum
V_d	Dwell Volume of the System
V_e	Elution Volume
V_I	Interstitial Volume of the Column
Vol.	Volume
V_P	Pore Volume of the Stationary Phase
V_R	Retention Volume
V_T	Total Volume of the System
w(DS)	Normalized Degree of Substitution Distribution

8. Bibliographic References

1. Hon, D. N.-S. *Cellulose* **1994,** 1, (1), 1-25.

2. Sjöström, E., In *Wood chemistry: Fundamentals and applications*, 2ed.; Academic Press: San Diego, **1993**.

3. Klemm, D.; Philipp, B.; Heinze, T.; Heinze, U.; Wagenknecht, W., Functionalization of cellulose. In *Comprehensive cellulose chemistry*, Wiley-VCH: Weinheim, **1998**; Vol. 2.

4. Edgar, K. J., Cellulose esters, organic. In *Encyclopedia of Polymer Science and Technology*, Mark, H. F., Ed. Wiley: New York, **2004**; Vol. 9.

5. Shelton, M. C., Cellulose esters, inorganic. In *Encyclopedia of Polymer Science and Technology*, Wiley: New York, **2003**; Vol. 9.

6. Balser, K.; Hoppe, C.; Eicher, T.; Wandel, M.; Astheimer, H. J.; Steinmaier, H.; Allen, J. M., Cellulose esters. In *Ullmann's Encyclopedia of Industrial Chemistry*, Wiley-VCH: Weinheim, **2004**.

7. Edgar, K. J.; Buchanan, C. M.; Debenham, J. S.; Rundquist, P. A.; Seiler, B. D.; Shelton, M. C.; Tindall, D. *Prog. Polym. Sci.* **2001,** 26, (9), 1605-1688.

8. Mahendran, R.; Malaisamy, R.; Mohan, D. *J. Macromol. Sci., Part A: Pure Appl. Chem.* **2002,** 39, (9), 1025-1035.

9. Baumann, M. G. D.; Conner, A. H., Carbohydrate polymers as adhesives. In *Handbook of adhesive technology*, 2ed.; Pizzi, A.; Mittal, K. L., Eds. Marcel Dekker: New York, **2003**.

10. Glasser, W. G. *Macromol. Symp.* **2004,** 208, (1), 371-394.

11. Edgar, K. J. *Cellulose* **2007,** 14, (1), 49-64.

12. Martin, J. R.; Johnson, J. F.; Cooper, A. R. *J. Macromol. Sci., Part C: Polym. Rev.* **1972,** 8, (1), 57-199.

13. Fischer, S.; Thümmler, K.; Volkert, B.; Hettrich, K.; Schmidt, I.; Fischer, K. *Macromol. Symp.* **2008,** 262, 89-96.

14. Miyamoto, T.; Sato, Y.; Shibata, T.; Tanahashi, M.; Inagaki, H. *J. Polym. Sci., Polym. Chem. Ed.* **1985,** 23, (5), 1373-1381.

15. Heinrich, J.; Mischnick, P. *J. Polym. Sci., Part A: Polym. Chem.* **1999,** 37, (15), 3011-3016.

16. Schützenberger, P. *Comptes Rendus* **1865,** 61, 485.

17. Steinmeier, H. *Macromol. Symp.* **2004,** 208, (1), 49-60.

18. Hummel, A. *Macromol. Symp.* **2004,** 208, (1), 61-80.

19. Wilson, J. D.; Tabke, R. S. *Tappi* **1974,** 57, (8), 77-80.

20. Wells, F. L.; Schattner, W. C.; Walker, A. *Tappi* **1963,** 46, (10), 581-586.

21. Kamide, K.; Saito, M. *Adv. Polym. Sci.* **1987,** 83, 1-56.

22. Funaki, Y.; Ueda, K.; Saka, S.; Soejima, S. *J. Appl. Polym. Sci.* **1993,** 48, (3), 419-424.

23. Malm, C. J.; Tanghe, L. J.; Laird, B. C. *J. Ind. Eng. Chem.* **1946,** 38, (1), 77-82.

24. Gedon, S.; Fengi, R., Cellulose esters, organic esters. In *Kirk-Othmer Encyclopedia of Chemical Technology*, Wiley: Hoboken, **2000**.

25. Heinze, T.; Koschella, A. *Polim.: Cienc. Tecnol.* **2005,** 15, (2), 84-90.

26. Liebert, T., Cellulose solvents – remarkable history, bright future. In *Cellulose solvents: For analysis, shaping and chemical modification*, Liebert, T. F.; Heinze, T. J.; Edgar, K. J., Eds. ACS Symposium Series: Washington, **2010**; Vol. 1033.

27. Tosh, B.; Saikia, C. N.; Dass, N. N. *Carbohydr. Res.* **2000,** 327, (3), 345-352.

28. Ramos, L. A.; Morgado, D. L.; El Seoud, O. A.; da Silva, V. C.; Frollini, E. *Cellulose* **2011,** 18, (2), 385-392.

29. Ass, B. A. P.; Frollini, E.; Heinze, T. *Macromol. Biosci.* **2004,** 4, (11), 1008-1013.

30. Ciacco, G. T.; Liebert, T. F.; Frollini, E.; Heinze, T. J. *Cellulose* **2003,** 10, (2), 125-132.

31. Wu, J.; Zhang, J.; Zhang, H.; He, J.; Ren, Q.; Guo, M. *Biomacromolecules* **2004,** 5, (2), 266-268.

32. Kosan, B.; Dorn, S.; Meister, F.; Heinze, T. *Macromol. Mater. Eng.* **2010,** 295, (7), 676-681.

33. El Seoud, O. A.; Heinze, T. *Adv. Polym. Sci.* **2005,** 186, 103-149.

34. Takaragi, A.; Minoda, M.; Miyamoto, T.; Liu, H. Q.; Zhang, L. N. *Cellulose* **1999,** 6, (2), 93-102.

35. Malm, C. J.; Tanghe, L. J.; Laird, B. C. *J. Am. Chem. Soc.* **1950,** 72, (6), 2674-2678.

36. Hiller, L. A., JR. *J. Polym. Sci., Part A-1* **1953,** 10, (4), 385-423.

37. Howlett, F.; Martin, E. *J. Text. Inst., Trans.* **1947,** 38, (4), T212-T225.

38. Malm, C. J.; Glegg, R. E.; Salzer, J. T.; Ingerick, D. F.; Tanghe, L. J. *Ind. Eng. Chem. Process Des. Dev.* **1966,** 5, (1), 81-87.

39. Usmanov, T. I.; Tashpulatov, Y. T.; Abdullaev, F. T.; Sultanov, A. Z. *Chem. Nat. Compd.* **1997,** 33, (5), 530-533.

40. Sjöholm, E., Size exclusion chromatography of cellulose and cellulose derivatives. In *Handbook of size exclusion chromatography and related techniques*, Wu, C.-S., Ed. Marcel Dekker Inc: New York, **2003**.

41. Vaca-Garcia, C.; Borredon, M. E.; Gaseta, A. *Cellulose* **2001,** 8, (3), 225-231.

42. Luo, J.; Sun, Y. *J. Appl. Polym. Sci.* **2006,** 100, (4), 3288-3296.

43. Goodlett, V. W.; Dougherty, J. T.; Patton, H. W. *J. Polym. Sci., Part A-1* **1971,** 9, (1), 155-161.

44. Tezuka, Y.; Tsuchiya, Y. *Carbohydr. Res.* **1995,** 273, (1), 83-91.

45. Kamide, K.; Okajima, K. *Polym. J.* **1981,** 13, (2), 127-133.

46. Sei, T.; Ishitani, K.; Suzuki, R.; Ikematsu, K. *Polym. J.* **1985,** 17, (9), 1065-1069.

47. Kowsaka, K.; Okajima, K.; Kamide, K. *Polym. J.* **1986,** 18, (11), 843-849.

48. Takahashi, S.-I.; Fujimoto, T.; Barua, B. M.; Miyamoto, T.; Inagaki, H. *J. Polym. Sci., Part A: Polym. Chem. Ed.* **1986,** 24, (11), 2981-2993.

49. Tezuka, Y.; Imai, K.; Oshima, M.; Chiba, T. *Macromolecules* **1987,** 20, (10), 2413-2418.

50. Kowsaka, K.; Okajima, K.; Kamide, K. *Polym. J.* **1988,** 20, (10), 827-836.

51. Nehls, I.; Philipp, B.; Wagenknecht, W.; Klemm, D.; Schnabelrauch, M.; Stein, A.; Heinze, T. *Papier* **1990,** 44, (12), 633-640.

52. Ho, F. F.-L.; Klosiewicz, D. W. *Anal. Chem.* **1980,** 52, (6), 913-916.

53. Reuben, J. *Carbohydr. Res.* **1986,** 157, 201-213.

54. Reuben, J. *Carbohydr. Res.* **1987,** 161, (1), 23-30.

55. Saake, B.; Altaner, C.; Lee, S.-J.; Puls, J. *Macromol. Symp.* **2005,** 223, (1), 137-150.

56. Heinze, T.; Erler, U.; Nehls, I.; Klemm, D. *Angew. Makromol. Chem.* **1994,** 215, (1), 93-106.

57. Verraest, D. L.; Peters, J. A.; Kuzee, H. C.; Raaijmakers, H. W. C.; van Bekkum, H. *Carbohydr. Res.* **1997,** 302, (3-4), 203-212.

58. Erler, U.; Mischnick, P.; Stein, A.; Klemm, D. *Polym. Bull.* **1992,** 29, (3-4), 349-356.

59. Saake, B.; Lebioda, S.; Puls, J. *Holzforschung* **2004,** 58, (1), 97-104.

60. Adden, R.; Müller, R.; Mischnick, P. *Cellulose* **2006,** 13, (4), 459-476.

61. Richardson, S.; Andersson, T.; Brinkmalm, G.; Wittgren, B. *Anal. Chem.* **2003,** 75, (22), 6077-6083.

62. Richardson, S.; Lundqvist, J.; Wittgren, B.; F., T.; Gorton, L. *Biomacromolecules* **2002,** 3, (6), 1359-1363.

63. Horner, S.; Puls, J.; Saake, B.; Klohr, E.-A.; Thielking, H. *Carbohydr. Polym.* **1999,** 40, (1), 1-7.

64. Kragten, E. A.; Kamerling, J. P.; Vliegenthart, J. F. G. *J. Chromatogr.* **1992,** 623, (1), 49-53.

65. Cohen, A.; Schagerlöf, H.; Nilsson, C.; Melander, C.; Tjerneld, F.; Gorton, L. *J. Chromatogr., A* **2004,** 1029, (1-2), 87-95.

66. Mischnick, P. *J. Carbohydr. Chem.* **1991,** 10, (4), 711-722.

67. Cuers, J.; Unterieser, I.; Burchard, W.; Adden, R.; Rinken, M.; Mischnick, P. *Carbohydr. Res.* **2012,** 348, 55-63.

68. Adden, R.; W., N.; Müller, R.; Mischnick, P. *Anal. Chem.* **2006,** 78, (4), 1146-1157.

69. Schagerlöf, H.; Richardson, S.; Momcilovic, D.; Brinkmalm, G.; Wittgren, B.; Tjerneld, F. *Biomacromolecules* **2006,** 7, (1), 80-85.

70. Bashir, S.; Critchley, P.; Derrick, P. J. *Cellulose* **2001,** 8, (1), 81-89.

71. Arisz, P. W.; Kauw, H. J. J.; Boon, J. J. *Carbohydr. Res.* **1995,** 271, (1), 1-14.

72. Saake, B.; Horner, S.; Puls, J., Progress in the enzymatic hydrolysis of cellulose derivatives. In *Cellulose derivatives: Modification, characterization, and*

nanostructures, Heinze, T. J.; Glasser, W. G., Eds. ACS Symposium: Washington, **1998**; pp 201-216.

73. Saake, B.; Puls, J.; Wagenknecht, W. *Carbohydr. Polym.* **2002,** 48, (1), 7-14.

74. Glöckner, G., In *Gradient HPLC of copolymers and chromatographic cross-fractionation*, Springer-Verlag: Berlin, **1991**.

75. Pasch, H.; Trathnigg, B., In *HPLC of polymers*, Springer-Verlag: Berlin-Heidelberg, **1998**.

76. Quarry, M. A.; Stadalius, M. A.; Mourey, T. H.; Snyder, L. R. *J. Chromatogr., A* **1986,** 358, (1), 1-16.

77. Stadalius, M. A.; Quarry, M. A.; Mourey, T. H.; Snyder, L. R. *J. Chromatogr.* **1986,** 358, (1), 17-37.

78. Glöckner, G.; Van den Berg, J. H. M. *J. Chromatogr.* **1986,** 352, 511-522.

79. Fischer, K.; Krasselt, K.; Schmidt, I.; Weightman, D. *Macromol. Symp.* **2005,** 223, 109-120.

80. Fitzpatrick, F.; Schagerlöf, H.; Andersson, T.; Richardson, S.; Tjerneld, F.; Wahlund, K.-G.; Wittgren, B. *Biomacromolecules* **2006,** 7, (10), 2909-2917.

81. Stefansson, M. *Carbohydr. Res.* **1998,** 312, (1), 45-52.

82. Oudhoff, K. A.; (Ab) Buijtenhuijs, F. A.; Wijnen, P. H.; Schoenmakers, P. J.; Kok, W. T. *Carbohydr. Res.* **2004,** 339, (11), 1917-1924.

83. Adden, R.; Müller, R.; Mischnick, P. *Macromol. Chem. Phys.* **2006,** 207, (11), 954-965.

84. Mischnick, P.; Adden, R. *Macromol. Symp.* **2008,** 262, (1), 1-7.

85. Saake, B.; Horner, S.; Kruse, T.; Puls, J.; Liebert, T.; Heinze, T. *Macromol. Chem. Phys.* **2000,** 201, (15), 1996-2002.

86. Mardles, E. W. J. *J. Chem. Soc., Trans.* **1923,** 123, 1951-1957.

87. McNally, J. G.; Godbout, A. P. *J. Am. Chem. Soc.* **1929,** 51, (10), 3095-3101.

88. Herzog, R. O.; Deripasko, A. *Cellulosechemie* **1932,** 13, 25-31.

89. Sookne, A. M.; Rutherford, H. A.; Mark, H.; Harris, M. *J. Res. Natl. Bur. Stand.* **1942,** 29, 123-130.

90. Rosenthal, A. J.; White, B. B. *J. Ind. Eng. Chem.* **1952,** 44, 2693-2696.

91. Kamide, K.; Manabe, S.-I.; Osafune, E. *Makromol. Chem.* **1973,** 168, 173-193.

92. Kamide, K.; Okada, T.; Terakawa, T.; Kaneko, K. *Polym. J.* **1978,** 10, (5), 547-556.

93. Kamide, K.; Matsui, T.; Okajima, K.; Manabe, S.-I. *Cellul. Chem. Technol.* **1982,** 16, (6), 601-614.

94. Greiderer, A.; Steeneken, L.; Aalbers, T.; Vivó-Truyols, G.; Schoenmakers, P. *J. Chromatogr., A* **2011,** 1218, (34), 5787-5793.

95. Floyd, T. R. *J. Chromatogr.* **1993,** 629, (2), 243-254.

96. Asai, T.; Shimamoto, S.; Shibata, T.; Kawai, T.; Teramachi, S. *Macromol. Symp.* **2006,** 242, (1), 5-12.

97. Kilz, P. *Chromatographia* **2004,** 59, (1-2), 3-14.

98. Pasch, H.; Hiller, W. *Macromolecules* **1996,** 29, (20), 6556-6559.

99. Pasch, H.; Adler, M.; Rittig, F.; Becker, S. *Macromol. Rapid Commun.* **2005,** 26, (6), 438-444.

100. Snyder, L. R.; Kirkland, J. J.; Dolan, J. W., Introduction to modern liquid chromatography. In 3ed.; Wiley: New York, **2010**.

101. Entelis, S. G.; Evreinov, V. V.; Gorshkov, A. V. *Adv. Polym. Sci.* **1986,** 76, 129-175.

102. Barth, H. G.; Boyes, B. E.; Jackson, C. *Anal. Chem.* **1998,** 70, (12), 251R-278R.

103. Radke, W. *Macromol. Theory Simul.* **2001,** 10, (7), 668-675.

104. Chang, T. *Adv. Polym. Sci.* **2003,** 163, 1-60.

105. Glöckner, G. *Adv. Polym. Sci.* **1986,** 79, 159-214.

106. Trathnigg, B.; Maier, B.; Gorbunov, A.; Skvortsov, A. *J. Chromatogr., A* **1997,** 791, (1-2), 21-35.

107. Raust, J.-A.; Brüll, A.; Sinha, P.; Hiller, W.; Pasch, H. *J. Sep. Sci.* **2010,** 33, (10), 1375-1381.

108. Philipsen, H. J. A. *J. Chromatogr., A* **2004,** 1037, (1-2), 329-350.

109. Cho, D.; Park, S.; Chang, T.; Avgeropoulos, A.; Hadjichristidis, N. *Eur. Polym. J.* **2003,** 39, (11), 2155-2160.

110. Ryu, J.; Park, S.; Chang, T. *J. Chromatogr., A* **2005,** 1075, (1-2), 145-150.

111. Skvortsov, A. M.; Gorbunov, A. A. *J. Chromatogr.* **1990,** 507, 487-496.

112. Chang, T.; Lee, H. C.; Lee, W.; Park, S.; Ko, C. *Macromol. Chem. Phys.* **1999,** 200, (10), 2188-2204.

113. Gorshkov, A. V.; Much, H.; Becker, H.; Pasch, H.; Evreinov, V. V.; Entelis, S. G. *J. Chromatogr.* **1990,** 523, 91-102.

114. Mengerink , Y.; Peters, R.; van der Wal, S.; Claessens, H. A.; Cramers, C. A. *J. Chromatogr., A* **2002,** 949, (1-2), 337-349.

115. Berek, D.; Janco, M.; Hatada, K.; Kitayama, T.; Fujimoto, N. *Polym. J.* **1997,** 29, (12), 1029-1033.

116. Kitayama, T.; Janco, M.; Ute, K.; Niimi, R.; Hatada, K.; Berek, D. *Anal. Chem.* **2000,** 72, (7), 1518-1522.

117. Pasch, H.; Rode, K. *Polymer* **1998,** 39, (25), 6377-6383.

118. Esser, K. E.; Braun, D.; Pasch, H. *Angew. Makromol. Chem.* **1999,** 271, 61-67.

119. Pasch, H.; Brinkmann, C.; Much, H.; Just, U. *J. Chromatogr.* **1992,** 623, 315-322.

120. Pasch, H.; Augenstein, M.; Trathnigg, B. *Macromol. Chem. Phys.* **1994,** 195, 743-750.

121. Pasch, H.; Augenstein, M. *Makromol. Chem.* **1993,** 194, (9), 2533-2541.

122. Falkenhagen, J.; Much, H.; Stauf, W.; Müller, A. H. E. *Macromolecules* **2000,** 33, (10), 3687-3693.

123. Macko, T.; Hunkeler, D. *Adv. Polym. Sci.* **2003,** 163, 61-136.

124. Buszewski, B.; Welerowicz, T. *Comb. Chem. High Throughput Screening* **2004,** 7, (4), 291-312.

125. Nunez, O.; Nakanishi, K.; Tanaka, N. *J. Chromatogr., A* **2008,** 1191, (1-2), 231-252.

126. Haky, J. E.; Vemulapalli, S.; Wieserman, L. F. *J. Chromatogr.* **1990,** 505, (2), 307-318.

127. Blackwell, J. A.; Carr, P. W. *Anal. Chem.* **1992,** 64, (8), 863-873.

128. Berthod, A. *J. Chromatogr.* **1991,** 549, (1-2), 1-28.

129. Claessens, H. A.; van Straten, M. A. *J. Chromatogr., A* **2004,** 1060, (1-2), 23-41.

130. Lloyd, L. L. *J. Chromatogr., A* **1991,** 544, (1-2), 201-217.

131. Glöckner, G. *J. Chromatogr.* **1987,** 403, 280-284.

132. Bashir, M. A.; Brüll, A.; Radke, W. *Polymer* **2005,** 46, (10), 3223-3229.

133. Bashir, M. A.; Radke, W. *J. Chromatogr., A* **2006,** 1131, (1-2), 130-141.

134. van der Horst, A.; Schoenmakers, P. *J. Chromatogr., A* **2003,** 1000, (1-2), 693-709.

135. Guiochon, G.; Marchetti, N.; Mriziq, K.; Schalliker, R. A. *J. Chromatogr., A* **2008,** 1189, (1-2), 109-168.

136. Siewing, A.; Schierholz, J.; Braun, D.; Hellmann, G. P.; Pasch, H. *Macromol. Chem. Phys.* **2001,** 202, (14), 2890-2894.

137. Siewing, A.; Lahn, B.; Braun, D.; Pasch, H. *J. Polym. Sci., Part A: Polym. Chem.* **2003,** 41, (20), 3143-3148.

138. Jiang, X.; van der Horst, A.; Lima, V.; Schoenmakers, P. J. *J. Chromatogr., A* **2005,** 1076, (1-2), 51-61.

139. Philipsen, H. J. A.; Klumperman, B.; van Herk, A. M.; German, A. L. *J. Chromatogr., A* **1996,** 727, (1), 13-25.

140. Adrian, J.; Esser, E.; Hellmann, G.; Pasch, H. *Polymer* **2000,** 41, (7), 2439-2449.

141. Gao, H.; Min, K.; Matyjaszewski, K. *Macromol. Chem. Phys.* **2006,** 207, (19), 1709-1717.

142. Gerber, J.; Radke, W. *Polymer* **2005,** 46, (22), 9224-9229.

143. Im, K.; Kim, Y.; Chang, T.; Lee, K.; Choi, N. *J. Chromatogr., A* **2006,** 1103, (2), 235-242.

144. Graef, S. M.; van Zyl, A. J. P.; Sanderson, R. D.; Klumperman, B.; Pasch, H. *J. Appl. Polym. Sci.* **2003,** 88, (10), 2530-2538.

145. Kilz, P.; Krüger, R. P.; Much, H.; Schulz, G., Two-dimensional chromatography for the deformulation of complex copolymers. In *Chromatographic characterization of polymers: Hyphenated and multidimensional techniques*, Provder, T.; Barth, H. G.; Urban, M. W., Eds. American Chemical Society: Washington D.C., **1995**; Vol. 247.

146. Schoenmakers, P. J.; Vivó-Truyols, G.; Decrop, W. M. C. *J. Chromatogr., A* **2006,** 1120, (1-2), 282-290.

147. Stoll, D. R.; Li, X.; Wang, X.; Carr, P. W.; Porter, S. E. G.; Rutan, S. C. *J. Chromatogr., A* **2007,** 1168, (1-2), 3-43.

148. Somsen, G. W.; Gooijer, C.; Brinkman, U. A. T. *J. Chromatogr., A* **1999,** 856, (1-2), 213-242.

149. DesLauriers, P. L.; Rohlfing, D. C.; Hsieh, E. T. *Polymer* **2002,** 43, (1), 159-170.

150. Kok, S. J.; Hankemeier, T.; Schoenmakers, P. J. *J. Chromatogr., A* **2005,** 1098, (1-2), 104-110.

151. Wheeler, L. M.; Willis, J. N. *Appl. Spectrosc.* **1993,** 47, (8), 1128-1130.

152. Willis, J. N.; Dwyer, J. L.; Liu, M. X. *Int. J. Polym. Anal. Charact.* **1997,** 4, (1), 21-29.

153. Albrecht, A.; Heinz, L.-C.; Lilge, D.; Pasch, H. *Macromol. Symp.* **2007,** 257, (1), 46-55.

154. Podzimek, S.; Vlcek, T.; Johann, C. *J. Appl. Polym. Sci.* **2001,** 81, (7), 1588-1594.

155. Wittgren, B.; Porsch, B. *Carbohydr. Polym.* **2002,** 49, (4), 457-469.

156. Pferfferkorn, P.; Beister, J.; Hild, A.; Thielking, H.; Kulicke, W.-M. *Cellulose* **2003,** 10, (1), 27-36.

157. Žagar, E.; Kržan, A. *Biomacromolecules* **2004,** 5, (2), 628-636.

158. Gao, W.; Liu, X. M.; Gross, R. A. *Polym. Int.* **2009,** 58, (10), 1115-1119.

159. Yau, W. W.; Hill, D. R. *Int. J. Polym. Anal. Charact.* **1996,** 2, (2), 151-171.

160. Zammit, M. D.; Davis, T. P. *Polymer* **1997,** 38, (17), 4455-4468.

161. Malmgren, T.; Mays, J.; Pyda, M. *J. Therm. Anal. Calorim.* **2006,** 83, (1), 35-40.

162. Liu, X. M.; Gao, W.; Maziarz, E. P.; Salamone, J. C.; Duex, J.; Xia, E. *J. Chromatogr., A* **2006,** 1104, (1-2), 145-153.

163. Dong, M. W., In *Modern HPLC for fractionating scientists*, Wiley: Hoboken, New Jersey, **2006**.

164. Striegel, A.; Yau, W. W.; Kirkland, J. J.; Bly, D. D., In *Modern size-exclusion liquid chromatography: Practice of gel permeation and gel filtration chromatography*, 2ed.; Wiley: Hoboken, New Jersey, **2009**.

165. Huglin, M. B., In *Light scattering from polymer solutions*, Academic Press: London-New York, **1972**.

166. Kratochvil, P., In *Classical light scattering from polymer solutions*, Elsevier Science: Amsterdam, **1987**.

167. Girod, S.; Baldet-Dupy, P.; Maillols, H.; Devoisselle, J.-M. *J. Chromatogr., A* **2001,** 943, (1), 147-152.

168. Zhang, F.; Roosen-Runge, F.; Skoda, M. W. A.; Jacobs, R. M. J.; Wolf, M.; Callow, P.; Frielinghaus, H.; Pipich, V.; Prévost, S.; Schreiber, F. *Phys. Chem. Chem. Phys.* **2012,** 14, (7), 2483-2493.

169. Zhbankov, R. G., In *Infrared spectra of cellulose and its derivatives*, Stepanov, B. I., Ed. Consultants Bureau: New York, **1966**.

170. O'Connor, R. T., Analysis of chemically modified cotton. In *Cellulose and cellulose derivatives*, Bikales, N. M.; Segal, L., Eds. Wiley-Interscience: New York, **1971**.

171. Noda, I.; Dowrey, A. E.; Haynes, J. L.; Marcott, C., Group frequency assignments for major infrared bands observed in common synthetic polymers. In *Physical properties of polymers handbook*, Mark, J. E., Ed. Springer-Verlag: Woodbury, New York, **2006**.

172. Harada, M.; Kitamori, T.; Teramae, N.; Hashimoto, K.; Oda, S.; Sawada, T. *Appl. Spectrosc.* **1992,** 46, (3), 529-532.

173. Kamide, K.; Okajima, K.; Kowsaka, K.; Matsui, T. *Polym. J.* **1987,** 19, (12), 1405-1412.

174. Deus, C.; Friebolin, H.; Siefert, E. *Makromol. Chem.* **1991,** 192, (1), 75-83.

175. Kondo, T. *J. Polym. Sci., Part B: Polym. Phys.* **1997,** 35, (4), 717-723.

176. Kern, H.; Choi, S. W.; Wenz, G.; Heinrich, J.; Ehrhardt, L.; Mischnick, P.; Garidel, P.; Blume, A. *Carbohydr. Res.* **2000,** 326, (1), 67-79.

177. Danhelka, J.; Kössler, I.; Bohackova, V. *J. Polym. Sci.: Polym. Chem. Ed.* **1976,** 14, (2), 287-298.

178. Marx-Figini, M.; Soubelet, O. *Polym. Bull.* **1982,** 6, (8-9), 501-508.

179. Marx-Figini, M.; Soubelet, O. *Polym. Bull.* **1984,** 11, (3), 281-286.

180. Siochi, E. J.; Ward, T. C. *J. Macromol. Sci., Part C: Rev. Macromol. Chem. Phys.* **1989,** C29, (4), 561-657.

181. Valtasaari, L.; Saarela, K. *Pap. Puu* **1975,** 57, (1), 5-10.

182. Tanner, D. W.; Berry, G. C. *J. Polym. Sci., Polym. Phys. Ed.* **1974,** 12, (5), 941-975.

183. Berry, G. C.; Leech, M. A. *ACS Symp. Ser.* **1981,** 150, 61-80.

184. Coppola, G.; Fabbri, P.; Pallesi, B.; Bianchi, U. *J. Appl. Polym. Sci.* **1972,** 16, (11), 2829-2834.

185. Hann, N. D. *J. Polym. Sci., Polym. Chem. Ed.* **1977,** 15, (6), 1331-1339.

186. Connors, W. J.; Sarkanen, S.; McCarthy, J. L. *Holzforschung* **1980,** 34, (3), 80-85.

187. Ludlam, P. R.; King, J. G. *J. Appl. Polym. Sci.* **1984,** 29, (12), 3863-3872.

188. Badger, R. M.; Blaker, R. H. *J. Phys. Colloid Chem.* **1949,** 53, (7), 1056-1069.

189. Das, B.; Choudhury, P. K. *J. Polym. Sci., Part A-1: Polym. Chem.* **1967,** 5, (4), 769-777.

190. Kamide, K.; Miyazaki, Y.; Abe, T. *Polym. J.* **1979,** 11, (7), 523-538.

191. Kamide, K.; Saito, M.; Abe, T. *Polym. J.* **1981,** 13, (5), 421-431.

192. Saito, M. *Polym. J.* **1983,** 15, (3), 249-253.

193. Elsdon, W. L.; Goldwasser, J. M.; Rudin, A. *J. Polym. Sci., Polym. Lett. Ed.* **1981,** 19, (10), 483-493.

194. Mori, S. *J. Appl. Polym. Sci.* **1976,** 20, (8), 2157-2164.

195. Song, M. S.; Hu, G. X.; Li, X. Y.; Zhao, B. *J. Chromatogr., A* **2002,** 961, (2), 155-170.

196. Olaru, N.; Olaru, L. *J. Appl. Polym. Sci.* **2004,** 94, (5), 1965-1968.

197. Mori, S. *Anal. Chem.* **1981,** 53, (12), 1813-1818.

198. Benoît, H.; Grubisic, Z.; Rempp, P.; Decker, D.; Zilliox, J. G. *J. Chem. Phys.* **1966,** 63, (11-12), 1507-1514.

199. Grubisic, Z.; Rempp, P.; Benoît, H. *J. Polym. Sci., Part B: Polym. Lett.* **1967,** 5, (9), 753-759.

200. Brun, Y. *J. Liq. Chromatogr. Relat. Technol.* **1999,** 22, (20), 3067-3090.

201. Brun, Y.; Alden, P. *J. Chromatogr., A* **2002,** 966, (1-2), 25-40.

202. Jiang, X.; van der Horst, A.; Schoenmakers, P. J. *J. Chromatogr., A* **2002,** 982, (1), 55-68.

203. Engelhardt, H.; Czok, M.; Schultz, R.; Schweinheim, E. *J. Chromatogr.* **1988,** 458, 79-92.

204. Glöckner, G.; Engelhardt, H.; Wolf, D.; Schultz, R. *Chromatographia* **1996,** 42, (3-4), 185-190.

205. Righezza, M.; Guiochon, G. *J. Liq. Chromatogr.* **1988,** 11, (9-10), 1967-2004.

206. Guiochon, G.; Moysan, A.; Holley, C. *J. Liq. Chromatogr.* **1988,** 11, (12), 2547-2570.

207. Righezza, M.; Guiochon, G. *J. Liq. Chromatogr.* **1988,** 11, (13), 2709-2729.

208. Gottlieb, H. E.; Kotlyar, V.; Nudelman, A. *J. Org. Chem.* **1997,** 62, (21), 7512-7515.

209. Jordan, S. L.; Taylor, L. T. *J. Chromatogr. Sci.* **1997,** 35, (1), 7-13.

210. Kok, S. J.; Arentsen, N. C.; Cools, P. J. C. H.; Hankemeier, T.; Schoenmakers, P. J. *J. Chromatogr., A* **2002,** 948, (1-2), 257-265.

211. Kok, S. J.; Wold, C. A.; Hankemeier, T.; Schoenmakers, P. J. *J. Chromatogr., A* **2003,** 1017, (1-2), 83-96.

212. Bashir, M. A.; Radke, W. *J. Chromatogr., A* **2007,** 1163, (1-2), 86-95.

213. Berkowitz, S. A. *J. Liq. Chromatogr.* **1983,** 6, (8), 1359-1373.

Curriculum Vitae

Name:	Hewa Othman Ghareeb
Date of Birth:	19.06.1979
Place of Birth:	Al-Sulaimaniyah, Iraq
Nationality:	Iraqi
Marital status:	Single

Academic career

October 2000 – July 2004	**BSc in Chemistry**, College of Science, Department of Chemistry, University of Al-Sulaimaniyah, Iraq (First best out of 20 graduates)
October 2004 – March 2005	Lab assistant, College of Science, Department of Chemistry, University of Al-Sulaimaniyah, Iraq
April 2005 – October 2005	Intensive German language courses (levels: A_1, A_2 and B_1) at Goethe Institute, Göttingen, Germany
October 2005 – October 2008	**MSc in Polymer Chemistry**, Technical University of Braunschweig, Germany Master thesis: *The short-molecule stabilization of titania nanoparticles* Under the supervision of Prof. Dr. H. Menzel
November 2008 – Today	**Doctoral student in Analytical Polymer Chemistry**, German Institute for Polymers (Deutsches Kunststoff-Institut, DKI), Darmstadt, Germany "On July 1st, 2012 DKI has been integrated to Fraunhofer Institute for Structural Durability and System Reliability LBF" Doctoral thesis: *Development of new analytical methods to characterize the heterogeneity of cellulose acetates* Under the supervision of Prof. Dr. M. Rehahn

Hewa Othman Ghareeb
Bleichstraße 6, App. 23
64283 Darmstadt

21.12.2012

Erklärung

Ich erkläre hiermit, dass ich meine Dissertation selbstständig und nur mit den angegebenen Hilfsmitteln angefertigt habe.

Darmstadt, den 21. Dezember 2012,

Hewa Othman Ghareeb

Hewa Othman Ghareeb
Bleichstraße 6, App. 23
64283 Darmstadt

21.12.2012

Erklärung

Ich erkläre hiermit, noch keinen Promotionsversuch unternommen zu haben.

Darmstadt, den 21. Dezember 2012,

Hewa Othman Ghareeb